UNIVERSIDADE ESTADUAL PAULISTA
"JÚLIO DE MESQUITA FILHO"

Instituto de Biociências Unesp Botucatu

STUDIES ON THE FUNCTION OF THE *LEISHMANIA MAJOR* TELOMERASE TERT COMPONENT IN TELOMERES MAINTENANCE, CELL PROLIFERATION, AND INFECTIVITY

MARK EWUSI SHIBURAH

BOTUCATU, SP

2024

UNIVERSIDADE ESTADUAL PAULISTA
"Júlio de Mesquista Filho"
INSTITUTO DE BIOCIÊNCIAS DE BOTUCATU

ESTUDOS SOBRE A FUNÇÃO DO COMPONENTE TERT NA MANUTENÇÃO DOS TELÔMEROS E NA PROLIFERAÇÃO CELULAR DE *L. MAJOR*

CANDIDATO: MARK EWUSI SHIBURAH
ORIENTADORA: PROFA. DRA. MARIA ISABEL NOGUEIRA CANO

Tese apresentada ao Instituto de Biociências, Campus de Botucatu, UNESP, como parte dos pré-requisitos necessários para obtenção do título de Doutor no Programa de Pós-Graduação em Ciências Biológicas (Genética)

BOTUCATU, SP
2024

UNIVERSIDADE ESTADUAL PAULISTA

"Júlio de Mesquista Filho"

INSTITUTO DE BIOCIÊNCIAS DE BOTUCATU

STUDIES ON THE FUNCTION OF THE *LEISHMANIA MAJOR* TELOMERASE TERT COMPONENT IN TELOMERES MAINTENANCE, CELL PROLIFERATION, AND INFECTIVITY

CANDIDATE: MARK EWUSI SHIBURAH

SUPERVISOR: PROF. DR. MARIA ISABEL NOGUEIRA CANO

Thesis presented to the Institute of Biosciences, Botucatu Campus, UNESP, as part of the prerequisites necessary to obtain the title of Doctor in the Postgraduate Program in Biological Sciences (Genetics)

BOTUCATU, SP

2024

UNIVERSIDADE ESTADUAL PAULISTA
"JÚLIO DE MESQUITA FILHO"

Catalog page/ Ficha catalográfica

FICHA CATALOGRÁFICA ELABORADA PELA SEÇÃO TÉC. AQUIS. TRATAMENTO DA INFORM.
DIVISÃO TÉCNICA DE BIBLIOTECA E DOCUMENTAÇÃO - CÂMPUS DE BOTUCATU - UNESP
BIBLIOTECÁRIA RESPONSÁVEL: MARIA CAROLINA A. CRUZ E SANTOS-CRB 8/10188

Shiburah, Mark Ewusi.
Studies on the function of the *Leishmania major* telomerase TERT component in telomeres maintenance, cell proliferation, and infectivity / Mark Ewusi Shiburah. - Botucatu, 2024

Tese (doutorado) - Universidade Estadual Paulista "Júlio de Mesquita Filho", Instituto de Biociências de Botucatu
Orientador: Maria Isabel Nogueira Cano
Capes: 20202008

1. Telomere. 2. DNA damage. 3. Leishmania. 4. Telomerase. 5. Cell cycle.

Palavras-chave: DNA damage; Leishmania; TERT knockout; Cell cycle; Loss of infectivity.

Minutes from the defense/ Ata da defesa

UNIVERSIDADE ESTADUAL PAULISTA

Câmpus de Botucatu

ATA DA DEFESA PÚBLICA DA TESE DE DOUTORADO DE MARK EWUSI SHIBURAH, DISCENTE DO PROGRAMA DE PÓS-GRADUAÇÃO EM CIÊNCIAS BIOLÓGICAS (GENÉTICA), DO INSTITUTO DE BIOCIÊNCIAS - CÂMPUS DE BOTUCATU.

Aos 18 dias do mês de janeiro do ano de 2024, às 09:00 horas, no(a) Sala de Pós-Graduação do Instituto de Biociências, realizou-se a defesa de TESE DE DOUTORADO de MARK EWUSI SHIBURAH, intitulada **ESTUDOS SOBRE A FUNÇÃO DO COMPONENTE TERT NA MANUTENÇÃO DOS TELÔMEROS E NA PROLIFERAÇÃO CELULAR DE L. MAJOR**. A Comissão Examinadora foi constituida pelos seguintes membros: Profa. Dra. MARIA ISABEL NOGUEIRA CANO (Orientador(a) - Participação Presencial) do(a) Departamento de Ciências Químicas e Biológicas / Instituto de Biociências UNESP Câmpus de Botucatu, Prof. Dr. ROBSON FRANCISCO CARVALHO (Participação Presencial) do(a) Departamento de Biologia Estrutural e Funcional / Instituto de Biociências de Botucatu - UNESP, PhD MAGALI CASANOVA (Participação Virtual) do(a) Faculty of Pharmacy and Adhesion and Inflammation Laboratory, PhD MIGUEL ANGEL CHIURILLO SIERVO (Participação por Parecer Circunstanciado) do(a) Department of Biological Sciences / University of Cincinnati, PhD MIGUEL GODINHO FERREIRA (Participação Virtual) do(a) Institute for Research on Cancer and Aging of Nice / Nice Université Côte d'Azur. Após a exposição pelo doutorando e arguição pelos membros da Comissão Examinadora que participaram do ato, de forma presencial e/ou virtual, o discente recebeu o conceito final: APROVADO . Nada mais havendo, foi lavrada a presente ata, que após lida e aprovada, foi assinada pelo(a) Presidente(a) da Comissão Examinadora.

Profa. Dra. MARIA ISABEL NOGUEIRA CANO

gov.br Documento assinado digitalmente
MARIA ISABEL NOGUEIRA CANO
Data: 18/01/2024 18:27:37-0300
Verifique em https://validar.iti.gov.br

Dedication

This work is dedicated to the God of my fathers and the memory of my beloved grandmother, Aba Ewusiwaa.

Acknowledgments

Sincerest gratitude to everyone who has been a part of my journey and the people of Sao Paulo whose taxes support FAPESP to push the frontiers of science!

Resumo

Mais de 98 países e territórios notificam casos de leishmaniose, uma doença que afeta quase um milhão de pessoas anualmente, e contra a qual não há tratamento e controle eficazes. Nosso objetivo foi estudar a função do componente transcriptase reversa da telomerase (TERT) em *Leishmania major* (LmTERT) e verificar se a LmTERT poderá ser considerada alvo para o desenvolvimento de novos medicamentos para tratar a leishmaniose. O componente TERT contém o núcleo catalítico da telomerase, a enzima responsável pelo alongamento dos telômeros e pela manutenção da estabilidade do genoma. Neste estudo utilizamos um sistema CRISPR-Cas9 já padronizado, para induzir o nocaute total e por substituição do gene TERT e inibição da telomerase em *L. major.* Southern blot usando sondas específicas, PCR e sequenciamento Sanger do tipo "primer-walking" confirmaram que as duas metodologias induziram a deleção eficiente dos dois alelos do gene TERT em *L. major.* O nocaute do gene *TERT* teve efeitos no crescimento do parasito, induzindo parada do ciclo celular e problemas na proliferação. O encurtamento progressivo dos telômeros, a marca registrada da ausência de TERT, foi observado tanto de forma qualitativa por Southern TRF como quantitativa por Flow-FISH. Além disso, as linhagens mutantes apresentavam aumento de danos ao DNA e problemas de replicação. As estruturas subcelulares das células nocaute LmTERT comparadas ao tipo selvagem por microscopia eletrônica e de varredura, evidenciaram modificações incomuns no citoplasma e uma abundância de autofagossomos, sugerindo um mecanismo autofágico pró-sobrevivência. Um mecanismo altruísta utilizado pelos parasitas foi abolido, e a análise proteômica demonstrou a existência de alterações na constituição do lipofosfoglicano (LPG) de superfície com expressões significativamente alteradas de leishmanolisina Gp63. Alterações nas proteínas do domínio META (expressas principalmente nas formas metacíclicas) e um número superior ao normal de parasitos de fase estacionária que aglutinam lectina de amendoim, foram igualmente observadas nas linhagens nocaute. Os resultados cumulativos que sugerem um comprometimento do potencial infeccioso do parasita foram confirmados pelo estudo in vivo de infecção em camundongos BALB/c e infecção in vitro usando macrófagos derivados da medula óssea de camundongos BALB/c. Foi observado desenvolvimento significativo de lesões nos camundongos infectados com parasitos controle contra aqueles infectados com as linhagens nocaute. Um índice de infectividade consistentemente mais alto foi observado para linhagens controle versus nocaute 48 horas pós-inoculação. Testes preliminares usando um inibidor não-nucleosídico da telomerase, o BIBR1532, resultou em telômeros mais curtos e diminuição do crescimento do parasito. Juntos, esses efeitos pleiotrópicos causados pela ausência ou inibição da LmTERT sugerem fortemente que ela apresenta grande potencial para ser explorada como alvo para o desenvolvimento de medicamentos contra a leishmaniose.

Palavras-chave: TERT, leishmaniose, encurtamento de telômeros, CRISPR-Cas9, autofagia, parada do ciclo celular, alterações de crescimento e ultraestruturais, proliferação celular comprometida, danos ao DNA, perda de infectividade, inibição da telomerase por BIBR1532

Abstract

Over 98 countries and territories have reported cases of leishmaniasis, a disease affecting nearly a million individuals annually but with ineffective remedies. Our goal was to study the function of the telomerase reverse transcriptase (TERT) in *Leishmania major* (LmTERT) and leverage this knowledge in developing new drugs. The TERT component contains the catalytic core of telomerase, the enzyme responsible for elongating telomeres and maintaining genome stability. A loss of function study using CRISPR-Cas9 and inhibition of the telomerase in *L. major* was conducted. Probe-specific Southern blot, PCR, and primer walk Sanger sequencing confirmed the efficient deletion of the *TERT* gene in *L. major*. The knockout of the *TERT* gene resulted in parasite growth defects, DNA fragmentation, cell cycle arrest, and problematic replication measured by flow cytometry. Progressive telomere shortening, the hallmark of TERT absence, was observed by Southern TRF and Flow-FISH assessments. We also assessed the subcellular structures of the LmTERT knockout cells against a wild type using scanning and electron microscopy and found unusual modifications in the cytoplasm, and an abundance of autophagosomes, suggesting a pro-survival autophagic mechanism. Changes in the metacyclic domain proteins were seen equally in the knockout lines. An altruistic mechanism used by the parasites was abolished. The cumulative results suggesting a compromise on parasite infective potential was confirmed by *in vivo* BALB/c mice infection study and *in vitro* bone-marrow derived macrophage infection. Significant lesion development was observed in the mice infected with control parasites against those infected with the knockout lineage. A consistently higher infectivity index was observed for control versus knockout lineages at 48 h post-inoculation. Consistent with the growth challenges and telomere shortening, preliminary tests of the inhibition of the telomerase using BIBR1532, a non-nucleoside small molecule, resulted in shorter telomeres and poor parasite growth. These results together suggest the usefulness of LmTERT to the parasite, putting the protein in a space to be explored for drug development against leishmaniasis.

Keywords: TERT, Leishmaniasis, telomere shortening, CRISPR-Cas9, Autophagy, Cell cycle arrest, growth, and ultrastructural changes, compromised cell proliferation, DNA damage, loss of infectivity, BIBR1532 inhibition.

THESIS ARRANGEMENT:

This thesis begins with a general introduction, followed by a section on the objectives, followed by a section entitled Introduction to the Chapters where the materials, methods, and results for the project are presented as two separate Chapters. Each chapter is presented as an article and begins with an introduction followed by a conclusion and references. A brief general conclusion section ends the chapters followed by a reference section referring specifically to citations from the general introduction.

To aid clarity, the lists of figures and tables are divided into various sections: e.g., a list of figures for the general introduction, a list of figures for Chapter 1, and a list of figures for Chapter 2.

Table of Contents

List of Figures in Introduction

List of figures in Chapter 1 (Page 24 - 92)

List of figures in Chapter 2 (Page 92 – 106)

List of tables

Tables in Chapter 1 (Pages 24-92)

List of Abbreviations

NTDs- Neglected Tropical Diseases

L. major- Leishmania major

LmTERT- *Leishmania major* TERT

ORF- Open Reading Frame

TERT- Telomerase reverse transcriptase

TEN- telomerase essential N-terminal

TRBD- telomerase RNA binding domain

RT- reverse transcriptase

CTE- C-terminal extension

TER- Telomerase RNA

TBE- template boundary element

STE- stem terminus element

CRISPR- Clustered Regularly Interspaced Short Palindromic Repeats

Cas9- CRISPR-Associated protein 9

T7RNAP- T7 RNA Polymerase

pTB007- Expression plasmid carrying Cas9, T7RNAP and Hygromycin genes used in transfection

Lm007- *Leishmania major* parasite carrying plasmid pTB007

sgRNA- single guide RNA

tracrRNA- trans-activating CRISPR RNA

DT- donor template

EdU- 5-ethynyl-2'-deoxyuridine

LPG- Lipophosphoglycan

PBS- phosphate-buffered saline

BIBR1532- 2-[[(E)-3-naphthalen-2-ylbut-2-enoyl]amino]benzoic acid

SCG- scβ-Galactosyltransferases

1. Introduction

The search for an alternative therapeutic strategy in treating leishmaniasis caused by protozoan parasites from the *Leishmania* genus is a matter of global public health interest [1]. *Leishmania* parasites have a digenetic lifecycle that involves living inside a mammalian host and a phlebotomine insect vector. This lifecycle imposes on the parasite a need to develop strategies to survive two different extreme environments using two major developmental phases: intracellular amastigotes and extracellular promastigotes, with observable differences but shared basic molecular and cellular characteristics [1–4].

Over 20 species of *Leishmania* can cause the disease and may manifest in different clinical forms depending on the parasite species and host immune system. The three main clinical forms of leishmaniasis are Cutaneous, Mucocutaneous, and Visceral [5,6]. Most of the cutaneous forms are self-healed in contrast to the dilacerating and mutilating mucocutaneous and the lethal visceral forms [6–9].

Over a million new leishmaniasis cases are reported annually [10]. According to the World Health Organization, 94% of leishmaniasis cases reported in 2017 were recorded in 7 countries, including Brazil (www.who.int/leishmaniasis/burden/en). In the last two decades, a great number of HIV/leishmaniasis coinfections have also been reported (Figure 1) [11,12]. Due to the challenges associated with existing treatment and control methods against the disease, an alternative therapeutic target has become necessary [13].

The WHO outlines a road map for tackling leishmaniasis by looking at the data from different perspectives, including mortalities from vector-disease transmission from 2021 to 2030. Efforts are still being made to combat the spread of leishmaniasis through several health interventions,

including the Elimination Programme of Kala-azar in Southeast Asia (https://www.who.int/publications-detail-redirect/who-wer9635-401-419). The 200 territories and countries that reported cases of leishmaniasis to the WHO show nearly 50% of these regions still have endemic cases of leishmaniasis (Figure 2 and Figure 3) [11].

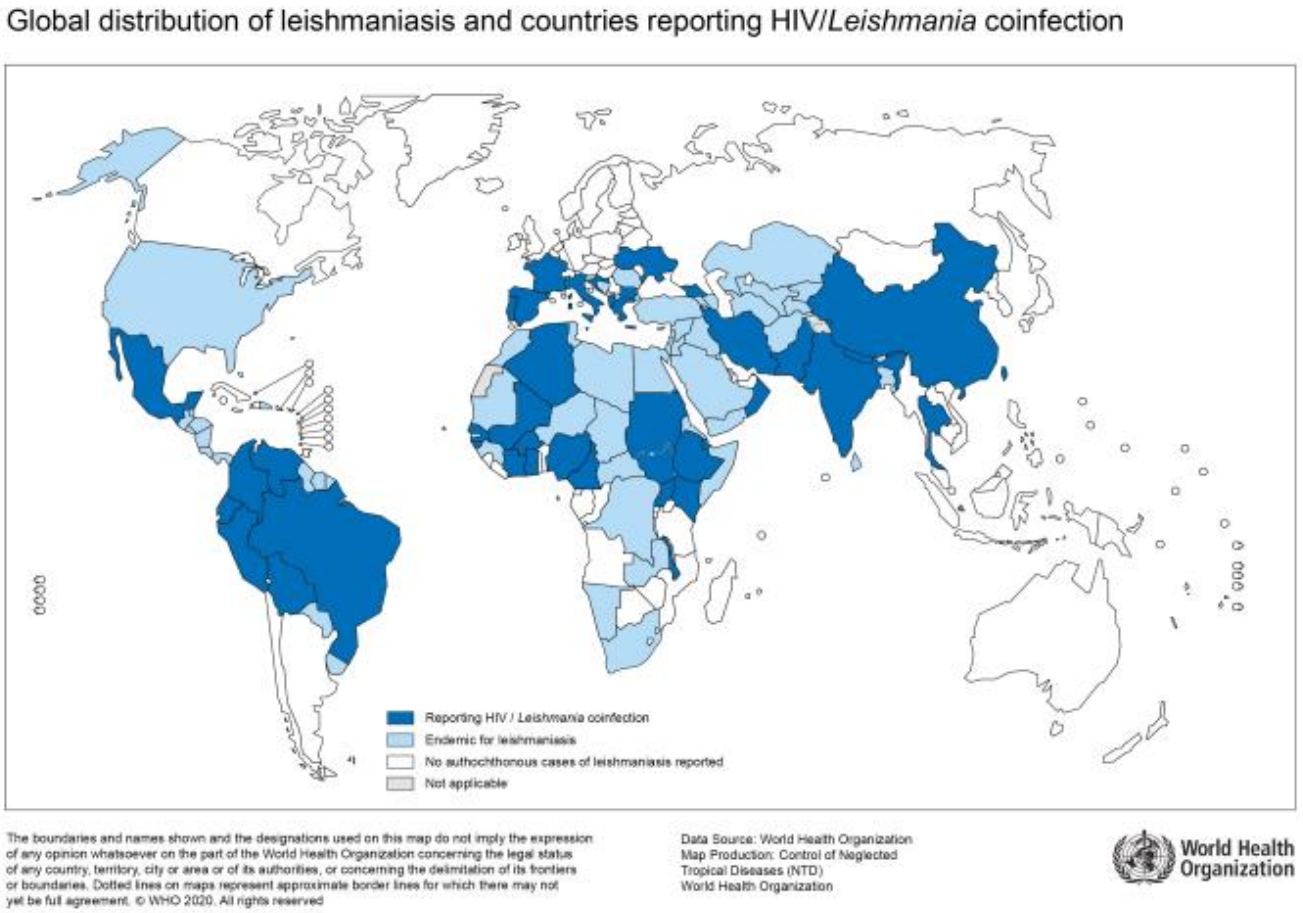

Figure 1. Distribution of leishmaniasis co-infection with HIV across the globe. The 2020 report on the global distribution of countries reporting cases of leishmaniasis co-infection with HIV. WHO classification of countries within the boundaries of Middle East and the Americas seems to have an increased incidence of co-infection cases. Source of image: WHO website.

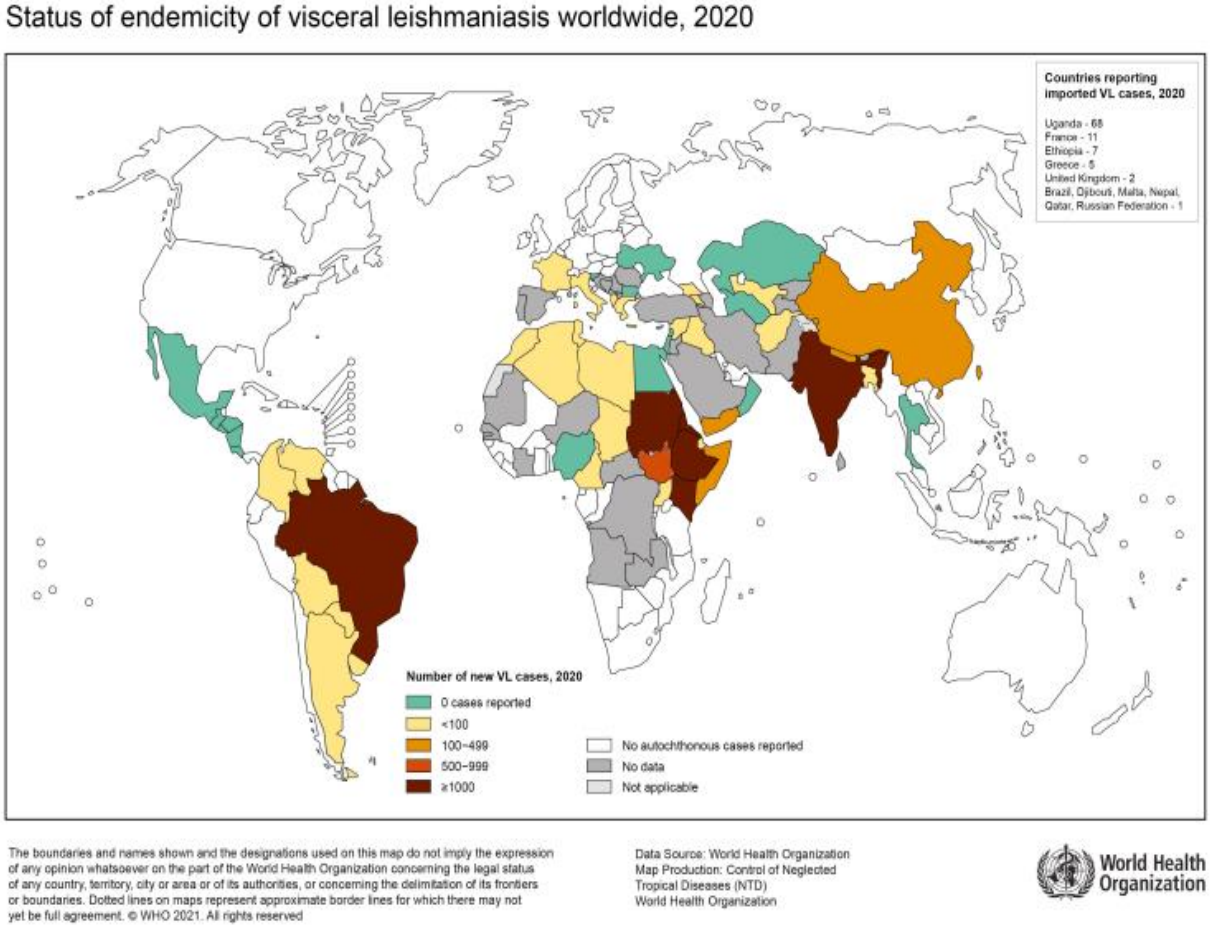

Figure 2. Visceral leishmaniasis distribution. The burden of visceral leishmaniasis across the globe. Some regions in Africa including Ghana, report no cases of Visceral leishmaniasis. Source: World Health Organization.

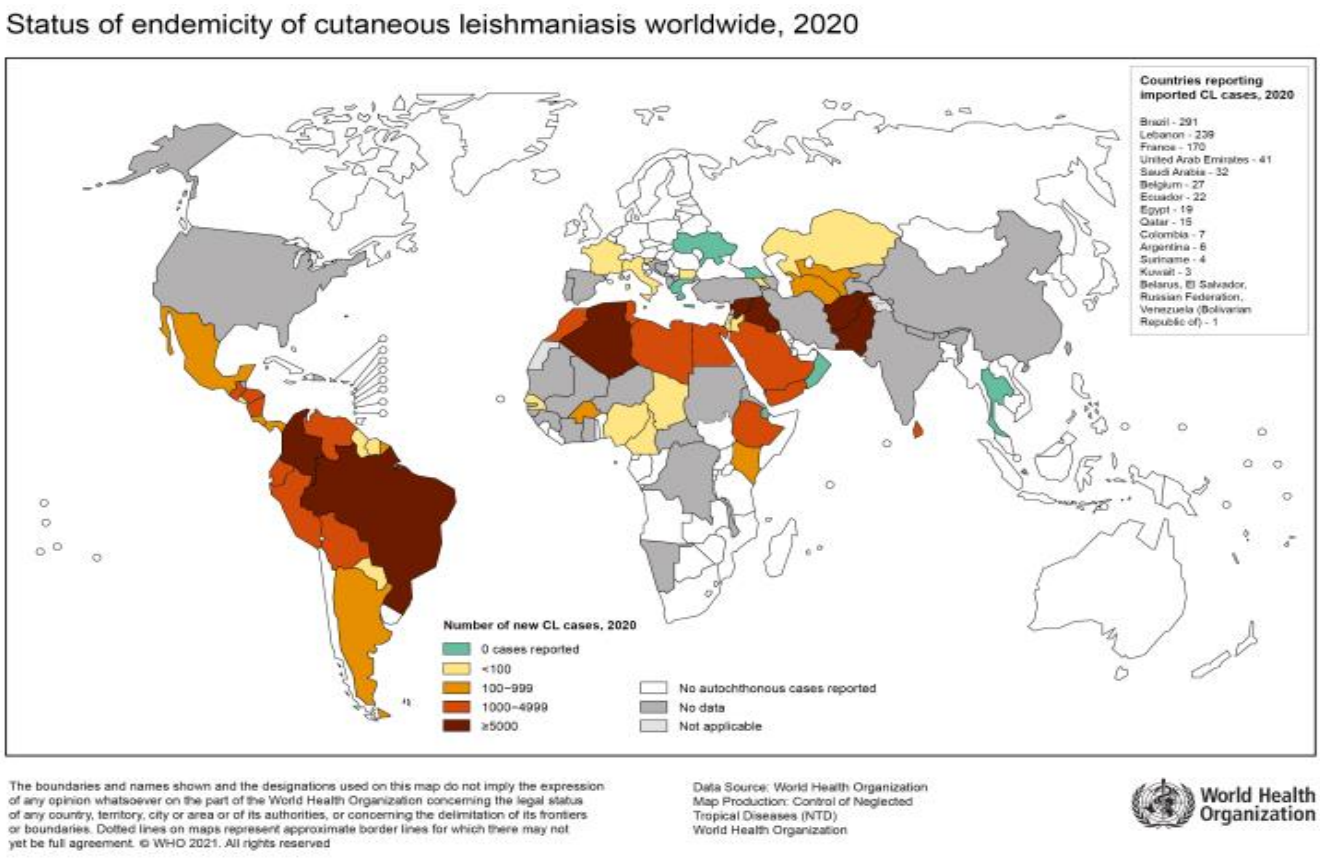

Figure 3. Cutaneous leishmaniasis global assessment. The global burden of cutaneous leishmaniasis in different countries described according to their impact in the various regions. Source: World Health Organization.

1.1 Leishmaniasis, a Neglected Tropical Disease and a quest for new remedies

The WHO classifies 20 conditions mainly identified in tropical regions under the umbrella name 'Neglected Tropical Diseases' (NTDs). Leishmaniasis is one such condition. A disease under the NTD classification like leishmaniasis affects largely impoverished communities where women and children are unduly affected (https://www.who.int/health-topics/neglected-tropical-diseases#tab=tab_1).

Even though there has been some progress in getting countries to fight these diseases, there is still little attention being paid to the development of new and effective remedies. Also, there is little

funding for studies involving these diseases and the social stigma associated with the disease has not gotten any better hence, its classification as 'neglected' remains [14]. The global public health menace of NTDs which includes leishmaniasis led the WHO to formulate a roadmap for the combat of these diseases under the title "*Ending the neglect to attain the Sustainable Development Goals: a road map for neglected tropical diseases 2021−2030*" [14].

As earlier stated, there is little attention for NTDs and thus, there are currently no vaccines available [12]. The Centres for Disease Control and Prevention (CDC), recommends the use of insecticide-treated nets, body covering dress, and the use of repellents as some measures one can take to prevent the bites of the invertebrate-vector-sandflies (https://www.cdc.gov/parasites/leishmaniasis/prevent.html). Due to the challenges with existing treatments, the CDC cautions medical practitioners in administering any treatment. Some of these challenges include highly toxic drugs such as the pentavalent antimonial and the high cost of others such as Amphotericin B. Liposomal amphotericin B and miltefosine can replace the antimonies and are recommended for the treatment of visceral and cutaneous leishmaniasis respectively. While miltefosine is also used in treating visceral leishmaniasis, it induces parasite drug-resistance and is not recommended for pregnant women due to its teratogenic effect. These existing treatments and control methods still do not satisfy the needs of the already impoverished communities, hence, the need to find new drug targets.

1.2 Biology of *Leishmania* parasites

Leishmania parasites have two life cycle stages: promastigote and amastigote. Being digenetic requires that they adapt and live in two host species as a heteroxenous organism (Figure 4) [4]. Sandflies, of the phlebotomine order, have been identified as key host agents and vectors for the spread of the parasite [2,3]. Inside the insect vector, the parasite exists as a highly proliferative

form named promastigote, which is elongate and displays an apparent flagellum that helps the parasite to migrate and survive through the digestive tract of the insect. Through the feeding of the insect on blood meal, the parasite is transferred to the mammals as metacyclic promastigotes, the non-proliferative but highly infectious developmental stage. The long metacyclic flagellum is believed to be the first point of contact with the host cells, as the parasites move anteriorly in the direction of the flagellum [4] Inside the mammalian host, metacyclics are engulfed by the host macrophages. While being engulfed, the parasite undergoes morphological changes and transform into amastigotes, a highly proliferative and rounded form with an imperceptible flagellum [2,4]. Several rounds of cell division inside the macrophages leads to alterations in the composition of the parasitophorous vacuole, which compromises the plasma membrane integrity and eventually overwhelms the macrophage defence system [4,15]. These activities disrupt the cells and leads to lysosomal exocytosis thereby releasing amastigotes to infect nearby macrophages [15]. This cycle reinitiates when other sandfly is infected during the feeding process [1]. Figure 4 contains a summary of the *Leishmania* spp. developmental cycle in both hosts.

This challenge of being exposed to different environments and extreme osmolarity changes, adds to the complexities of the parasites' survival mechanisms [16].

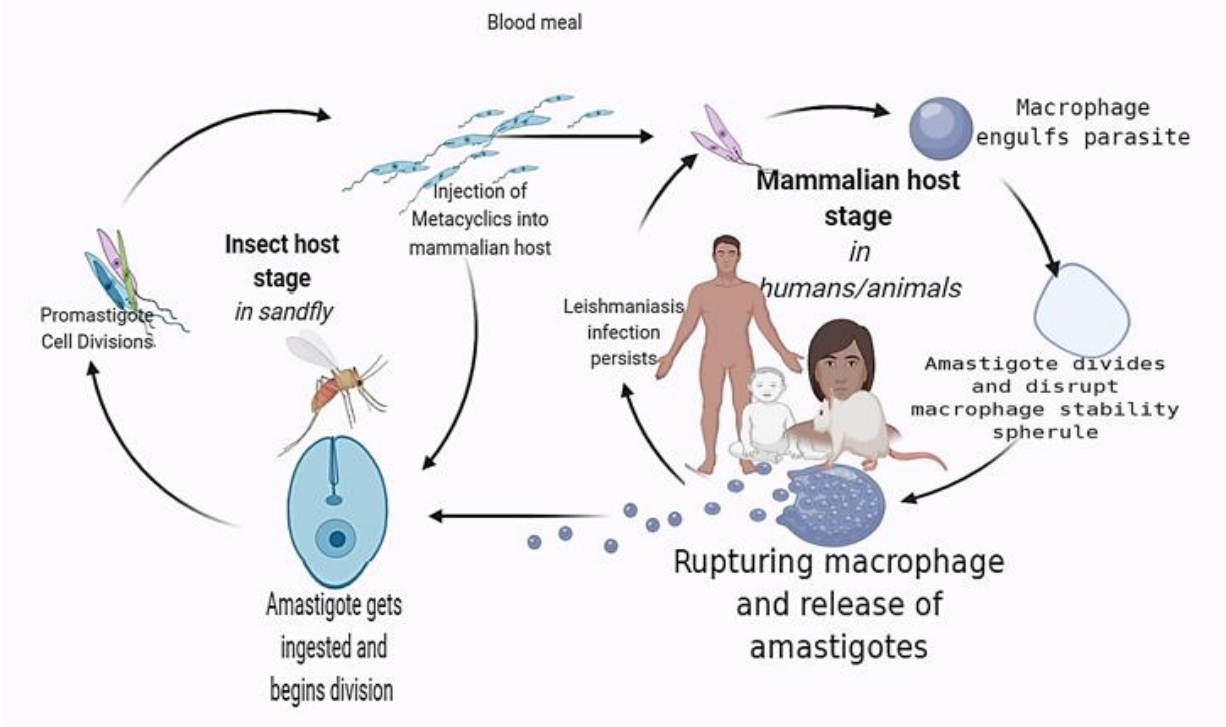

Figure 4. Life cycle of the *Leishmania* parasite. The parasite lives inside of the mammalian host as an amastigote and spreads by disrupting the macrophages to infect others. During the blood meal of the insect host on a mammalian host, the amastigote form is picked up and then undergoes several transitions inside of the invertebrate insect to become a promastigote. These two different environments stress the parasite and have mechanisms that threaten their survival. Image was designed with tools from Biorender.

1.2.1 The Cell morphology and link to pathogenicity

The changes that take place inside the macrophage where the highly infective metacyclic promastigote transitions into an amastigote, leads to a reduction in the cell surface to volume ratio and a reduction in the length of the once protruding flagellum [4]. Among the other trypanosomes, *Leishmania* seems to be the only parasite that conserves its flagellum after changing states or environments [4]. This ostensibly suggests a level of relevance of this structure to the parasite. Host-parasite interaction, morphogenesis, virulence, cell division and mitochondrial DNA segregation are some of the few importance ascribed to the flagellum, whose motility is linked to the paraflagellar rod [4,15].

Another key important feature of these parasites that distinguishes them from most other eukaryotes is the possession of kinetoplast DNA which exist as catenated minicircles and maxicircles; with the minicircles being highly abundant in the 100s as compared to a dozen of maxicircles [3]. During parasite morphogenesis in the insect host, the flagellar pocket, which serves as the major interface for the parasite and the host, also undergoes changes. This change helps prevent the acidic and protease-rich parasitophorous vacuole to attack the susceptible regions of the parasite [4]. This phenomenon of parasite defence mechanism may explain why the trypanolytic factor in the parasitophorous vacuole is unable to act against amastigotes but immobilizes metacyclics [4,15,17].

The adaptation of the parasite to its host is quite interesting. Amastigotes have been found to exhibit slower growth than promastigotes. This seems to be an adaptation to not exceedingly overwhelm the host immune mechanisms so the host can survive for a longer time and thus, increases the chances of transmission [15].

Consequently, cell morphology has been ruled out as a major contributor to the spectrum of diseases observed, but it is without a doubt a key influencer on cell survival [4]. There are about 5 developmental morphologies under which the *Leishmania* parasite can be described. Procyclic promastigotes is the stage within the blood-meal, the parasite has a basal length between 6.5 to 11.5 μm and has a shorter flagellum than the cell body length [15]. Nectomonad promastigote arise from procyclic forms and has a basal length of about 12 μm [1]. During the migration within the midgut of the insect, Nectomonads transform into Leptomonad promastigote with a body length of 6.5-11 μm and, unlike the procyclic stage, the flagellum length exceeds the cell body [1,4]. Leptomonads give rise to metacyclic promastigotes which is considered to be the most infective stage. Metacyclics have a body length less than 8 μm but a very long flagellum [1,2,4]. Another form that

has been described but debated is the Haptomonads. This stage of the parasite has been described as probably slow dividing or aberrant cells [15].

Promastigotes half their cell length during cell division or population doubling such that different daughter cells result from the division; one maintains the old structures/morphology while the other takes a new shorter flagellum [1,4].

1.3 Telomeres, End replication problem and Hayflick limit

Telomeres are ribonucleoprotein structures found mostly at the ends of eukaryotic chromosomes as hexameric nucleotide repeats [18]. It was first discovered in the protozoan, *Tetrahymena thermophilia* ribosomal DNA (rDNA) as a short tandemly repeated sequence and later found to be present at the chromosome ends of other organisms [19,21–23]. Telomere sequence is usually rich in guanine, (i.e., human telomeric repeat 5'-TTAGGG-3') with slight variations in sequence and length among organisms [19]. Telomeres are an essential part of most eukaryotic chromosomes and crucial to genome stability and the survival of most eukaryotic organisms [18].

In normal cells that lack telomerase activity, for example, the adult somatic cells, cells undergoing cell division lose segments of their chromosome ends at each round of the cell division. This phenomenon is what was first described by Olovnikov and Watson as the end replication problem (Figure 5). The bidirectional replication in eukaryotes proceeds in a manner where there is the leading strand synthesis and the lagging strand synthesis. The leading strand synthesis, although requiring an RNA primer to initiate synthesis, proceeds uninterrupted in a 5' to 3' direction following the replication fork direction. The lagging-strand synthesis contrastingly requires several RNA primers to initiate each replication due to the inverse directionality to the replication fork relative to the 5'-3' direction of the strand. The RNA primers are removed during replication by an exonuclease and replaced by DNA sequences, resulting in the formation of Okazaki fragments,

which are ligated at the end of the process to give the full strand [19,24]. During the exonuclease activity, the removal of the last primer on the lagging strand results in a terminal gap that cannot be replicated by conventional DNA polymerases because of the lack of a free 3' hydroxyl group (-OH) to which a nucleotide could be added, generating a 3' G-overhang at the terminus of the newly synthesized strand [19,24,25]. In addition, the nucleases Apollo and Exo 1 promote a resection at the leading strand ends generating also a 3' G-overhang [25].

Repetitive rounds of DNA replication without telomere elongation induces progressive telomeres shortening, which continue until the telomeres reach a critical limit, signalling cells to stop dividing [19,24]. When cells get to the point where they are unable to further replicate, they are said to have reached their Hayflick limit; the maximal number of cell divisions a cell is allowed to undergo. From this point on, cells experience increased telomere shortening, lose some cell cycle checkpoints and can enter into replicative senescence, and cell cycle arrest (Figure 7) [19]. Some cells can escape senescence and enter crisis, dying by apoptosis; just a few cells escape crisis and with an unstable genome and short telomeres, reactivate telomere elongation by telomerase (see Topic 1.4) and immortalize. With the aid of other genomic instability effects, such as the expression of anti-apoptotic signals and the inability to repair damaged DNA, and in some specific cases, after virus infection, cells acquire tumorigenic profiles. It is widely known that 85-90% of somatic cancer cells can proliferate indefinitely and maintain short telomeres [25].

As mentioned earlier, protected telomeres evade DNA damage responses (DDR), telomere fusions, and recombination events. They also play a role in chromosome stability and genome integrity. One mechanism utilized by telomeres is the formation of telomere and displacement loops (T-loop and D-loop, respectively), where the 3'-G overhang invades the duplex DNA to form a lariat structure (Figure 6A) [18,26]. The overhang can also be folded in a different conformation to give the G-quadruplex structure (Figure 6B). Here, four guanines associate with each other by

overpowering kinetic barriers to achieve intramolecular folding [19]. G-quadruplexes are held together by the Hoogsteen base pairing rules [27]. These abilities hinge on, among other factors, the six members of the shelterin complex and their functions [26,28–30]. Both t-loops and G-overhangs are maintained by the association of protein complexes and telomeric DNA forming a high order structure that protect telomeres from fusion and degradation [29].

Additionally, adjacent to telomeres are the subtelomeric regions, which in most eukaryotes are transcriptionally active and reported to be sources of the transcription of telomeric repeats containing RNAs (TERRA); long non-coding RNAs involved in the regulation of telomere length by its association with telomeric proteins and formation of telomeric R-loops [19,25].

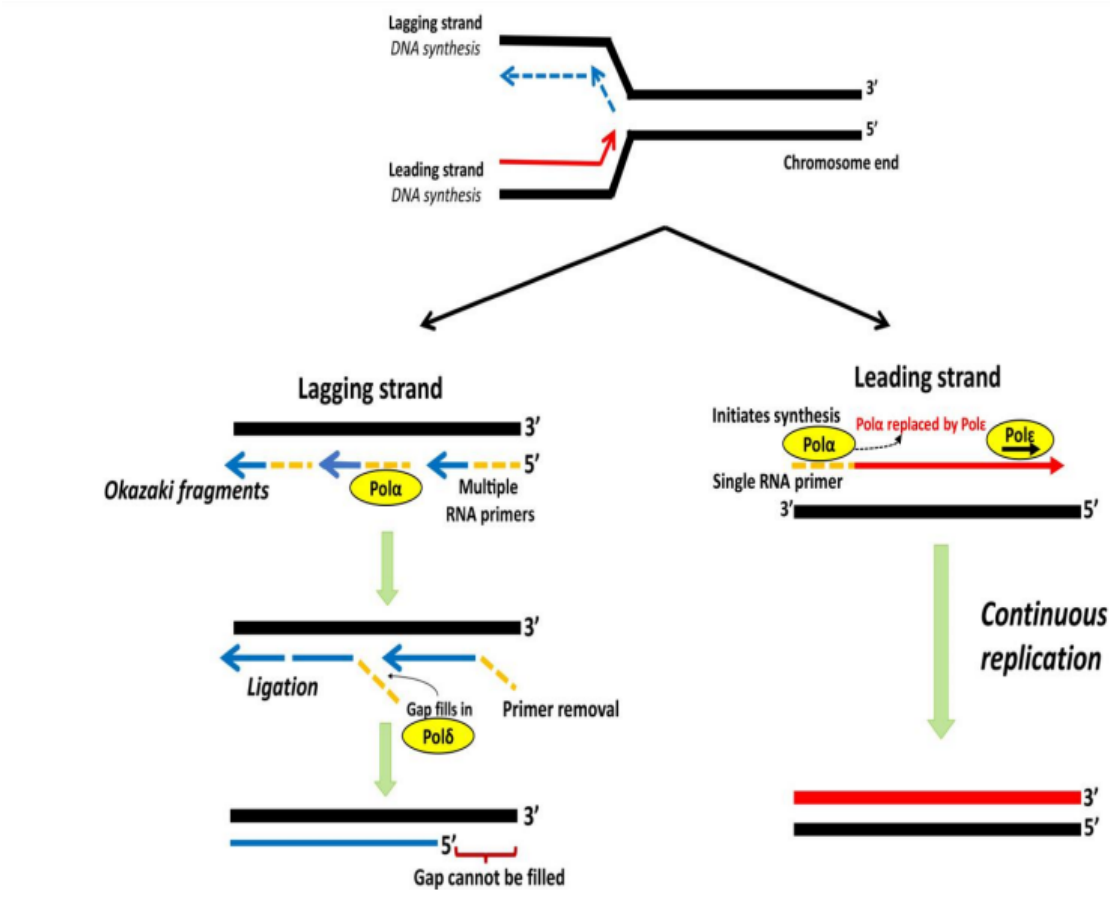

Figure 5. A cartoon of the end replication problem. In semiconservative DNA replication, the leading strand is replicated continuously without any hindrance by the DNA polymerase Polα and Polε after the primase synthesizes the

first RNA primer. There is the synthesis of several RNA primers in replicating the lagging strand, which then get elongated. In both cases the replication proceeds in the 5' to 3' direction. The individual fragments formed from the replication of the lagging strand is termed as Okazaki fragments. Degradation of the RNA primers leaves a gap at the 5' end which remains unfilled and becomes a substrate for the telomerase activity in telomerase positive cells. Image source: [19]

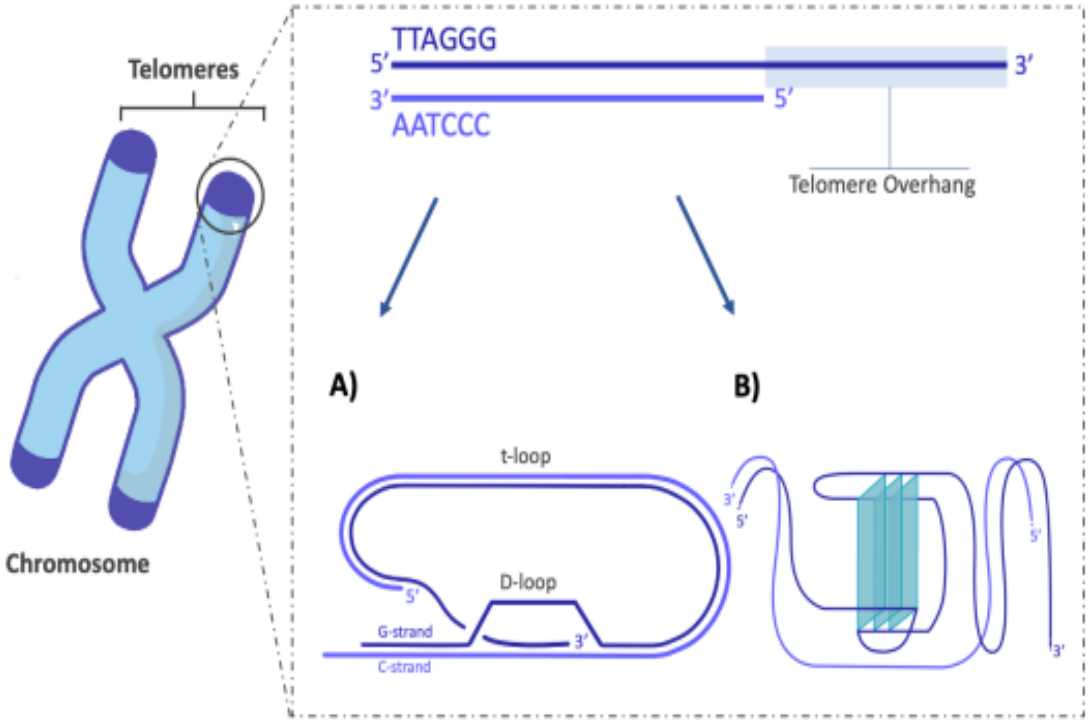

Figure 6. Schematic representation of the 3'-G overhang structural conformations. The formation of T and D loops represented in **(A)**. The folding of the telomere ends on itself and invasion of the duplex DNA results in this conformation. In **(B)** G-quadruplex structure formation from the intramolecular interactions of guanines at the telomeres overhang. These structures function to protect the chromosome end. Source: [25].

1.3.1 The Shelterin complex

The shelterin complex, also sometimes referred to as the telosome, is a sextuple-telomere-specific protein complex, which is constitutively expressed in the cells and collaborates among its member proteins as well as with other factors to regulate the activities of telomerase in the maintenance of telomere length [28,29,31,32].

Telomeric Repeat-binding Factor 1 (TRF1), Telomeric Repeat-binding Factor 2 (TRF2), Adrenocortical dysplasia homolog (ACD) also referred to as TINT1/PTOP/PIP1 (TPP1), Protection of Telomeres 1 (POT1), Repressor/Activator Protein 1 (RAP1), and TRF1 Interacting Nuclear factor 2 (TIN2) are the distinct proteins that constitute the shelterin complex in humans and some other mammalian species [28,33,34].

While telomeres are considered a common denominator of most eukaryotic chromosomes, the shelterin complex itself is not. The shelterin-like complex in certain species has components orthologous to that of the human while others lack the shelterin complex completely [31,32]. The fission yeast, as an example, has orthologues that differ slightly in structure and function from the human shelterin complex but fulfil the core function of ensuring homeostasis at the telomere region [35]. Budding yeast, unlike fission yeast, lack the shelterin complex but possess the RAP1 component which together with Rif1-2 proteins and the telomere-end binding protein CDC13, engages in organizing telomere events in the organism [36].

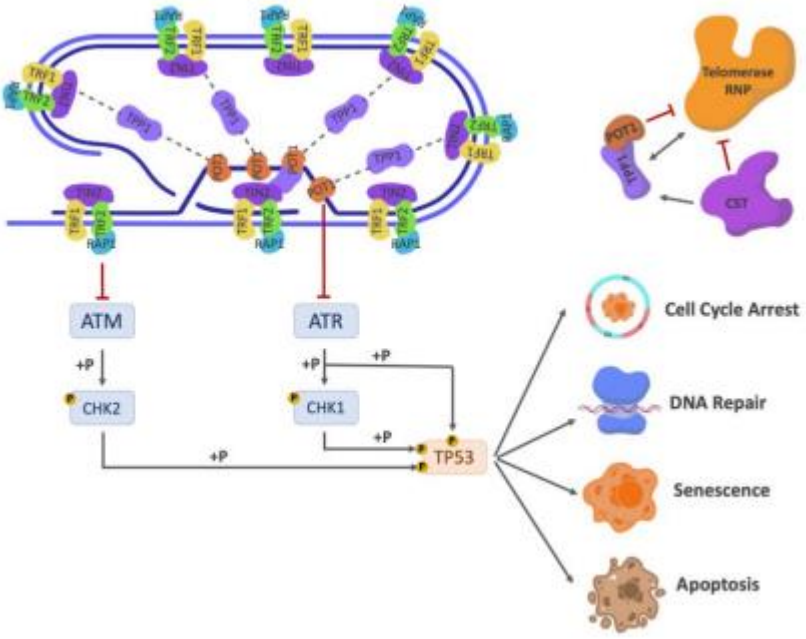

Figure 7. The association of telomeres with the shelterin complex. The shelterin complex is composed of six proteins that act to 'shelter' the telomeres. They act to regulate the length of telomeres and trigger of other cell events. The absence of any of these proteins has consequences on the integrity of the genome. Some cellular events that could be associated with the absence of the shelterin complex include senescence, apoptosis, DNA damage, and cell cycle arrest. The CST complex, made up of the Conserved telomere protection component 1 (CTC1), Suppressor of cdc13a (STN1), and telomeric pathway with STN1 (TEN1), is also depicted here. These proteins, together with the shelterin complex, control events at the telomeres. The CST complex resolves replication forks and can unfold the G-quadruplex conformation. Image Source: [25]

1.3.2 Features of telomeres in *Leishmania* spp.

Leishmania spp. telomeres possess a conserved TTAGGG sequence [37]. Conte, and Cano [37], showed that the telomeres in *Leishmania amazonensis* are polymorphic in nature and suggested it is regulated at the chromosome level. A key characteristic of telomeric regions in trypanosomes is the presence of a modified thymine referred to as Base J (β-D-glucosyl-hydroxymethyl uracil), which is considered an epigenetic marker and an RNA polymerase II transcription terminator. In most *Leishmania* spp. such as *L. major*, 98% of base J is found at the telomeres, which locally inhibits DNA cleavage by frequently cutting restriction enzymes [3]. *Leishmania* spp. chromosome ends also contain at the subtelomeric region, the *Leishmania* conserved telomere associated sequence (LCTAS); the organization of these sites differs between species, but differently from *T.*

brucei and *T. cruzi,* they do not contain sequences of genes encoding virulent antigens, such as the Variant Surface Glycoproteins (VSG) in *T. brucei* [16,38]. In *Leishmania* spp. the subtelomeric regions are part of LCTAS, they harbor a plethora of housekeeping genes which may be functionally relevant to the parasite biology [39].

The LCTAS sequences in *Leishmania* also vary from species to species. In *L. major* and *L. amazonensis*, LCTAS are organized as tandemly repeated sequences of about 100bp repeated two to three times; this is not the case in the multicopy chromosome of *L. braziliensis,* which has been termed as minichromosome telomere associated sequence of about 1.6kb length [37,40]. Also, at the ends of all chromosome sequences comprising the LCTAS are two conserved sequence boxes (CSB1 and CSB2) (Figure 8) intercalated by CCCTAA sequences similar to the structure found in *Saccharomyces cerevisiae* [40]. These sequences vary from chromosome to chromosome in distribution and organization [37].

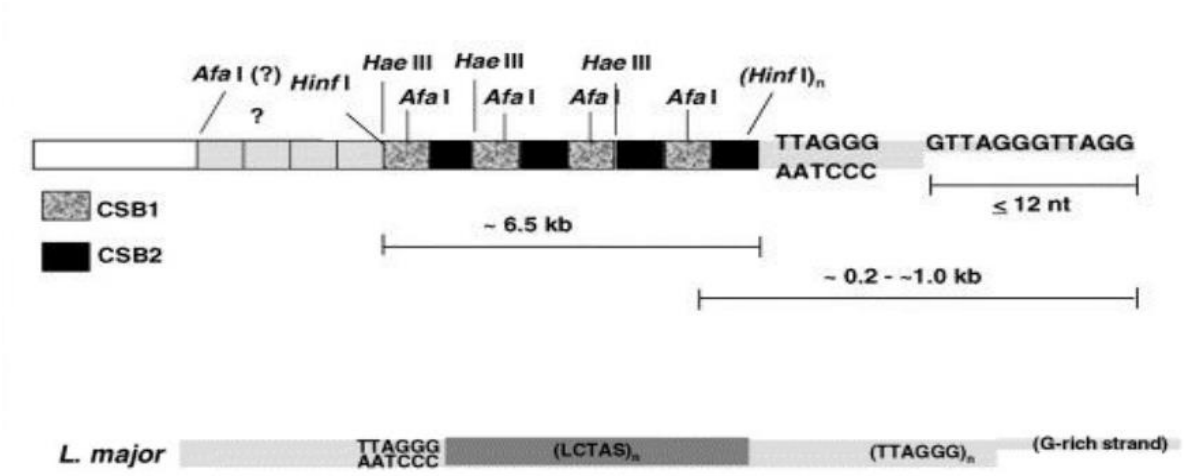

Figure 8. *L. major* and *L. amazonensis* chromosome termini. The organization of chromosome termini in both *Leishmania* species shows the sites for frequent cutting restriction enzymes at LCTAS and intercalating the CSB1 and CSB2. The G-rich overhang is also depicted along with mean nucleotide lengths. The average size of parasites telomeres and LCTAs are shown in kb. Image adapted and modified from [37].

1.4 The telomerase enzyme

Germinative, and embryonic mammalian cells contrary to adult somatic cells, have their telomeres not restricted by a Hayflick limit. This is due to the activity of a ribonucleoprotein enzyme known as telomerase, which can elongate telomeres [23,41–44]. Telomerase is a ribonucleoprotein complex minimally composed by a specialized reverse transcriptase (TERT) and a long non-coding RNA which bears the template sequence copied by TERT at the end of the chromosomes to elongate telomeres [43–45]. The telomerase enzyme is responsible for ensuring proper telomere maintenance using its core subunit, the TERT component, and other accessory proteins [46,47]. Cano et al. [23], and Giardini et al. [48–50]), both reported the existence of telomerase activity and the TERT component in different *Leishmania* species. They showed that the parasite's enzyme is conserved, although there are some genus-specific amino acid substitutions present [48].

The TERT subunit serves as the catalytic subunit of the telomerase enzyme and contains four conserved structural domains: the telomerase essential N-terminal (TEN), telomerase RNA binding domain (TRBD), the reverse transcriptase (RT), and the C-terminal extension (CTE) (Figure 9) [48,51].

The TERT in metazoans has 11 motifs showing moderate variations and high synteny in its TERT sequence with humans. For protozoa, sequence analysis of the key domains between *Leishmania* and humans has inconsistent reports [48,52]. Giardini and colleagues in 2006 reported a finding that suggested that the TERT in *Leishmania* possessed all the canonical domains (TEN, TRBD, RT and CTE) and the 11 motifs, but in a 2017 report by Lai and colleagues, they disagree with this position, citing the number of identical amino acids at the N terminal to be insufficient proof of a GQ motif at the TEN domain in *Leishmania* [48,52]. However, in the Telomerase

Database (https://telomerase.asu.edu/sequences-tert) the GQ motif remains annotated in the *Leishmania* TERT amino acid sequence. The GQ motif is reported to be essential for the telomere maintenance mechanism of the TERT gene and its manipulation can potentially influence cell growth and telomerase activity [41,45]. Nonetheless, a well-established fact about the GQ motif is its absence in *T. brucei*, which may partly explain why the 2005 study by Dreesen and colleagues on parasite's TERT knockdown did not show any impact on cell growth besides the possible existence of alternative compensating mechanism [26,45,52]. The GQ motif is also reported to aid in the multimerization of the telomerase as well as the dissociate activity when bound to the telomerase RNA (TER) [53]. Whilst the RT domain serves the catalytic role of the protein, the TRBD domain facilitates binding with the telomerase RNA [45].

The telomerase RNA, as earlier stated, provides the template sequence for the *de novo* synthesis of telomeric repeats to chromosome termini. Unlike the TERT, the telomerase RNA (TER) seems more divergent, showing no conservation at the sequence level, although some maintain a more conserved secondary structure [45,54,55]. The TER can be described as having a template region used in the synthesis and a non-template region whose function has been linked to the telomerase enzyme activity and seem to be conserved between organisms [54]. The non-template region comprises of the template boundary element (TBE) that associates with the TERT RBD domain, a pseudoknot, and the stem terminus element (STE) [45]. An important and well conserved domain of the TER is the CR4/5 domain, which in flagellates is termed Helix IV [45,56].

The *Leishmania* telomerase RNA component described by our group is one of the largest TERs described; about 2,100 nucleotides in length; being 100 nucleotides shy of the *Plasmodium falciparum* TER and it contains a 12-nucleotide-long template sequence and other structural and functional domains shared with some TER described in ciliates and the *Tb*TER (Vasconcelos et al., 2014). The *Tb*TER, however, has been found to lack a pseudoknot component structure [51]. Figure

10 summarizes the differences and similarities in the TER structure from evolutionarily distant eukaryotes.

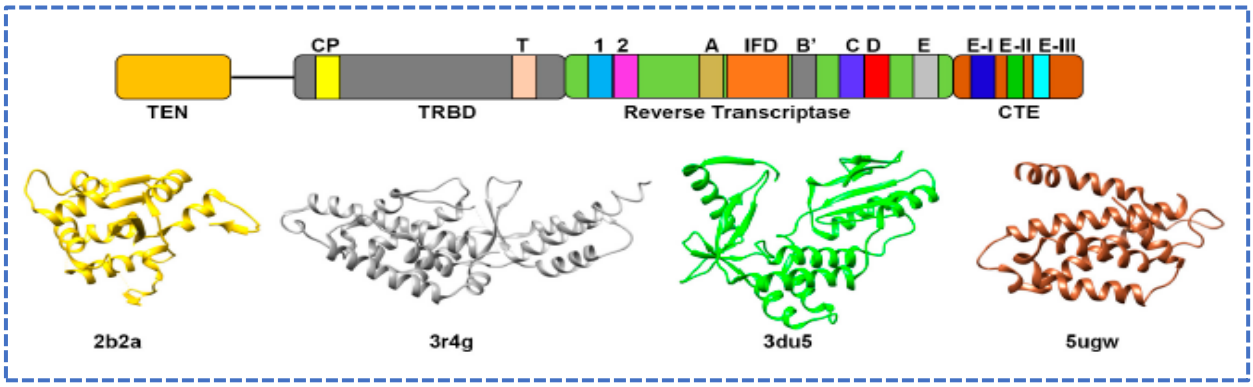

Figure 9. Graphic representation of TERT domains and motifs. The telomerase essential N-terminal (TEN), telomerase RNA binding domain (TRBD), the reverse transcriptase (RT), and the C-terminal extension (CTE) are the protein core domains. The TEN and TRBD domains are connected via a linker. TEN domain (PDB ID: 2b2a) and TRBD domain (PDB ID: 3r4g) from *Tetrahymena thermophila,* RT domain (PDB ID: 3du5) from *Tribolium castaneum* and CTE/thumb domain (PDB ID: 5ugw) from *Homo sapiens*. Image reproduced from [51]

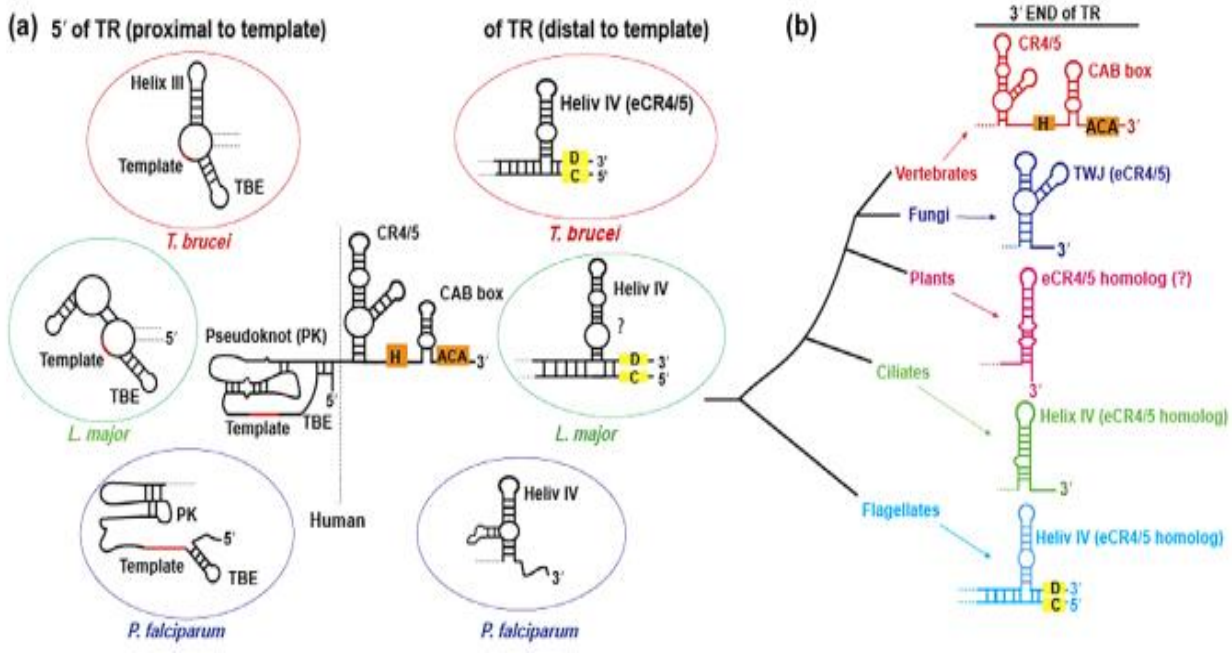

Figure 10. Secondary Structure of Telomerase RNA (TER) in different organisms. Different organisms and their telomere RNA structure. (a) Depiction and comparison of the structure of Human TER to important parasites. The image features the predicted TER structure in *L. major* and *P. falciparum,* and the authenticated TER of *T. brucei.* The template boundary element and the highly conserved Helix IV domain is also represented along with the vertebrate

homologue CR4/5. (b) Cladogram depicting the homology in CR4/5 domain to the Helix IV of the other class of organisms. Image processed from [45].

1.5 Alternative mechanisms in telomere maintenance: ALT pathways

Some cells are able to continue proliferation without telomerase. The phenomenon of cells to survive without telomerase have been elucidated in cancer cells, yeast and trypanosoma [47,57,58]. The ability of these cells to continuously proliferate against the Hayflick limit was traced to the presence of other mechanisms that they utilize in maintaining their telomeres in the absence of the telomerase enzyme activity. These mechanisms are collectively called alternative lengthening of telomeres (ALT) and are independent of telomerase activity although some can coexist with the telomerase without any impact on their activity [59–62]. Cells with ALT show some peculiar characteristics including the display of ALT associated PML bodies (APBs), heterogeneous telomere length, abundant extrachromosomal telomere repeat (ECTR) and telomere sister chromatid exchange (T-SCE) [63,64]. The ALT pathway uses telomeric DNA as a copy template for the replication of other telomeres to elongate them via recombination. In a chromosome orientation fluorescent *in situ* hybridization (CO-FISH) experiment, ALT cells give off more than one signal per chromosome extremity instead of one due to the exchange between telomere and a repeat sequence. Also, in ALT cells one can find telomeres with no detectable signals in the FISH [62]. Londoño-Vallejo et al., [62], found that in the presence of telomerase activity, ALT activity is even higher than in 'solo-ALT' cells and they have all chromosome extremities displaying signals in CO-FISH. ALT cells have high levels of DNA damage proteins at the telomeres due to the uncapping of the telomeres [62,64] Good evidence of ALT is observing extremely long telomeres in the absence of telomerase [59,60].

1.6 Justification: Telomerase as a drug target in *Leishmania*

As stated earlier, leishmaniasis affects millions globally, nevertheless there are no satisfactory remedies, thus the need to find new therapeutics. Knowledge about telomerase involvement in cancer progression and immortalization, its silence in somatic cells, and the dominant negative role of TERT in cancer cells has gained it the reputation as a universal drug target. A number of telomerase inhibitors are under consideration for use as therapeutics against cancer. Many of these drugs are yielding results with promising signs of anti-cancer properties [47].

The knockout of TERT in other eukaryotic cells such as human cells, yeast, and mice has been shown to result in a decline in cell proliferation, telomere shortening, and failure in tissue renewal, besides the replicative senescence and other cell phenotypes [69–72]. Some of these studies further report on the anti-apoptotic role of TERT and the haploinsufficiency of the TERT and TER components when heterozygotes cell lines were generated [70–72]. However, in the study of telomerase-negative cells with excessively long telomeres, researchers found a mechanism that used different route to elongate telomeres; an alternative lengthening of telomeres mechanism (ALT) [64]. The presence of ALT in cancer cells has brought a new challenge for therapeutics that target only the core telomerase pathway. Thus, new methods of abolishing ALT in cancers has been proposed [59,64].

Telomerase activity is highly correlated to the roles of the TERT in conjunction with other accessory proteins of the ribonucleoprotein complex such as the chaperone HSP90 [66]. In humans, HSP90 acts as a chaperone for the proper conformation and activity of telomerase [45]. In a recent report from our group on *L. amazonensis,* inhibition of *L*HSP90 resulted in cells presenting telomere shortening, inhibition of telomerase activity and growth defects, strongly suggesting that the TERT in *Leishmania* shares some similar function with other organisms [67].

There is little data on the function of telomerase in *Leishmania* biology. But Campelo and colleagues [68], showed that in the presence of hydrogen peroxide, LmTERT was found to be redistributed among cellular components outside the *L. major* nucleus. The authors argued that this observation points to the possible roles of the parasite's TERT beyond its canonical function in telomere maintenance. They also showed that the overexpression of the LmTERT increased parasite growth rate and protected cells from oxidative stress [68]. Together, these results point to the relevance of TERT in telomere synthesis and parasite biology.

Dreesen and colleagues showed dissenting data in cell proliferation and phenotype in TERT knockout strains of *T. brucei* [26] . The authors reported no significant effect on cell viability after several months of culture, *e*ven though their result on the impact on telomere length corroborates with telomere shortening reported in other studies [26]. They observed the average rate of telomere shortening in their cells to be about 4.5 bp per population doubling. They also found the telomeric regions harbouring VSG sites to shorten in the absence of the TERT gene. Dreesen and co-authors conclude by raising questions on the usefulness of the TERT as a drug target due to the slow rate of telomere shortening and non-retardation in growth after several months of cultivation [26]. Despite, the results obtained by Dreesen and colleagues, we find the evidence by other studies of therapeutic value of telomerase in *Leishmania* to be convincing [68].

To this end, my thesis work focused on understanding the functional roles of TERT in *Leishmania major*, and to provide insights on its usefulness as a drug target against leishmaniasis.

2. Objectives

2.1 Main objective

The main objective is to perform functional studies on the TERT component of *Leishmania major* telomerase, using three different methodologies: treatment with BIBR1532 specific inhibitor of telomerase, knockout by gene replacement of the TERT component, using CRISPR-Cas9, and overexpression of the TERT gene.

2.2 Specific Objectives

After these perturbations, we specifically aimed to:

1) Evaluate the cell proliferation of promastigote forms of *L. major* using growth curves

2) Analyse the cell cycle profile of promastigote forms

3) To test the ability of promastigotes to transform into metacyclic forms

4) Perform *in vitro* test of telomerase activity

5) Assess changes in telomere length

6) Evaluate cell death induction

7) Assess the alterations in cell and organelle morphology

8) Assess DNA damage signalling

9) Estimate the infective potential on macrophage cultures and Balb/c mice.

3. Materials, Methods, Results, and Discussion : Introduction to the chapters

This section is organised into two chapters. Each chapter is presented in the format of independent scientific articles that touch on the main objective of the thesis. Based on this, each chapter has its own short introduction, succinct materials and methods, discussion and references.

Chapter 1: **Ablation of telomerase reverse transcriptase in *Leishmania major* results in a senescent-like phenotype and loss of infectivity.** This chapter deals with the deletion of the TERT in *Leishmania major* using a well-established CRISPR-Cas9 system for trypanosomatids. It goes on to evaluate the various effects of the absence of TERT on the parasite biology and highlights the possibility of the TERT gene as a useful drug target. The information presented in this chapter is already published as a preprint under the doi: https://doi.org/10.1101/2023.11.10.566596 and submitted for peer-review, and publication in traditional journal.

Chapter 2: **A brief report on the consequences of BIBR1532 inhibition of telomerase in *Leishmania major*.** This chapter section predominantly discusses preliminary results from the inhibition of telomerase using a small molecule (BIBR1532) specific for telomerase inhibition. This work is still ongoing in the lab.

3.1 Chapter 1

Ablation of telomerase reverse transcriptase in *Leishmania major* results in a senescent-like phenotype and loss of infectivity

Mark Ewusi Shiburah[1,2], Beatriz Cristina Dias de Oliveira[1], Habtye Bisetegn[1], Débora Andrade Silva[1], Luiz Henrique de Castro Assis[1], Rubem Menna Barreto[3], Marcos Meuser Batista[3], Maria de Nazaré Correia Soeiro[3], Benedito D. Menozzi[4], Helio Langoni[4], Juliana Ide Aoki[5], Adriano Capellazzo Coelho[5], Maria Isabel N. Cano[1,*]

[1] Department of Chemical and Biological Sciences, Institute of Biological Sciences, UNESP, Botucatu, Sao Paulo, Brazil
[2] Animal Research Institute, Council for Scientific and Industrial Research (CSIR-ARI), Accra, Ghana
[3] Laboratório de Biologia Celular do Instituto Oswaldo Cruz, Fiocruz, Manguinhos, Rio de Janeiro, Brazil
[4] Department of Animal Production and Preventive Veterinary Medicine, UNESP, Botucatu, Sao Paulo, Brazil
[5] Department of Animal Biology, Institute of Biology, UNICAMP, Campinas, Sao Paulo, Brazil

[*] Corresponding author
Email: maria.in.cano@unesp.br (M.I.N.C)

Abstract

The lack of efficient human vaccines and effective nontoxic drugs for leishmaniasis necessitates a search for new therapeutic targets. The telomere environment could provide potential targets against leishmaniasis. TERT, the telomerase reverse transcriptase component, has been on the radar for new therapeutic options against several diseases for more than two decades. In this study, we constructed a full deletion (*Lm*TERT-/-) and an ORF disruption (*Lm*N420) of the gene encoding the TERT component of *Leishmania major*. *Lm*TERT-/- and *Lm*N420 parasites showed replicative and proliferative defects, growth impairment, cell cycle alterations, increased DNA damage, and progressive telomere shortening. Blockage of parasite altruism and the presence of autophagosomes characteristic of a senescent-like phenotype were also detected. *Lm*TERT-/- and *Lm*N420 parasites caused either micro lesion development or no visible lesions in mouse footpads and reduced infectivity in macrophages. While our checks to see if telomere erosion had reached the *SCG* genes involved in lipophosphoglycan modification showed no changes, our proteomic assessment revealed a downregulation of a metacyclic-associated protein. Complementation of the knockout lineages using the WT *Lm*TERT restored some of the lost phenotypes. Therefore, we speculate that the pleiotropic effects of the loss of *Lm*TERT advance the case for using it as a drug target against the parasite.

Keywords: *Leishmania* spp.; DNA replication; *TERT* knockout; growth impairment; cell cycle arrest; DNA damage; telomere shortening; autophagy; loss of infectivity; senescence

Author Summary

Leishmaniasis affects several impoverished communities, but there are no effective drugs for treatment. The ones that exist are too expensive for the demographic affected. We decided to study a protein component (*Lm*TERT) that maintains the integrity of most eukaryotic genomes. We tried to understand how the absence of this protein in *Leishmania* affects the parasite. We found that *Lm*TERT absence causes DNA damage and telomere shortening. Also, we found the depletion of *Lm*TERT promotes proliferative and other defects reminiscent of senescence. We further showed that inactivating *Lm*TERT abolishes parasite altruism and infectivity while causing protein deregulation. Our study provides insights into how useful TERT is to the parasite and can serve as a possible target for drug design.

Introduction

Over a million new cases of leishmaniasis are reported annually across 98 territories and countries [1–4]. New therapeutics are crucial due to the absence of licensed vaccines and the inefficiency of currently available disease control and treatment methods [5–8]. The search for an alternative therapeutic strategy in treating leishmaniasis is thus a matter of global public health concern [1,5,9,10].

Telomeres are essential to most eukaryotic chromosomes, including *Leishmania* spp., and are crucial to genome stability and survival [11–16]. A proper understanding of the mechanisms and roles of telomeres in parasite survival would provide answers in the search for new and parasite-specific drug targets [17–20]. *Leishmania* spp. telomeres comprise the conserved tandem 'TTAGGG' sequence elongated by telomerase [21–23]. The telomerase component of *Leishmania* is mainly composed of telomerase RNA (TER) and telomerase reverse transcriptase (TERT) [24–29]. *Leishmania* TERT conserves all the canonical structural and functional domains found in most TERT but presents amino acid substitutions specific to the genus [24,26,30–33]. An active TERT adds new telomeric repeats to the chromosome ends. This activity of TERT helps to prevent the incidence of genomic instability, apoptosis, and cell senescence, among many other cell defects due to TERT inactivity [27,34–38].

In this study, we set out to inactivate the TERT in *Leishmania major,* a causative agent of tegumentary leishmaniasis, and assess the impact of this manipulation on the parasite's biology. We generated two distinct TERT mutants, one bearing the full knockout of both *TERT* alleles (denoted *Lm*TERT-/-*)* and the other, an endogenous deletion of portions of the open reading frame (ORF) of the *TERT* alleles (denoted *Lm*N420). We generated both mutants using the CRISPR-Cas9 approach outlined by Beneke and colleagues [39]. The results presented here undoubtedly show

that TERT ablation significantly influenced several biological processes in the parasite, including cell proliferation, telomere shortening, blockage of parasite altruism, and autophagy, leading to a senescence-like phenotype and loss of *in vivo* and *in vitro* infectivity capacity [40,41]. We assessed whether progressive telomere shortening would affect the telomeric copies of *SCG* genes involved in lipophosphoglycan modifications [42,43]. However, our preliminary results showed that most of the *SCG* genes were unaffected. Interestingly, we found differential expression in proteins, including downregulation of a META domain protein. Together, our results advance the case for using *Lm*TERT as a therapeutic target.

Results

Deletion of whole and parts of *LmTERT* is deleterious to *Leishmania major*

Given the role of TERT in other eukaryotes and the recommended checklist for essential genes provided by Wang and colleagues [44], we hypothesized that deleting the entire *TERT* gene may lead to the immediate death of the parasite. Hence, the strategy was to attempt a complete and partial deletion of the *L. major TERT* gene using the CRISPR–Cas9 knockout system (S1 and S2 Figs) [39,45,46]. We used the *Lm*007 lineage (S1A-S1C Figs) to generate both knockout lineages (S2A Fig). In both deletion strategies, we selected different clones and expanded them into clonal-population lineages. We phenotypically studied the different clonal lineages and chose one of each to continue the experiments since they showed similar growth and telomere length profiles. Successful *Lm*TERT deletion was confirmed using PCR, Southern blotting, and Sanger sequencing (S2B-S2C Figs).

We checked for phenotypic changes and found that the depletion of *Lm*TERT induced growth defects in the parasite. Compared to the control (*Lm*007), *Lm*TERT-/- and *Lm*N420 promastigotes at passages 7 and 20 showed lower cell density in the logarithmic and early stationary growth phase. This growth defect was particularly evident in the delayed time for the knockout parasites to reach the stationary growth phase (Fig 1A). The growth defect was permanent even after 20 passages. Between passages 7 and 20, the parasites showed a consistent and significant difference in growth on days 2, 3, and 4 (Fig 1A). We further evaluated the proliferative capacity of the parasites by incubating log-phase parasite cultures with EdU (5-ethynyl-2'-deoxyuridine). After EdU labelling, most knockout lineages were identified as not committed to replication (Fig 1B, right panel). Under

50% of *Lm*TERT-/- and *Lm*N420 promastigotes at passages 7 and 20 were proliferating after EdU incorporation, against approximately 80% of proliferating cells in the control, *Lm*007 (Fig 1B, left panel).

Considering the importance of the surveillance system in cell growth [20,47–49], it was necessary to see how much of an influence the ablation of *Lm*TERT has on the cell-cycle progression of the parasites, which may also explain the observed growth and replication impairments. We processed promastigote forms with propidium iodide. Data obtained on the DNA content at the log and stationary phases (Fig 1C) revealed changes in the cell cycle progression pattern of knockout lines compared to the control. Knockout cells (*Lm*N420 and *Lm*TERT-/-) showed measurable delays or transient arrest in the G0/G1 phase at the log phase (Fig 1C). At both P7 and P20, a high number of knockout parasites, *Lm*N420 (50.88% and 58.05%) and *Lm*TERT-/- (48.06% and 52.26%), were recorded at the log G0/G1 phase versus *Lm*007 (44.87% and 53.91%) (Fig 1C, Panel 1). In contrast, lower percentages of cells were recorded for the knockout lineages at the log G2/M phase, *Lm*N420 (20.50% and 20.22%) and *Lm*TERT-/- (23.18% and 17.75%) against *Lm*007 (27.03% and 20.22%) (Fig 1C, Panel 2). These data suggest an interruption in the cell cycle progression of the knockout parasites and a possible defective transitioning system that could impact parasite development [48].

In the absence of TERT, we expected an increase in DNA damage. This theory was founded on the observed telomere attrition (see Fig 4) and the detected delays in cell cycle progression (Fig 1C). At the log phase of growth, the parasites generally had low DNA damage signals averaging 4.5% for *Lm*007, 0.2% for *Lm*N420, and 3.5% for *Lm*TERT-/-. At the stationary growth phase, this increased drastically to about 38.16% and 36.24% for the TERT-depleted parasites (*Lm*N420 and *Lm*TERT-/-, respectively) compared to an average of 22.48% for *Lm*007 (Fig 1D). Here, we

establish an association between the observed DNA damage and the recorded delays in cell cycle progression in the knockout lineages.

A

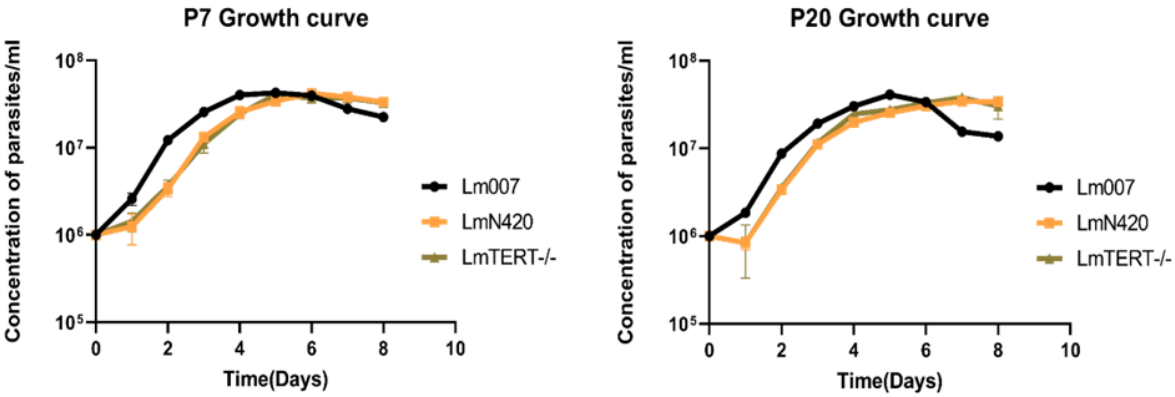
P7 Growth curve
Concentration of parasites/ml
10^8
10^7
10^6
10^5
0
2
4
6
8
10
Time(Days)
Lm007
LmN420
LmTERT-/-
P20 Growth curve
Concentration of parasites/ml
10^8
10^7
10^6
10^5
0
2
4
6
8
10
Time(Days)
Lm007
LmN420
LmTERT-/-

B

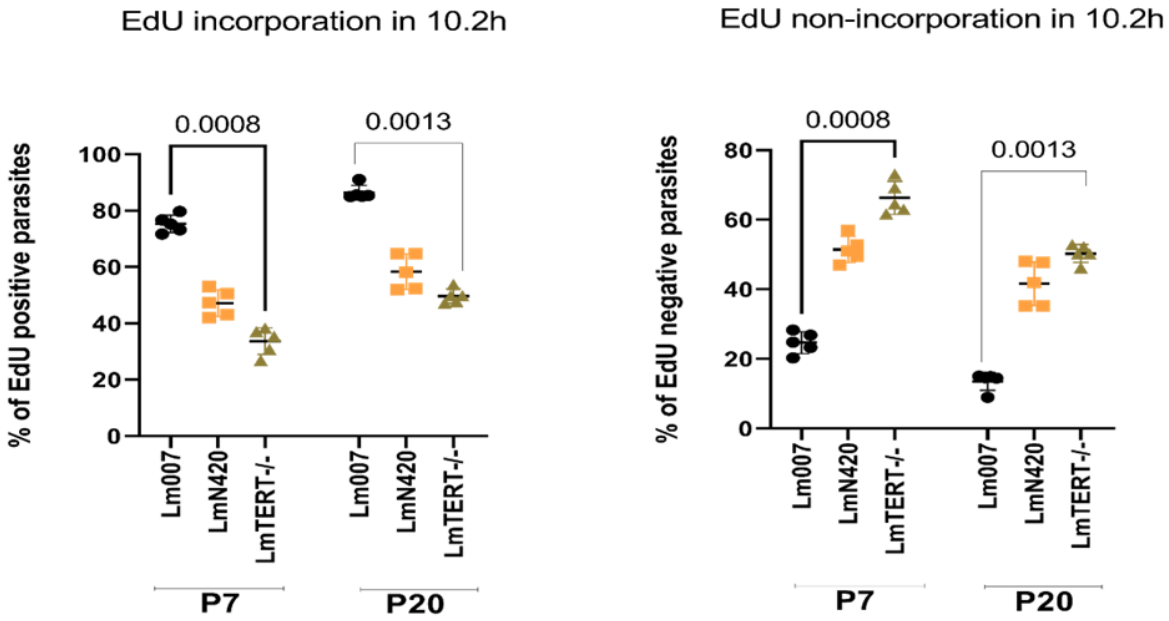
EdU incorporation in 10.2h
% of EdU positive parasites
0.0008
0.0013
100
80
60
40
20
0
Lm007
LmN420
LmTERT-/-
Lm007
LmN420
LmTERT-/-
P7
P20
EdU non-incorporation in 10.2h
% of EdU negative parasites
0.0008
0.0013
80
60
40
20
0
Lm007
LmN420
LmTERT-/-
Lm007
LmN420
LmTERT-/-
P7
P20

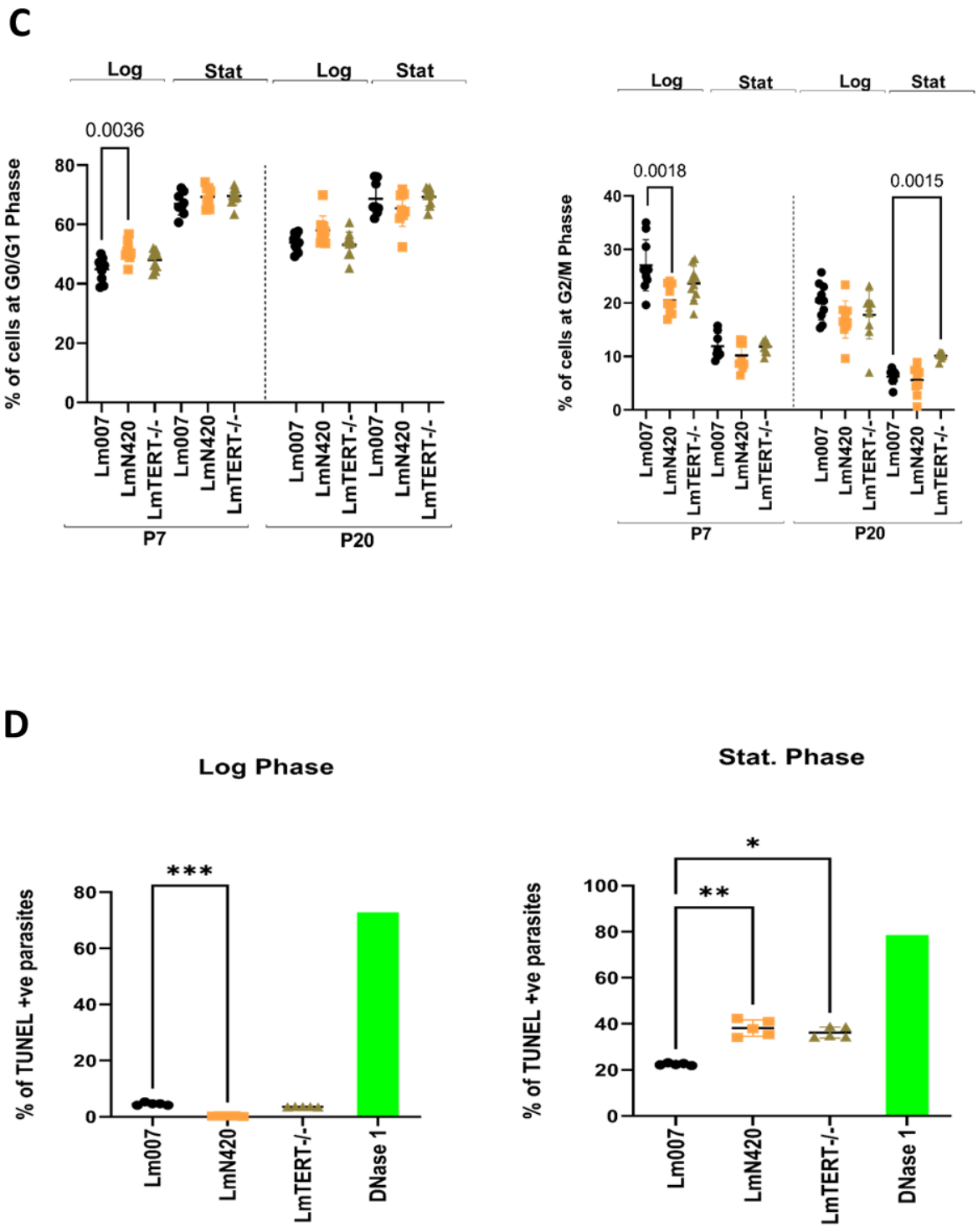

Fig 1. Defective growth, DNA synthesis, and accumulation of DNA damage in TERT-depleted parasites. (A) Growth curves comparing the growth profile of TERT-depleted parasites and *Lm*007 at P7 and P20. The following symbols represent the significant differences between treatments: *, Both edited lines differ from *Lm*007; & only *Lm*N420 is significantly different from *Lm*007; #, only *Lm*TERT-/- is significantly different from *Lm*007. Statistical

analysis was performed using the Mann-Whitney test on the means of three parallel experiments for each treatment group. (B) Parasites' ability to synthesize DNA was represented by their EdU uptake (left panel) and nonresponsive parasites to DNA synthesis (right panel). Kruskal-Wallis test was used as the statistical treatment for five technical replicates from two independent experiments for each group. (C) Graphs from data on parasite challenges in cell cycle progression (D) TUNEL data showing accumulation of DNA damage in parasites after TERT depletion. Data from a single experiment with five technical replicates was used in the Kruskal-Wallis statistical test. All data in this Fig is represented as mean ±SD, and significance was tested at $P \leq 0.05$.

TERT-deficient parasites lacked cell death and had an increased number of stationary phase promastigotes negative for peanut lectin agglutinin (PNA)

One of the clauses given by the Nomenclature Committee on Cell Death (NCCD) in declaring cell death is the compromise in the plasma membrane, which symbolizes a point of no return for such cells [50,51]. We used an Annexin-PI assay to check parasite death by membrane turnover and permeabilization. The control parasites (*Lm*007) showed lower viability records (56.78% and 62%) at P7 and P20, respectively, when compared with *Lm*N420 (94.40% and 95.16%) and *Lm*TERT-/- (91.50% and 94.14%) (Fig 2A). In addition, *Lm*007, in contrast to the TERT-depleted parasites (*Lm*N420 and *Lm*TERT-/-), was nearly tenfold more PI/Annexin-positive, showing an average of 37.72% versus 3.83% and 6.64% in *Lm*N420 and *Lm*TERT-/-, respectively, at P7 (Fig 2B).

We performed a metacyclic selection assay to ascertain the parasites' normal development. We collected parasites grown for up to 7 days at the stationary phase for P7 and P20 and performed PNA agglutination [52]. The results presented in Fig 2C show a surprisingly high number of promastigotes negative for PNA in the knockout lineages. There were differences for *Lm*N420 and *Lm*TERT-/- against *Lm*007, as shown in the left and right panels of Fig 2C, respectively. Additionally, the *Lm*TERT-/- remarkably quadrupled its previous count at P20 and was fourfold higher than *Lm*007 at P20 (Fig 2C, right panel). At the stationary phase, *Leishmania* promastigotes

cultures should have more Annexin-V-positive cells and fewer parasites negative for PNA [53,54]. The unexpectedly low permeability, Annexin-V binding of the knockout parasites at the stationary phase, and the increased number of PNA-negative parasites suggest a modification in the parasites' plasma membranes after TERT ablation.

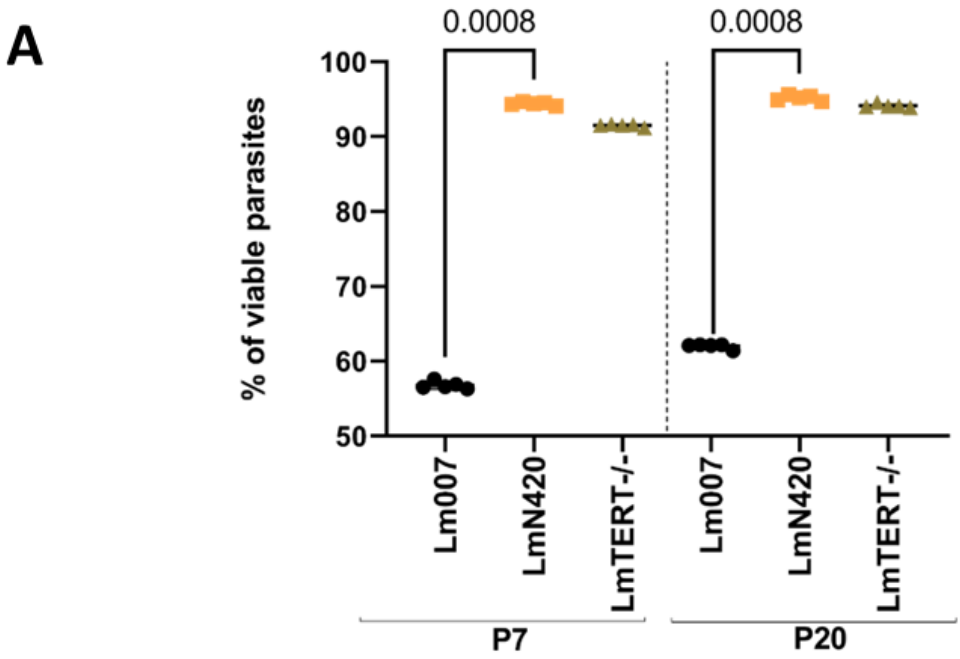

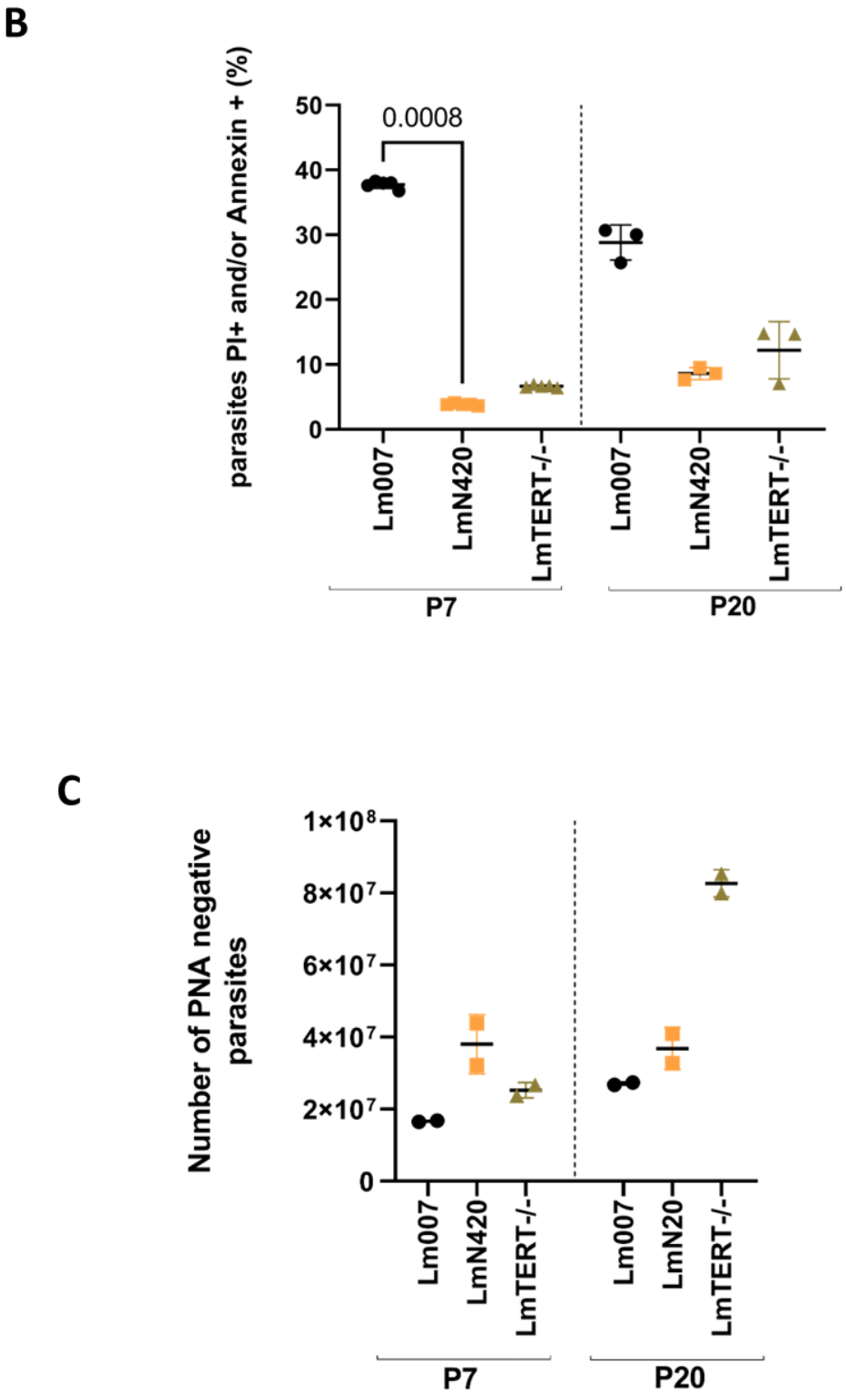

Fig 11. Absence of cell death and increased PNA-negative parasites among the TERT-depleted *L. major* promastigotes. (A) and (B) Parasites at the stationary phase were stained with Annexin-V and propidium iodide to determine viability. (A) The graph represents parasites that are positive for both stains, indicative of no cell death

(quadrant-Q4, Fig. S3C). An FMO control was performed by treating *Leishmania* parasites with only PBS, and no staining procedure was conducted on these parasites to represent an intact membrane. (B) The graph shows the percentages of parasites found in quadrants Q2 and Q3, Fig. S3C. Positive control was performed by treating *Leishmania* parasites with 20% formaldehyde for approximately 10 min to cause membrane turnover before being subjected to a staining procedure. The negative control was parasites with no stain. (C) The graph shows the number of parasites that are negative for lectin agglutination. Kruskal-Wallis test was used in the statistical treatment of graphs presented in this Fig to establish significance at $P \leq 0.05$. Graphs (A) and (B) represent two independent experiments of at least three technical replicates. Graph (C) is representative of two experiments conducted in parallel.

Ultrastructural analysis of *L. major* wild-type promastigotes and TERT-deficient parasites shows senescent-like phenotypes

To check eventual ultrastructural alterations in TERT-depleted promastigotes, wild-type and mutant parasites of different passages *in vitro* (P5 and P20) were processed for scanning and transmission electron microscopy. Our findings demonstrated a lack of morphological alteration when *L. major* promastigotes (with and without TERT deletion) were examined by scanning electron microscopy (SEM). Parasites presented characteristic morphology in all experimental conditions, such as elongated shapes and free flagella. At the same time, round and intermediate forms could also be observed, in addition to dividing promastigotes (Fig 3, SEM panel), showing a heterogeneous population of cells in culture.

Transmission electron microscopy (TEM) evaluated wild-type promastigotes displaying typical organelles, such as the nucleus, mitochondrion, kinetoplast, endoplasmic reticulum, and flagellum (Figs 3A and 3D). In contrast, 100% of the TERT-deficient promastigotes at P5 (Figs. 3B and 3E, TEM panels) and P20 (Figs. 3C and 3F, TEM panels) presented cytosolic vacuolization (V) and the formation of autophagosomes and blebs in the plasma, flagellar and flagellar pocket membranes. Also, mitochondrial insults such as organelle swelling and inner concentric membrane structures characteristic of autophagy were noted (Figs. 3B, 3C, 3E, and 3F, TEM panels). The features observed here, the prolonged delays in cell cycles, and the replication troubles detailed earlier are reminiscent of a cell undergoing senescence [40,41,55,56].

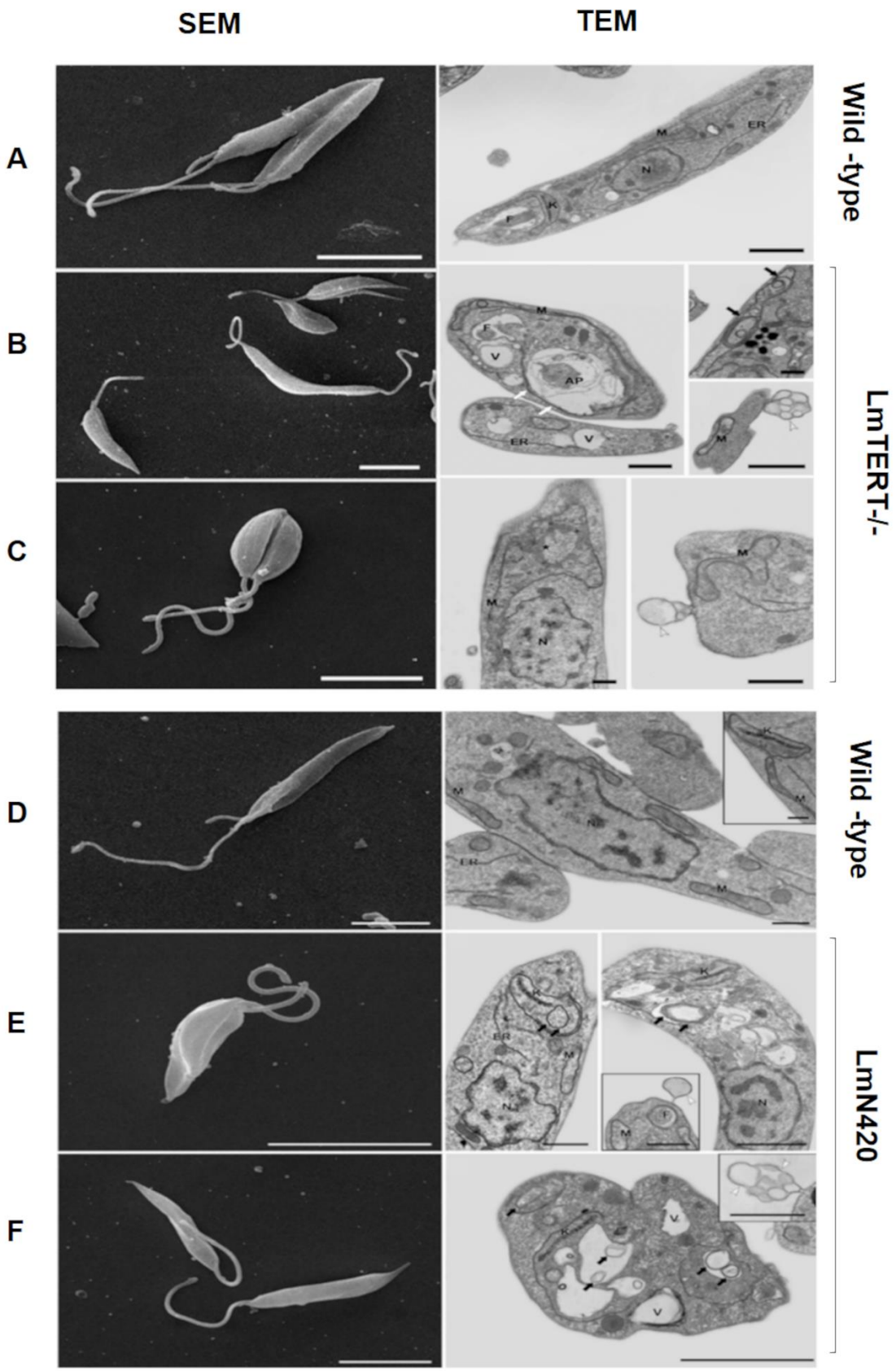
SEM
TEM
A
B
C
D
E
F
Wild -type
LmTERT-/-
Wild -type
LmN420
M
ER
N
K
F
V
AP

Fig 3. TERT-depleted parasites show a senescent-like phenotype. Left panels (A-F), scanning electron microscopy (SEM) (bars = 5 μm) and Right panels (A-FI), transmission electron microscopy (TEM) (bars = 1 μm) of wild-type, LmTERT-/-, LmN420 promastigotes. In the top and bottom panels, the wild-type parasites (A, D) show typical, elongated morphology and normal appearance of organelles, including the nucleus (N), mitochondrion (M), kinetoplast (K), endoplasmic reticulum (ER), and flagellum (F). In the top panel, promastigotes TERT-/- at P5 (B, SEM) and P20 (C, SEM) show classical elongated bodies and flagella. Their analyses by TEM show cytosolic vacuolization (V), formation of autophagosomes (AP), blebs in the flagellum and flagellar pocket (white arrowheads), mitochondrial phenotypes such as organelle swelling (*), and the presence of inner concentric membrane structures (black arrows). In the bottom panel, promastigotes LmN420 showed no morphological alteration by SEM obtained at P5 (C) and P20 (F), with parasites presenting characteristic morphology such as elongated shape and free flagellum. Additionally, round and intermediate forms were observed, in addition to dividing promastigotes. When evaluated by TEM, LmN420 promastigotes at P5 (E, TEM) and P20 (F, TEM) presented cytosolic vacuolization, blebs in the plasma, flagellar and flagellar pocket membranes (white arrowheads), and the presence of concentric membrane structures inside mitochondria (black arrows).

Telomere attrition in TERT-depleted *L. major* promastigotes and recovery after complementation reveals the role of TERT in parasite telomere maintenance

A characteristic feature of most organisms with interrupted TERT activity is a reduction in telomere length [34,41,57]. TERT is responsible for the polymerization of telomeric ends. Its ablation leads to an incomplete telomerase holoenzyme and terminates telomere length maintenance, resulting in continuous attrition of these ends [18,25,58–62]. Whether the TERT in *Leishmania major* has similar roles as in other eukaryotes was evaluated here by Southern telomere restriction fragment (TRF) assessment and Flow-FISH. Telomere attrition was evident in the TERT-depleted parasites at passages 7 and 20 (Figs. 4A and 4B). Proportional changes in telomere length, calculated using arbitrary fluorescence units (a.u.) of molecules of equivalent soluble fluorochrome (MESF) (Table 1), showed an approximately 50% reduction in telomere size after TERT inactivation.

We performed a complementation strategy by introducing an episomal plasmid carrying wild-type TERT back into the respective knockout lineages. We denoted the complementation lineages as NAB and TAB for *Lm*N420 and *Lm*TERT-/-, respectively. The telomere profiles from these

lineages revealed an average increase in telomere size compared to their respective knockouts (Fig 4B, left panel). Approximately 25-30% of the lost telomeres were recovered (Fig 4B, right panel). These data point to the critical role of TERT in maintaining chromosomal termini in these parasites.

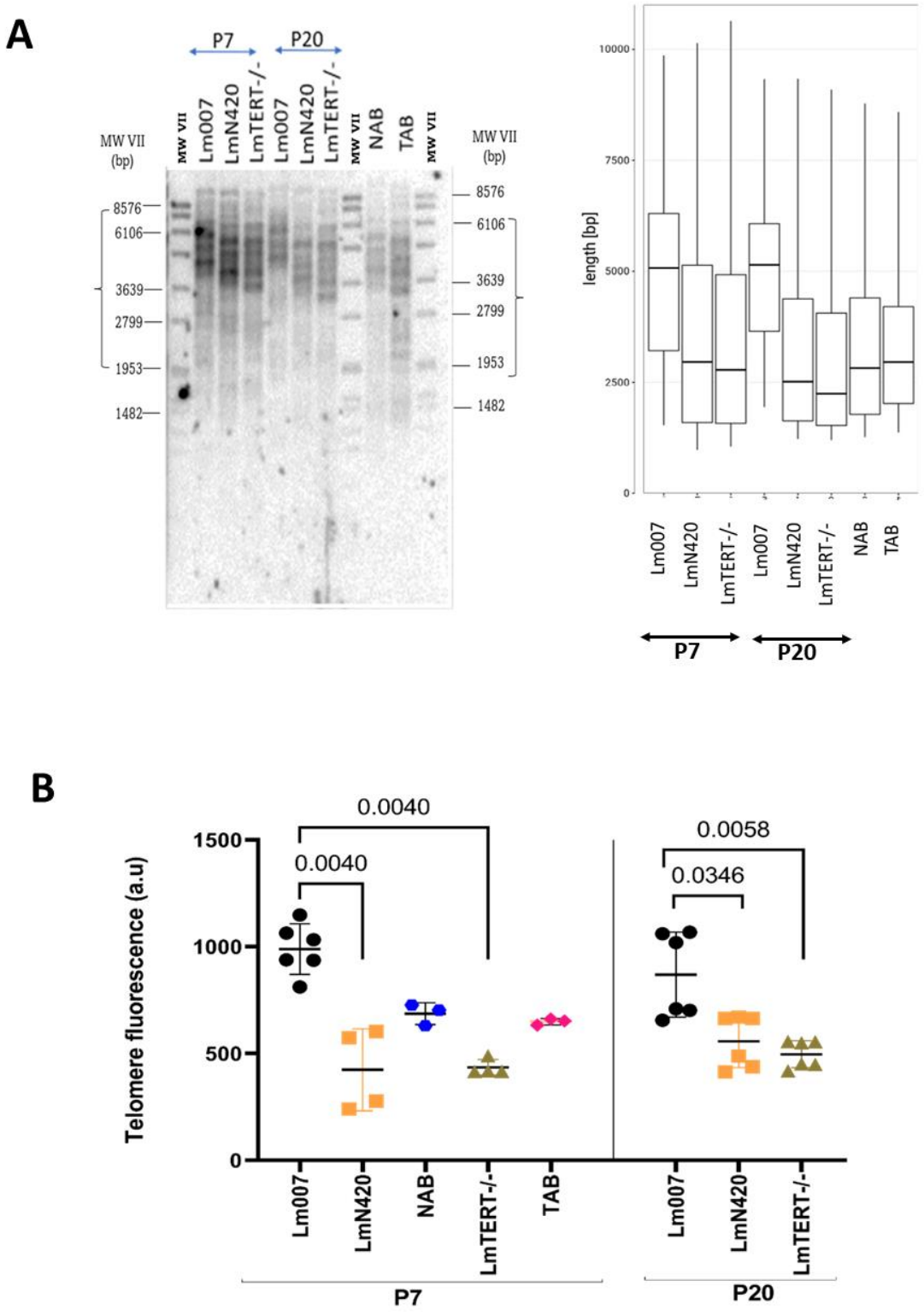

Fig 4. TERT depletion induces telomere attrition in *L. major* promastigotes. The deletion of *Lm*TERT leads to a observable attrition in telomeres. (A) The Southern blot image shows the different groups at passage 7 (left panel),

passage 20 (middle panel), and after complementation with the episomal expression of wild-type TERT (NAB and TAB) in the right panel. A WALTER assessment of the TRF was equally done (B) The fluorescent values were obtained by calculating the MESF for *Lm*007, *Lm*N420, and *Lm*TERT-/-, as well as NAB and TAB at P7 (left panel) and P20 (right panel). Significance was obtained after Kruskal-Wallis test was used as treatment of data obtained from at least three technical replicates of two independent experiments. Graphs are shown with mean ± SD data. P≤0.05.

Table 1 Comparative changes in telomere size

Parasites groups	Mean MESF (a.u)		Proportional change	
	P7	P20	P7	P20
*Lm*007	988.5	868.8	1	1
*Lm*N420	423.8	556.8	0.429	0.641
*Lm*TERT-/-	435.3	496.8	0.440	0.572

TERT-depleted parasites showed reduced or no capacity to infect BALB/c mice models, and bone marrow-derived macrophages from BALB/c

Due to the low Annexin-positive and high number of PNA-negative promastigotes, we questioned the infective capacity of the knockout lineages. We conducted concurrent Annexin-V and *in vivo* infectivity assays (Figs 5A and 5B). An *in vitro* infectivity assay using bone marrow-derived macrophages (BMDMs) from BALB/c mice was also performed at 24 h, 48 h, and 72 h (Figs 5C and 5D). Data from the *in vivo* infection assay showed a significant difference in lesion development between the mice infected with the knockout lineages and the *Lm*007-infected group. All mice in the *Lm*007 treatment group developed their first visible lesion at 50 days post-inoculation. In contrast, mice infected with *Lm*TERT-/- cells had only two out of the three showing

microlesions 61 days post-infection. None of the three mice infected with the *Lm*N420 cells presented any lesion development during data collection (61 days post-inoculation). In addition, one mouse from the *Lm*N420 group was experimentally separated for further monitoring. This mouse showed no visible lesions up to 70 days post-inoculation.

The sizes of the inoculated and non-inoculated footpads were measured using Vernier calipers, and the difference was estimated as the swelling size (Fig 5B, graph). At a mean size of approximately 5 mm, the *Lm*007-infected mouse paw was about twice the size observed in *Lm*TERT-/- and that of *Lm*N420. A mean difference of 1.9 mm and 2.5 mm was observed between *Lm*007 versus *Lm*TERT-/- and *Lm*N420, respectively (Fig 5B, graph). Concurrently, serological tests using indirect immunofluorescence (IIFA) reported a negative presence of infection in mice inoculated with the knockout lineages using different titrations. We only obtained positive signals from the experiment's positive control and the mouse group infected with *Lm*007 (Supplementary Figs 4B and 4C).

In agreement, macrophage infection studies using BMDMs at a parasite-to-macrophage ratio of 10:1 revealed reduced infection in TERT-deficient lineages. At 24 h, the *Lm*007-infected macrophages had less infection compared with the knockout (*Lm*N420 and *Lm*TERT-/-) and complementation lineages (NAB and TAB) (Fig 5C). However, at 48 h, the percentage of macrophages infected with *Lm*007 increased from a mean of 8.357% to 56%. In contrast, the percentage of cells infected with *Lm*N420 declined from 23.47% at 24 h to 13.33% at 48 h. Similarly, infection with *Lm*TERT-/- declined from 27.24% to 7.409%. Complementation lineages, NAB and TAB, progressively increased from 32.18% and 17.33%, respectively, to 57.90% and 19% at 48 h. A continuous increase in the percentage of infected macrophages was recorded for TAB (39%) at 72 h. In comparison, a continuous decline was recorded for the knockout lineages (*Lm*N420 and *Lm*TERT-/-). The decline was observed in the controls *Lm*007 (27.33%) and NAB

(56%) at 72 h, which were nevertheless higher than the knockout lineages. An infectivity index, calculated by finding the product of the mean number of amastigotes per macrophage and the percentage of macrophages infected, also revealed a similar pattern of infection as the percentage of macrophages infected (Fig 5D). These results imply that *Lm*TERT influences the infectivity of *Leishmania major* parasites and their growth inside the host cells.

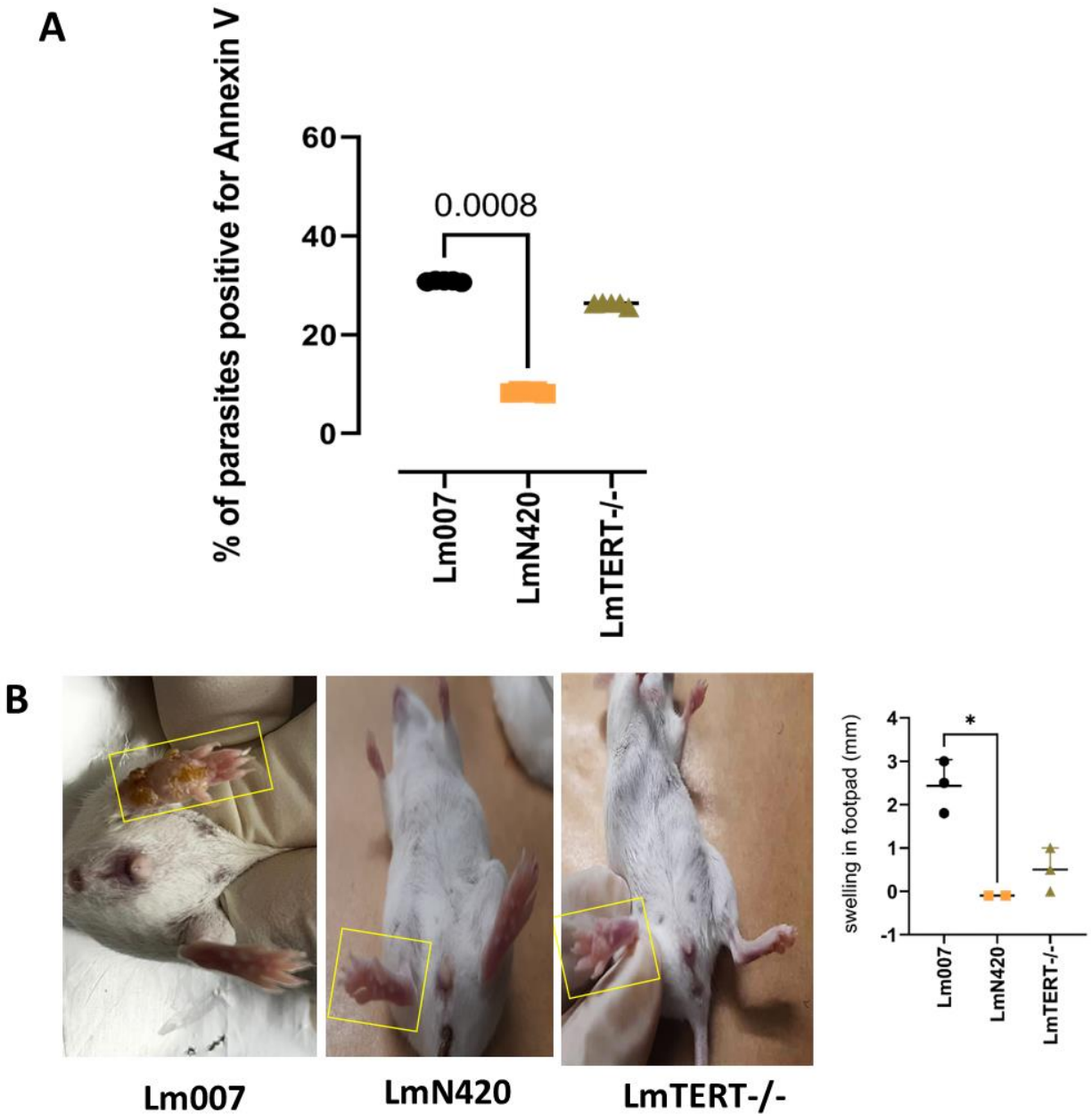
A
% of parasites positive for Annexin V
60
40
20
0
0.0008
Lm007
LmN420
LmTERT-/-
B
Lm007
LmN420
LmTERT-/-
swelling in footpad (mm)
4
3
2
1
0
-1
*
Lm007
LmN420
LmTERT-/-

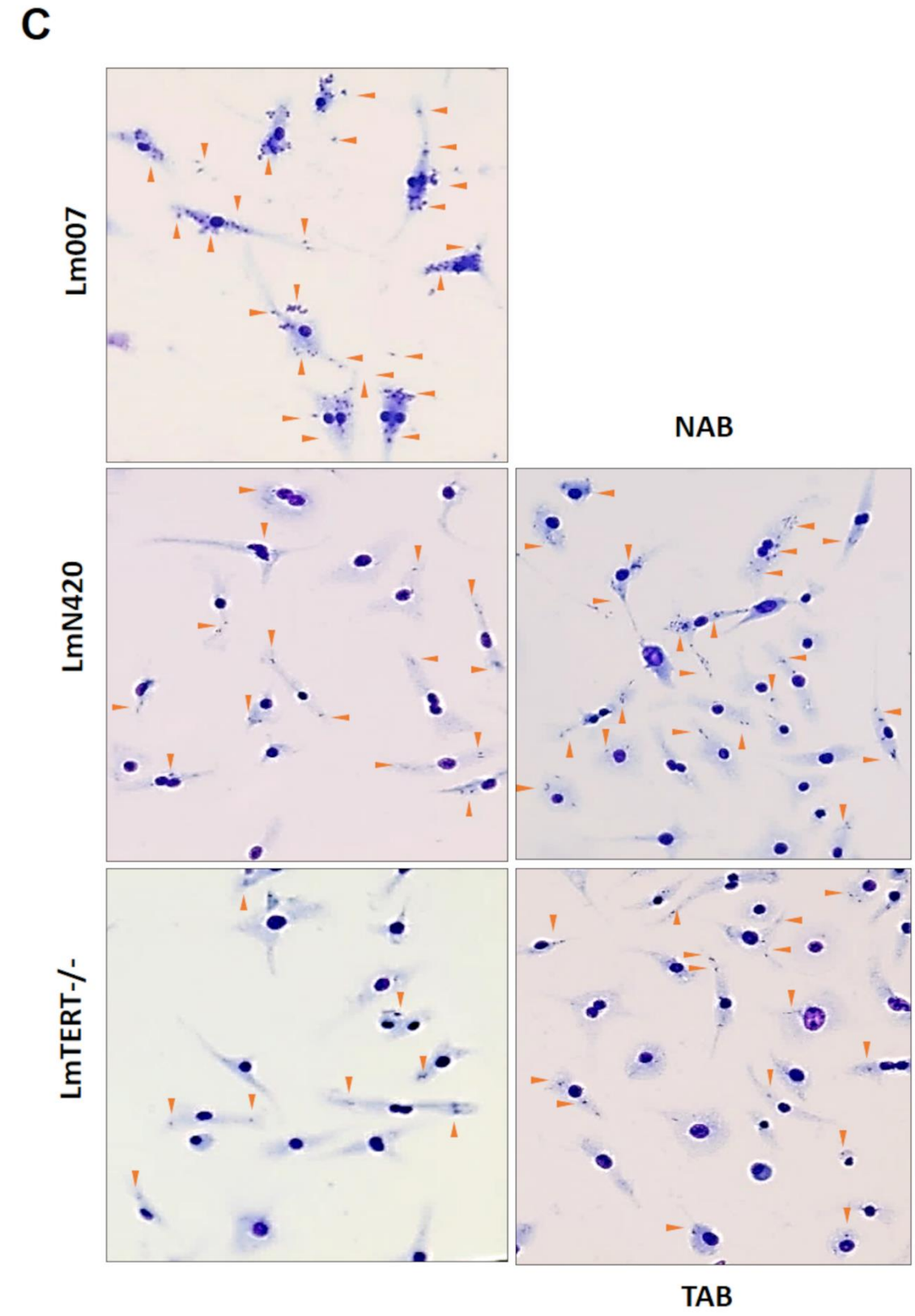
C
Lm007
LmN420
LmTERT-/-
NAB
TAB

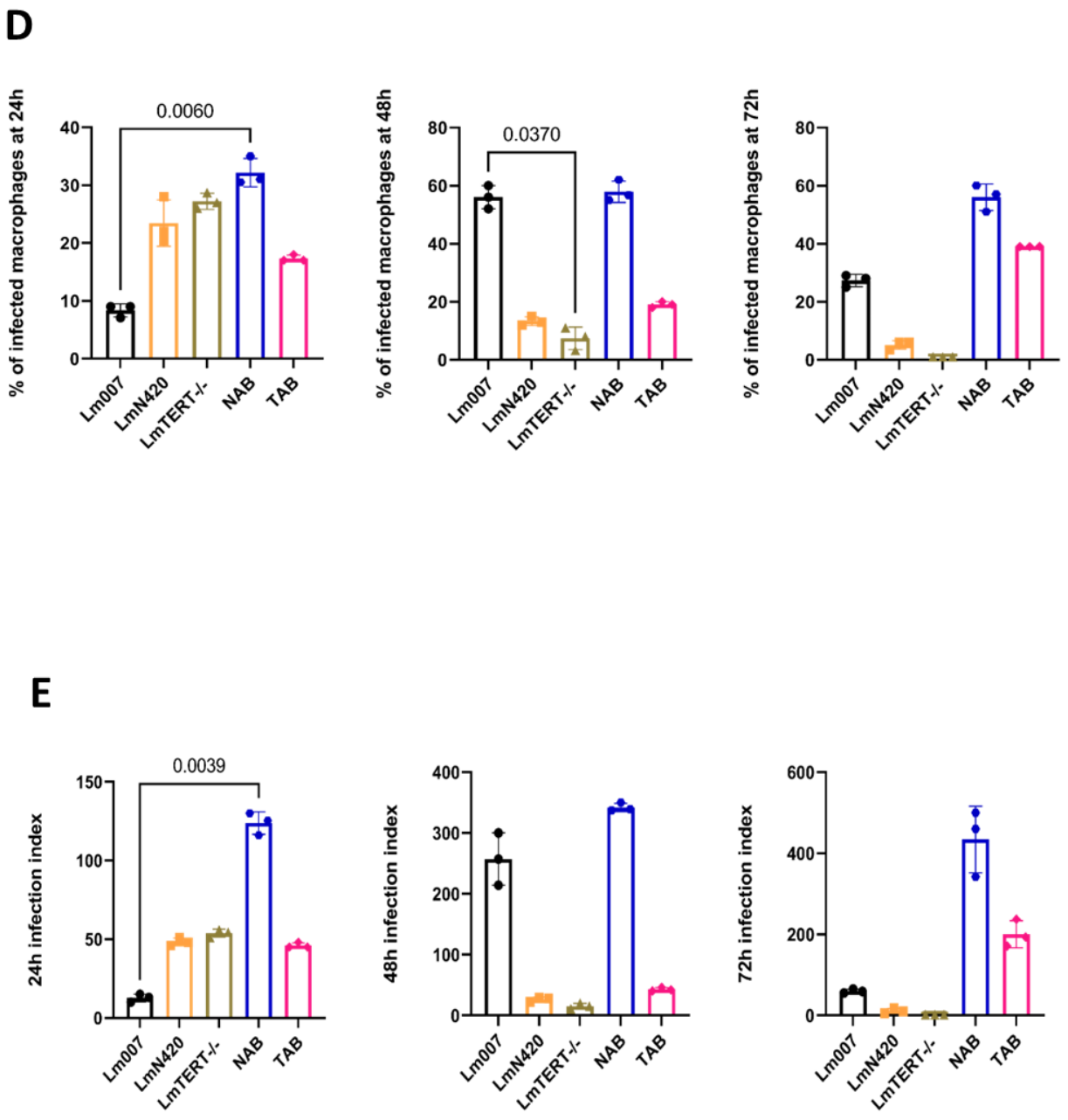

Fig 5. TERT-depleted parasites showed reduced or no capacity to infect BALB/c mouse models and bone marrow macrophages. (A) The graph shows that Annexin assays were conducted concurrently during inoculation using the parasites from the same cultures used in mouse inoculation. Positive control was performed by treating *Leishmania* parasites with 20% formaldehyde for approximately 10 min to cause membrane turnover before taking them through a staining procedure. (B) Lesion size determined after 61 days post-inoculation is represented in the graph. Representative images of mouse footpads infected with *Lm*007, *Lm*N420, and *Lm*TERT-/- are shown from left to right. (C) Images showing some macrophages invaded by amastigotes. Arrows point to the number of amastigotes per macrophage. (D) The graph of macrophage infections performed, including data from complementation parasite infection. (E) This graph shows the infection index and representative images of macrophage infection. Data from approximately 300 macrophages per treatment group (three replicates in parallel) were subjected to Kruskal-Wallis test.

Telomeric scβ-Galactosyltransferases (*SCG* genes) remain undisturbed

Linking the results observed in the telomere attrition, metacyclic selection assay, and the infectivity of parasites, we checked for the telomeric scβ-Galactosyltransferases (*SCG* genes) involved in lipophosphoglycan (LPG) modification in the parasites. We reasoned that the shortening of telomeres may have impacted these genes, resulting in modifications in their roles as LPG modulators [42,43,63]. Due to the high sequence identity (>90%) between the *SCG* genes, we only designed primers for the sets with less similarity. Performing ordinary PCR with specific primers, we confirmed that telomeric erosion had not reached the point of completely eroding some of the genes (S5 Fig).

Mass spectrometry confirms protein deregulation in TERT- depleted parasites

While the *SCG*s amplified were still present, our further analysis of the *Lm*TERT-/- and *Lm*007 proteomes by mass spectrometry showed changes in protein regulation. Differential protein expression analysis revealed 104 proteins (S7 Fig) being significantly upregulated or downregulated. Among the downregulated proteins were the stage-regulated metacyclic proteins (META domain-containing protein) (S7B Fig). META domain proteins are expressed less in the knockout compared to the *Lm*007. The proteomic data suggest that the increased PNA-negative promastigote numbers from the metacyclic selection assay (Fig 2C) may not be true metacyclics. Instead, they may be promastigotes whose plasma membrane composition has been altered, thereby affecting the lipophosphoglycan constitution and subsequent agglutination by PNA. Another interesting result in the proteomics assessment was the upregulation of a TPR-repeat

(tetratricopeptide repeat) containing protein (S7CFig). TPR motifs are known facilitators of protein-protein interactions. They are present in proteins involved in different biological functions, such as in the orthologues of EST1p (ever-short telomere 1 protein), an evolutionarily conserved regulator of telomerase activity [64,65].

Discussion

Telomerase reverse transcriptase (TERT) is an essential component of telomerase. Nonetheless, the extent of its relevance to *Leishmania* parasite biology and survival has been unexplored. Consequently, this study sought to understand the effects of TERT deletion on parasite morphology, cell cycle progression, cell proliferation, cell fate, cell organelle organization, infectivity, and telomere homeostasis. We show that the absence of TERT does not lead to the immediate death of parasites as hypothesized but does affect vital parasite biology, including *in vivo* and *in vitro* infectivity and the regulation of parasite surface lipophosphoglycan constitution.

The absence of the TERT in *Leishmania major,* unlike *Trypanosoma brucei,*[60] shows detrimental effects on parasite growth, causing the cells to reach the stationary phase later than *Lm*007. The delay resulted in the difference in timing where the decline phase for the control parasites happened earlier than the knockouts, likely due to nutrient depletion and other conditions associated with stationary phase cultures, such as changes in the culture media pH [66]. The ability of cells to go through the various stages of development hinges on their transitions across the distinct phases of the cell cycle. In the presence of genomic perturbations, cells activate checkpoints to ensure that the integrity of their genome is uncompromised. In addition, cell cycle checkpoints guarantee that the next generation of cells has the necessary cellular supplies to survive, grow, and reproduce [20,48,67]. Our data indicate that *Lm*TERT-/- and *Lm*N420 are challenging in synthesizing DNA. The data also suggests the likely initiation of checkpoints due to DNA damage

leading to arrest in cell cycle progression. From our data, we posit a role of TERT in DNA synthesis and cell cycle progression. Interestingly, these challenges do not seem to hinder the continuous growth of the parasite. Damasceno and colleagues [68] demonstrated that *L. major* could continue with other cell cycle processes even with a checkpoint activation. Our data agree with their observation [68].

The telomere attrition recorded here due to TERT manipulation and a similar report by Dreesen *et al*. [58] on *T. brucei* indicates the significance of TERT in maintaining telomeres in these ancient eukaryotes. The reduction in telomere length signifies the loss of the protective cap at the end of the chromosome, triggering a senescent-like state [19,69]. There are reports of telomerase-deficient cells using alternative telomere maintenance mechanisms for survival [70–73]. These post-senescence survivors activate alternative lengthening of telomere (ALT) strategies, such as recombination and chromosome circularization, to maintain short telomeres [74]. Although not much evidence is provided here, based on the observed phenotypes and concurrent events in other cell types, we suspect that there is a population of our TERT-deficient parasites that use an ALT mechanism to continue to proliferate despite having short telomeres. Telomere uncapping led to an accumulation of DNA damage signals as TERT-deficient parasites grew from the log into the stationary phase [40,54,75–81]. Similar observations have been reported in *Saccharomyces cerevisiae,* whereby telomere uncapping led to the accumulation of DNA damage as cell division proceeded [82].

While the use of Annexin-V as a marker for apoptosis in *Leishmania* has been called into question, some relevant studies have shown a strong relationship between this assay and parasite infectivity and cell fitness. Annexin-V labeling demonstrates changes to the parasite plasma membrane [51,53,83–89]. Based on this, we declare cells as either dead or alive without stressing the type of death [90]. The low levels of Annexin-V-positive cells recorded for *Lm*N420 and

*Lm*TERT-/- indicate intact membranes and, thus, viable parasites. The presence of Annexin-V-positive cells in culture has been reported to serve as an altruist, helping in manipulating host cell defences to facilitate the intracellular survival of the fittest parasite [91]. We suspected abolished infectivity in TERT-ablated parasites based on the Annexin data. This suspicion was confirmed by the *in vivo* and *in vitro* infectivity results. The absence of infection in mice inoculated with *Lm*TERT-/- revealed by the indirect immunofluorescence assay suggests that the microlesion observed in the footpad likely did not develop from infection with the knockout *Leishmania* parasites. While indirect immunofluorescence detection of *Leishmania* is a qualitative measure with the disadvantage of false-negative or positive results, it is an effective method for detecting cutaneous leishmaniasis [92,93]. Furthermore, the controls used in our study show high robustness in the sensitivity and specificity of the tests (S4 Fig). The infectivity index recorded after infecting BMDMs corroborates these observations and incontrovertibly indicates that TERT is involved in parasite infectivity.

In addition, the formation of autophagosomes revealed by electron microscopy results points to the initiation of cellular control by autophagy [90]. Autophagy is a molecular pathway described in *Leishmania* as a cell control mechanism directly involved in survival and infectivity [50,68,90]. Basmaciyan and colleagues [94] have shown that autophagic *Leishmania* parasites have lower Annexin-positive signals, a phenomenon corroborated by our results here. Therefore, it is likely that in the absence of TERT, *Leishmania* parasites use an autophagic mechanism similar to macroautophagy in mammalian cells. Macroautophagy allows cells to break down their cytosolic materials and organelles to produce energy for survival under adverse conditions [94,95]. Given this information, we propose a suggestive role of TERT in parasite pro-survival-autophagy.

Another question is whether the selected metacyclic parasites are actual metacyclics or metacyclic-like' parasites. Metacyclics are considered a key determinant of *Leishmania* virulence,

but the data obtained here are contrary [96]. Despite this observation, Zandbergen and colleagues [54] reported a positive correlation between virulence and Annexin-positive *Leishmania* parasites. The authors consider the presence of Annexin-positive parasites as a better determinant of infection than the number of metacyclic parasites. Our Annexin, infectivity, and METAs results corroborate their report [54]. As a result of the modifications in the plasma membrane and the protein deregulation observed, we believe the promastigotes obtained from TERT-depleted lineages are parasites lacking the necessary potential for PNA binding. *Leishmania* parasites are known to have specific lipophosphoglycan (LPG) at each growth phase. Although our results from the amplification of *SCG* genes do not conclusively suggest that telomeric erosion has affected them, it is impossible to confirm whether their protein expression or function was compromised. Additionally, it is unclear to what extent the other unamplified members of the *SCG* gene family influence the LPGs [42,43].

In conclusion, our study has revealed evidence of TERT involvement in maintaining and regulating *L. major* telomeres*,* parasite infectivity, the cell cycle, surface protein expression, metacyclogenesis, DNA damage machinery, and prosurvival autophagy. We provide several lines of evidence on how the absence of *Lm*TERT leads to pleiotropic effects that can be likened to senescence in yeast and other cells. We propose a model in which the absence of *Lm*TERT leads to telomere shortening, thereby triggering cell cycle arrest and DNA damage responses that cause cells to enter a replicative senescent state. We suspect these cells survive using prosurvival autophagic mechanisms and maintain short telomeres using an unknown ALT mechanism. Future studies will try to elucidate the exact ALT mechanism utilized by these parasites. On the other hand, the TPR-containing protein overexpressed by the TERT-/- parasites can be a starting point by determining its relatedness and relevance in comparison with that of the EST1-TPR in *S. cerevisiae,* which was found to be relevant in telomere homeostasis [65]. The consistent results

from the full-gene knockout and the ORF-disrupted knockout, along with the complementation results, further strengthen the notion that the absence of TERT was responsible for the observed pleiotropic defects. As such, *Lm*TERT can serve as a drug target against leishmaniasis.

Materials and methods

Resource availability statements

Materials availability

Leishmania mutant lines and oligonucleotides generated in this project are available upon request to the lead contact.

Data availability

All data reported in this paper can be found at **doi: 10.5281/zenodo.10148737,** along with the respective statistical treatments and results obtained. Proteomic data are available via ProteomeXchange with identifier **PXD046289**.

Experimental model and subject details

WT *Leishmania major* Friedlin strain (MHOM/IL/1980/FRIEDLIN) was used to generate the *Lm*007 lineage, which was used to generate knockout lineages. Knockout lineages served as background lines for the respective complementation lineages. Experiments were conducted at two key passages, passage 7 and passage 20. Depending on the assay, these experiments used logarithmically growing parasites and stationary phase parasites. All parasites were cultivated with the M199 (Cultilab) culture medium supplemented with 10% Foetal Bovine Serum, 41.75 mM Hepes (Amresco), 0.35 g/l $NaHCO_3$ (Sigma), 104.38 µm Adenine (Sigma), 0.001% Biotin (Sigma), 10000 U/mL penicillin/streptomycin solution and kept at 26 °C [97]. For the selection of single, independent clones, promastigotes were plated on solid M199 media in the presence of 20% FBS mixed 1:1 with 2% Agar (bacteriological grade) supplemented with specific antibiotics. The resistance gene carried by the parasite lineage determined the choice of antibiotics. Female Balb/c

mice at six weeks old were also used in the experiment. Mice were fed ad libitum and housed in an authorized facility.

Gene editing

Design and synthesis of oligonucleotides

SgRNAs were obtained following similar strategies described by Beneke *et al.* [45] and Yagoubat *et al.* [98]. A set of oligonucleotide sequences for the gene ID *Lmj*F.36.3930 (*Lm*TERT component) was designed using information from the LeishGEdit (http://www.leishgedit.net/mysql/primersearch.php). Another oligonucleotide set was designed using the Eukaryotic Pathogen CRISPR guide RNA/DNA Design Tool (EuPaGDT) (http://grna.ctegd.uga.edu/), maintaining default parameters. Whereas LeishGEdit sgRNA targeted the UTR regions of the gene, the EuPaGDT-designed sgRNAs targeted the endogenous region of the gene, 420bp and 4022bp from the start codon for the 5' and 3' cut, respectively. Two sets of oligonucleotides were designed from the LeishGEdit site to amplify a DNA fragment from a pTplasmid [39]. Two fragments of plasmids that confer resistance to different selection drugs (neomycin and puromycin) were used to amplify a donor template (DT). Puromycin and Neomycin donor templates were used in the full TERT knockout replacement, whereas only the Neomycin donor template was used in the *Lm*N420 deletion.

Parasite transfections and clonal lineage selection

The Cytomix buffer, composed of 120 mM KCl, 0.15 mM $CaCl_2$, 10 mM K_2HPO_4, 25 mM HEPES, 2 mM EDTA, and 2 mM $MgCl_2$, was used in the deletion procedures. Briefly, 2×10^8 cells were centrifuged at 1000 g for 10 min, washed with the buffer at a similar speed, and the pellet resuspended in 500 µL of the buffer. To generate *Lm*N420, NAB, *Lm*007, and TAB, two pulses

from the Bio-Rad gene pulser system were used with the following conditions: 25 μF and 1500 Volts (3.75 kV), with 10 s wait period between the pulses [97]. The Amaxa nucleofector system (Lonza) generated the *Lm*TERT-/-; a single pulse of the X-001 program was used [45,68]. Clonal lineages were selected by plating in the presence of specific antibiotics. Using two different systems to generate knockout lineages increased the confidence in attributing observed phenotypes to the gene manipulation rather than a possible confounding effect of the system.

Flow cytometry techniques

Assessment of DNA content

A total of 5×10^6 cells were harvested from log phase and stationary phase cultures followed by resuspension in 90% methanol, incubated at -20 °C for 30 min. Two PBS washes were performed on permeabilized cells before staining with 40 μg/mL propidium iodide and 100 μg/mL RNAse A (Amresco). Stained cells were incubated at 37 °C for 30 min, then at 4 °C for at least 30 min before collection with a flow cytometer (BD Biosciences C6 Acuri). 20-30,000 events were collected in specific PE-A and PE-H gates for further deconvolution or data analysis using FlowJo vX 10.0.7r2 (Tree Star, Inc., Ashland, OR). During analysis, events between treatments were maintained within a difference of 1,000 events. The same gating strategy with adjustments to capture an equal number of events in each instance [99–101].

EdU labelling of parasites

20 μM of EdU (Sigma) was added to the culture medium at the exponential growth phase [102]. Cells were incubated for 10.2 h in the EdU before collection for processing. Cells were permeabilized and incubated in the click-IT reaction cocktail for 30-45 min, then were washed and resuspended in 200 μl of propidium iodide buffer before, incubated at 37 °C for 30 min and later 4

°C for 30 min. A similar procedure for collection and analysis was followed, as in DNA content analysis above [103–106].

Annexin-V and cell membrane integrity assessment

1 x 10^6 stationary phase parasites were collected, washed with PBS, and resuspended in 100 µl of Binding buffer, 2 µl of Annexin V, and 100 µg/mL of Propidium Iodide (Bio-Rad). The mix was incubated at room temperature for 15 min before analysis. Channels FITC-A and PE-H were used because this Annexin-V is conjugated to FITC 20,000-30,000 single events were collected using the Flow cytometer, and data analysis was performed using FlowJo vX 10.0.7r2 (Tree Star, Inc., Ashland OR) [53].

Flow-FISH telomere length assessment

2 x 10^7 cells were collected and then permeabilized with 90% Methanol at -20 °C overnight. Hybridization buffer was added to controls for non-detection, and for the treatment, 300 µl of Hybridization buffer containing TelC probe (1:10,000) was added. The cells are flickered and incubated at 85 °C for 15 min, followed by overnight room-temperature incubation. Cells were washed and incubated at 40 °C, followed by resuspension in PI solution and incubated at 37 °C for 30 min before being transferred to 4 °C for 30 min. 10,000 to 20,000 events were collected for analysis. MESF values were calculated using the manufacturer-recommended program.

Tunel evaluation of DNA damage

2 x 10^7 parasites were fixed with 4% paraformaldehyde (Sigma) and 0.2% Triton X-100 permeabilization. Permeabilized cells were equilibrated and incubated with the nucleotide mix and Terminal Deoxynucleotidyl Transferase, Recombinant (rTdT) enzyme (Promega). Cells were then incubated at 37 °C for 60 min, protected from direct light, followed by treatment with 0.1% Triton

(Bio-Rad) containing 5mg/mL BSA(Promega) dissolved in PBS. Procedures for staining cells for the assessment of DNA content were followed. Finally, 10,000-20,000 events were collected by flow cytometry.

Transmission (TEM) and scanning electron microscopy (SEM) analysis

Leishmania major procyclic promastigotes of *Lm*007, *Lm*N420, and *Lm*TERT-/- each at passages 7 and 20 were washed twice with 0.1 M phosphate buffer saline (PBS) and fixed at 4 °C for 40 min with 2.5% glutaraldehyde (GA) diluted in 0.1 M Na-cacodylate buffer (pH 7.2). For TEM analysis, the parasites were washed three times with 0.1M sodium cacodylate buffer and post-fixed for 15 min with 1% osmium tetroxide (OsO_4), 0.8% potassium ferricyanide and 5 mM $CaCl_2$ in 0.1 M cacodylate buffer, pH 7.2. Then, samples were washed with the same buffer, dehydrated in an ascending acetone series, and embedded in PolyBed 812 resin as previously described [107]. Ultrathin sections were stained with uranyl acetate and lead citrate and examined under a Jeol 1200 EX transmission electron microscope (Tokyo, Japan) at Centro Nacional de Biologia Estrutural e Bioimagem (CENABIO). Alternatively, for SEM analysis, fixed parasites adhered on glass coverslips coated with 0.1% poly-L-lysine and post-fixed as described above. Then, samples were dehydrated in a crescent ethanol series (30-100 %), dried using the critical point method with CO2, mounted on aluminium stubs coated with a 20 nm gold layer, and examined with a Jeol JSM6390LV scanning electron microscope (Tokyo, Japan) Platform Rudolf Barth in Instituto Oswaldo Cruz, FIOCRUZ [108].

Metacyclic selection

Approximately 1 x 10^8 cells of stationary phase parasite culture were centrifuged at 2,300 x g for 5 min and washed twice with PBS 1X. The supernatant was discarded, and metacyclic solution (PBS1X, 0.1 mg/mL of lectin PNA (Sigma), and 5 mM EDTA) was added to the samples. The mixture was allowed to incubate at room temperature for 1 h, and the supernatant was collected as metacyclics by low-speed centrifugation [52,96].

Bacterial transformation and confirmation of *Lm*TERT presence

Thermo-competent XL-1 blue bacteria were incubated with 10 ng of plasmid for 30 min. After the incubation period, the sample was transferred to a prewarmed incubator at 42 °C for 2 min and set on ice for 5 min. SOB media was supplemented with 100 µl of 1 M $MgCl_2$, 100 µl of 1 M $MgSO_4$, and 900 µl was added to the samples before setting to incubate rotating at 37 °C for an hour. A solid plate of LB agar was prepared, and aliquots of the transformed bacteria were cultured overnight. A single colony from the overnight incubation was selected and expanded in LB broth by overnight incubation at 37 °C. After the overnight expansion, the protocol for Midi-Prep extraction of DNA was followed as directed by the manufacturer to extract the DNA of the plasmid. Restriction fragment analysis was done using *Cla*1 and *Pst*1 restriction enzymes to confirm the extracts.

DNA and RNA extraction

DNA extraction was performed using the Qiagen kit and following the protocol provided by the manufacturer. About 1 x 10^8 parasites from passages 7 and 20 were taken through the protocol. The final elute of the DNA was RNase-treated before quantification. Proteinase K and RNase treatment were performed at 56 °C and 37 °C, respectively. For RNA extraction, about 1 x 10^8 cells were

treated with Trizol (Invitrogen) to extract the RNA. RNA and DNA were quantified by BioTek Epoch Microplate Spectrophotometer (BioTek), and quality checks were done by EtBr-stained agarose gel electrophoresis.

PCR, Sanger sequencing, and RT-qPCR

PCRs were performed using either the Taq polymerase (Invitrogen) in reactions requiring downstream usage of PCR products or the GoTaq green master mix (Promega), where downstream application was not required. A primer walk strategy was designed along the edited regions using SnapGene V.3.2.1. We amplified the edited regions of the genome. PCR products were purified using the PureLink™ Quick Gel Extraction and PCR Purification Combo Kit (Invitrogen). The purified PCR products were Sanger sequenced at a core facility (IBTEC). Assembly of contigs from fragments and further analysis were done using Geneious V.7.1.3.

To perform RT-qPCR, 1µg of extracted RNA from passage 7 was DNase (Thermo scientific) treated and converted to cDNA using the iScript™ cDNA Synthesis Kit (Bio-Rad). Primers for *Lm*TERT (target) and RPN8 (reference) were used to check the expression of the reintroduced, wildtype *Lm*TERT in knockout lineages by qPCR. The primer sequences are listed in the S1 Table. qPCR reactions were performed using a StepOnePlus™ Real-Time PCR System (Applied Biosystems). Each reaction contained a 2.5 ng cDNA template, 100 nM of forward and reverse primers, 5 µl SYBR Green PCR Master Mix (Bio-Rad), and nuclease-free water. The qPCR cycling conditions consisted of an initial denaturation at 95 °C for 10 min, followed by 40 cycles of denaturation at 95 °C for 15 sec, annealing at 60 °C for 30 sec, and extension at 72 °C for 30 sec. The threshold cycle (Ct) values were determined for each sample, and relative gene expression levels were calculated using the 2^-ΔΔCt method, with normalization to the reference genes

(RPN8). All qPCR experiments were performed in triplicate, and the results are presented as mean ±SD.

Terminal restriction fragments profile obtained by telomeric Southern blot

Genomic DNA extracted from the parasites at passages 7 and 20 were digested with 5 U *Rsa*1 (Roche) at 37 °C overnight. Terminal restriction fragments (TRF) were fractionated in a 0.8% EtBr-stained agarose gel and transferred to the Hybond N+ nylon membrane (Cytivia) overnight. The membrane was crosslinked after the transfer and taken through stringent washes before being hybridized with a 5'-DIG-labelled telomeric probe (TELC) (5'-DIG-CCCTAACCCTAACCCTAACCCTAACCCTAA). The hybridization signals were developed with an anti-DIG-HRP conjugate antibody and CSPD-Star (Roche).

Protein studies

Protein extraction and western blot

Whole-cell lysates from parasites at P7 were obtained by washing twice with phosphate-buffered saline (PBS) at 3500 x g for 5 min. 1 mL of Buffer A (20 mM Tris-HCl, 1 mM EGTA, 1 mM EDTA, 15 mM NaCl) supplemented with 1 mM spermidine, 0.3 mM spermine, and 1 mM DTT was added to cells and incubated in liquid nitrogen for 1 min. Tubes were recovered from liquid nitrogen and placed on ice to defrost. 0.5 % Nonydet p-40 and protease inhibitor were added to the extract and centrifuged at maximum speed for 20 min. The supernatant was recovered as total protein extract, and the pellet was discarded. 10 % SDS-polyacrylamide gel was prepared, and samples were loaded into wells in the gel and subjected to electrophoresis to separate the bands in two steps. Samples were run against a standard molecular weight marker at 80 V, 400 mA, and 400

W for 1 h in the first step, then at 120 V, 400 mA, and 400 W for another hour in the second step. Transfer to Immun-Blot® PVDF membrane for protein blotting (Bio-Rad) was done in a Tris-glycine transfer buffer (25 mM tris and 192 mM Glycine) overnight at 90 mA and 120 V at 4 °C evenly cooled temperature. A blocking solution was prepared using a blotting-grade blocker (Bio-Rad) at a 1% (w/v) concentration with PBS/TWEEN 20 (PBST) solution. Primary antibodies were prepared in the blocking solution at appropriate dilutions. Following the manufacturer's instructions, the ECL™ western blotting analysis system (GE Healthcare) was used on the membrane to generate signals (Genesys V.1.7.2.0).

Proteomic analysis

The protein extracts of promastigote forms of *Lm*TERT-/- and *Lm*007 were obtained following a modified version of the protocol described by Fragaki *et al.* [109], using 1 x 10^9 promastigotes on the last day of the exponential phase. Briefly, the cells were collected by centrifugation at 2500 x g for 5 min at 4 ºC and washed twice with 1 mL of sterile phosphate-buffered saline (PBS) using the same parameters for the centrifugation steps. The washed cells were resuspended in 500 µL of lysis buffer 1, which was composed of 10 mM Hepes, 1.5 mM $MgCl_2$, 10 mM KCl, 0.5 mM dithiothreitol (DTT), 0.5% NP40, and 1x protease inhibitors cocktail (Sigma-Fast-Ethylenediaminetetraacetic acid (EDTA)-free). This first lysis step aimed to release the cytoplasmatic proteins, and after the cell resuspension by vortex, the microtube was kept on ice for 30 min. The cytoplasmatic proteins in the supernatant were recovered by centrifugation at 2000 x g for 10 min at 4 ºC. The nuclear proteins were further obtained in two steps. First, the pellet was treated with 50 U of DNAse I (Thermo Scientific) for 20 min at room temperature in 300 mM Hepes pH 7.5, 8 mM $MgCl_2$, 200 mM KCl, and 1,5 x protease inhibitors cocktail. Then, 50 µL of lysis buffer 2 (120 mM Hepes pH 7.5, 1.5 M KCl, 500 mM sucrose, 0.4 mM EDTA, and 1 mM

DTT) was added, and the microtube was incubated on ice for 20 min. Nuclear proteins were recovered by centrifugation at 16100 x g for 15 min at 4 ºC. The protein extracts were quantified using PierceTM B.C.A. Protein Assay kit (Thermo Fischer Scientific) according to the manufacturer's instructions. Approximately 300 µg of proteins were submitted to a precipitation step using acetone/methanol. After resolubilization, 50 µL of 50 mM Hepes pH 7.9 protein concentrations were obtained using the same B.C.A. procedure mentioned above. For the in-solution protein digestion procedure, 100 µg of total protein was denatured in 7 M urea. The disulfide bonds were reduced with 10 mM DTT for 40 min at room temperature, and cysteine residues were carbamidomethylated by incubation with 40 mM of iodoacetamide for 40 min at room temperature. The excess of iodoacetamide was consumed following incubation with 10 mM DTT for 10 min at room temperature. For proteolysis, the protein solutions were diluted to 700 mM urea with 50 mM Hepes pH 7.5, and aliquots containing 1 µg of proteins were saved as the non-digested sample for posterior comparison. Trypsin (Sigma) was added in a 1:50 (m/m) ratio, and the reactions were incubated at 30 ºC for 18 h. After proteolysis, the solutions were acidified with formic acid and concentrated by vacuum centrifugation. Then, the peptides were desalted employing the Stage Tip approach with C18 membranes (3M) and following the procedure described by Rappsilber et al. [110]. The desalted peptides were dried by vacuum centrifugation, dissolved in 30 µL of 0.1% formic acid, and quantified using the Qubit TM Protein Assay kit (Thermo Fischer Scientific). The volume containing 10 µg of peptides was dried by vacuum centrifugation and labelled with TMT as described by Zecha et al. [111]. The reactions were split into cytosolic and nuclear proteins and followed the same labeling scheme: the fractions from *Lm*007 were labelled with tag 127N, and those from *Lm*TERT-/- were labelled with tag 128N.

LC-MS/MS analysis

The peptide fractions (cytosolic and nuclear) were dissolved in 0.1% formic acid (FA), and 100 ng was analysed by LC-MS/MS. Samples were loaded onto a 2 cm precolumn (nanoviper C18, 3 μm) in an EASY-nLC 1200 system (Thermo Fischer Scientific). The liquid chromatography was performed using a 15 cm C18 analytical column (nanoviper C18, 2 μm). The peptide elution followed a gradient of 0.1% FA as phase A and 100% ACN/0.1% FA as phase B with a constant flow rate of 300 nL/min. The starting condition was 5% B, reaching 28% B in 80 min, 10 min to 40% B, and finally, the gradient was increased to 95% B in 2 min, remaining in this condition for 12 min. The nLC system was in tandem with an Orbitrap Fusion Lumos mass spectrometer (Thermo Fischer Scientific) operated in positive mode. The automatic gain control (A.G.C.) was set to 4 x 10^5 ions and a maximum fill time of 50 ms, while the mass range was fixed to 400-1600 m/z with high resolution (120,000 full-width half maximum (FWHM) at m/z 200). Data-dependent acquisition was selected, and a cycle time of 3 seconds was achieved. Higher energy collision-induced dissociation (H.C.D.) was applied for peptide fragmentation using 38 as normalized collision energy (N.C.E.). The fragmentation step was performed at high resolution (50,000 FWHM) with an A.G.C. target of 1 x 10^5 and a maximum injection time of 200 ms using an isolation window of 0.7 m/z. The MS/MS selection intensity threshold was set to 2.5 x 10^4 and a dynamic exclusion of 60 s.

Data analysis

Database search was performed using MaxQuant software (version 2.0.3.0) [112] and in collaboration with Professor André Zelanis (UNIFESP). All raw files of LC-MS/MS of the two peptide fractions (cytosolic and nuclear) were submitted to database search against a fasta file of protein sequences from *L. major* (Friedlin 2021) available in TriTrypDB [113] (8508 sequences in

March 2023). Database search was carried out considering the 10plex TMT labeling as the type of analysis. The reporter ion analysis was specified at the MS2 level, considering a mass tolerance of 0.003 Da, and the 'direct mode' was selected. The precursor ion fraction (P.I.F.) was set to 0.75, and no normalization method was applied. Trypsin was chosen as the enzyme in a specific mode. As dynamic modifications, the occurrence of methionine oxidation (+15.9949 Da) and deamidation of N.Q. (+0.9840), and Protein N-term acetylation (+42.0106) were considered. Cysteine carbamidomethylation was considered a fixed modification (+57.0215). The search mode "match between runs" was enabled in all searches. A false discovery rate (F.D.R.) < 1% was set at P.S.M. (Peptide Spectrum Match) and protein levels. The results were analysed using the Perseus software (version 2.0.9.0). Only protein groups with two or more peptides were considered as identified.

Infectivity studies

Inoculating mice with *Leishmania major*

Parasites were cultured until they reached the stationary phase (day 7). BALB/c Female mice at 6 weeks old were brought in from a mice facility and nurtured until 7 weeks 4 days when they were inoculated with 40 µl of PBS containing about 2 x 10^6 of parasites from *Lm*007, *Lm*TERT-/- and *Lm*N420 in suspension. Inoculation was performed in the right hind footpad of each mouse for all treatment groups using a needle and syringe. Feeding and water were provided ad libitum, with regular monitoring and changes in bedding material. Three mice were used per treatment, and lesion development was followed. Mice were euthanized 61 days post-inoculation. 100 µl of blood was collected before being euthanized. Both hind footpads were measured, and the size of the swelling was determined. The study was conducted under the guidelines for the care and use of laboratory animals.

Macrophage derivation from bone marrow and infection

Bone marrow-derived macrophages (BMDMs) were obtained from femurs and tibias of BALB/c mice. The cells were incubated in RPMI 1640 medium supplemented with penicillin (100 U/mL), streptomycin (100 µg/mL), L-glutamine (2 mM), sodium pyruvate (1 mM), 20% fetal bovine serum and 20% L929 conditioned medium as macrophage stimulating factor source, for 7 days at 37 ºC and 5% CO_2. After differentiation, BMDMs were collected by centrifugation at 600 x g for 10 min at 4ºC and counted in the Neubauer chamber. 3 x 10^5 cells were incubated in RPMI medium, as described in sterile coverslips (Olen) in 24-well plates (Nest) overnight at 37ºC and 5% CO_2. Non-adherent cells were removed, and infection was performed with *Lm*007*, Lm*N420*, Lm*TERT-/-*,* NAB, and TAB promastigotes in the stationary growth phase (MOI 10:1) for 3 h at 34 ºC and 5% CO_2. After 3 h, the cultures were washed with PBS, and the infection was evaluated after 24, 48, and 72 h. The infection was evaluated by determining the percentage of infected macrophages and the number of intracellular amastigotes after counting 300 Panotic-stained (Laborclin) macrophages. The percentage of infection was determined by the equation $(\frac{Number\ of\ infected\ macrophages)}{total\ number\ of\ macrophages} \times 100)$. The infection index was determined by multiplying the percentage of infected macrophages by the mean of intracellular amastigotes per infected macrophage [114].

Indirect immunofluorescence assay of *Leishmania major* infection

Samples from infected mice were tested for antibodies against *Leishmania* spp. Using the indirect immunofluorescent assay test (IIFA) [115]. The antigen for sensitization of the slides was produced using *L. major*-like antigen promastigotes (international code MHOM/BR/1976/JOF provided by Osvaldo Cruz Institute, FIOCRUZ, Rio de Janeiro, and maintained at the Zoonosis Diagnostic Service at FMVZ, UNESP, Botucatu, São Paulo, Brazil) kept in tubes containing 9 mL

of liver infusion broth and tryptose medium and 5 mL of Novy-McNeal-Nicolle medium. After drying, the slides were kept at −20 °C until use. The antibodies by *Leishmania* were studied using serial serum dilutions of 1:40, 1:80, 1:160, 1:320, and 1:640. The dilution process was performed in microplates, using 190 µL of phosphate-buffered saline (PBS) (pH 7.2). Serial dilution started with 10 µl of the serum sample in the first well (1:20). Subsequently, 100 µl of PBS was added into the next five wells by pipetting a 100 µL volume from the prior dilution into the next well (after homogenization) until reaching the fifth well. The last 100 µl volume was discarded. This procedure was repeated with positive and negative control serum samples. Each serum dilution (10 µL) was pipetted into the slide wells, including the positive and negative controls. The slides were incubated inside a moist chamber at 37 °C for 30 min. Afterward, they were washed twice with PBS for 10 min and dried in the incubator at 37 °C. Anti-immunoglobulin G (IgG) specific to mice, conjugated with the fluorescein isothiocyanate, was diluted according to the manufacturer's instructions (Bethyl Labs. / Fortis Life Sciences (USA), using Evans Blue solution with PBS (1:5) and adding 10 µl to each slide dilution. The slides were again incubated for 30 min at 37 °C in a moist chamber, washed with PBS, dried in the incubator, assembled with buffered glycerol (pH 8.5), and covered with coverslips. The slides were examined using an immunofluorescence microscope (Magnification of 40×). After reading the controls, the highest dilution of the serum for which complete fluorescence occurred of the promastigotes was considered the cut-off point, equal or superior to dilution 40 [116].

Statistical Analysis

Data collected, unless otherwise stated, were from at least two independent experiments with at least 3 technical replicates in each assay and subjected to statistical treatment using GraphPad Prism V.9. Statistical analysis was done with either Mann-Whitney test or Kruskal-Wallis test with further

Dunnett analysis for multi-group comparisons. All graph is represented as mean ±SD, and significance was tested at $P \leq 0.05$ at all times. Exact P values are shown only where significance was found.

Ethics statement

Animal procedures were approved by the Ethics Committee for Animal Experimentation of the Instituto de Biologia, Universidade Estadual de Campinas (UNICAMP) (protocol: 5719–1/2021) for experiments using mice.

Acknowledgments

We thank Professors Paolo Di Mascio and Graziella E. Ronsein for the Mass spectrometry analyses performed at the Redox Proteomics Core of the Mass Spectrometry Resource at Chemistry Institute, University of Sao Paulo. We thank Jose Buratini Jnr and Thaisy Tino Dellaqua for their assistance performing the RT-qPCRs. We also thank Robson Francisco Carvalho, Florencia M. Barbé-Tuana, Theresa Teixeira, and Nuhu Osman Attah for their critical reading and suggestions regarding the project and this manuscript. We extend our appreciation to members of the Telomeres Laboratory for their diverse contributions to the project.

Funding

This work was supported by the São Paulo State Research Foundation (FAPESP, Fundação de Amparo à Pesquisa do Estado de São Paulo) under grant 2018/04375-2 and Conselho Nacional de Desenvolvimento Científico e Tecnológico, Brazil, CNPq under grant 302433/2019-8 to MINC. ACC is a FAPESP Young investigator (grant 2016/21171-6). MES and BCDO are doctoral fellows from FAPESP (grants 2020/00316-1 and 2019/25985-6). HB is a doctoral fellow from CNPq (grant

403634/2022-9). DAS and LCA are post-doctoral fellows from FAPESP (grants 2021/05523-8 and 2021/04253-7, respectively).

Author contributions

Conceptualization: M.E.S. and M.I.N.C.; **Methodology:** M.E.S., B.C.D.O., H.B., D.A.S., L.C.A., R.M.B., M.M.B., M.N.C.S., B.D.M., H.L., J.I.A., A.C.C., and M.I.N.C.; **Validation:** M.E.S.; B.C.D.O.; **Formal Analysis:** M.E.S., D.A.S., R.M.B., M.M.B., M.N.C.S., B.D.M.; **Investigation:** M.E.S., B.C.D.O., H.B., D.A.S., L.C.A., R.M.B., M.M.B., B.D.M., J.I.A.; **Resources:** M.E.S., D.A.S., M.N.C.S., B.D.M., H.L., A.C.C., and M.I.N.C.; **Data Curation:** M.E.S. and D.A.S.; **Writing – Original Draft:** M.E.S.; **Writing – Review & Editing:** M.E.S., B.C.D.O., H.B., D.A.S., L.C.A., M.N.C.S., B.D.M., J.I.A., A.C.C., and M.I.N.C.; **Visualization:** M.E.S. and M.I.N.C.; **Project Administration:** M.I.N.C.; **Supervision:** M.I.N.C.; **Funding Acquisition:** M.I.N.C.

References

[1] Karmakar S, Ismail N, Oliveira F, Oristian J, Zhang WW, Kaviraj S, et al. Preclinical validation of a live attenuated dermotropic *Leishmania* vaccine against vector transmitted fatal visceral leishmaniasis. Commun Biol 2021;4. https://doi.org/10.1038/s42003-021-02446-x.

[2] Lage DP, Ribeiro PAF, Dias DS, Mendonça DVC, Ramos FF, Carvalho LM, et al. A candidate vaccine for human visceral leishmaniasis based on a specific T cell epitope-containing chimeric protein protects mice against *Leishmania* infantum infection. NPJ Vaccines 2020;5. https://doi.org/10.1038/s41541-020-00224-0.

[3] Kanyina EW. Characterization of visceral leishmaniasis outbreak, Marsabit County, Kenya, 2014. BMC Public Health 2020;20. https://doi.org/10.1186/s12889-020-08532-9.

[4] Sunter J, Gull K. Shape, form, function, and *Leishmania* pathogenicity: from textbook descriptions to biological understanding. Open Biol 2017;7. https://doi.org/10.1098/rsob.170165.

[5] Volpedo G, Pacheco-Fernandez T, Holcomb EA, Zhang WW, Lypaczewski P, Cox B, et al. Centrin-deficient *Leishmania mexicana* confers protection against New World cutaneous leishmaniasis. NPJ Vaccines 2022;7. https://doi.org/10.1038/s41541-022-00449-1.

[6] Karmakar S, Volpedo G, Zhang W-W, Lypaczewski P, Ismail N, Oliveira F, et al. Centrin-deficient *Leishmania mexicana* confers protection against Old World visceral leishmaniasis. NPJ Vaccines 2022;7:157. https://doi.org/10.1038/s41541-022-00574-x.

[7] Duncan R, Gannavaram S, Dey R, Debrabant A, Lakhal-Naouar I, Nakhasi HL. Identification and Characterization of Genes Involved in *Leishmania* Pathogenesis: The Potential for Drug Target Selection . Mol Biol Int 2011;2011:1–10. https://doi.org/10.4061/2011/428486.

[8] Zhang WW, Karmakar S, Gannavaram S, Dey R, Lypaczewski P, Ismail N, et al. A second generation leishmanization vaccine with a markerless attenuated *Leishmania* major strain using CRISPR gene editing. Nat Commun 2020;11. https://doi.org/10.1038/s41467-020-17154-z.

[9] Handman E, Kedzierski L, Uboldi AD, Goding JW. Fishing for anti-*Leishmania* drugs: Principles and problems. Adv Exp Med Biol 2008;625:48–60. https://doi.org/10.1007/978-0-387-77570-8_5.

[10] Kweku MA, Odoom S, Puplampu N, Desewu K, Nuako GK, Gyan B, et al. An outbreak of suspected cutaneous leishmaniasis in Ghana: lessons learnt and preparation for future outbreaks. Glob Health Action 2011;4. https://doi.org/10.3402/gha.v4i0.5527.

[11] Barbé-Tuana F, Kich Grun L, Pierdoná V, Dias De Oliveira BC, Paiva SC, Shiburah ME, et al. Human genome structure, function and clinical considerations. 2021. https://doi.org/https://doi.org/10.1007/978-3-030-73151-9_7#DOI.

[12] Srinivas N, Rachakonda S, Kumar R. Telomeres and telomere length: A general overview. Cancers (Basel) 2020;12. https://doi.org/10.3390/cancers12030558.

[13] Bryan TM. G-quadruplexes at telomeres: Friend or foe? Molecules 2020;25. https://doi.org/10.3390/molecules25163686.

[14] Calado R, Young N. Telomeres in disease. F1000 Med Rep 2012;4. https://doi.org/10.3410/M4-8.

[15] T Van der Ploeg LH, C Liu AY, Borst P. Structure of the Growing Telomeres of Trypanosomes. vol. 36. 1964.

[16] Teixeira MT, Gilson E. Telomere maintenance, function and evolution: The yeast paradigm. Chromosome Research 2005;13:535–48. https://doi.org/10.1007/s10577-005-0999-0.

[17] Lira CBB, Giardini MA, Neto JLS, Conte FF, Cano MIN. Telomere biology of trypanosomatids: beginning to answer some questions. Trends Parasitol 2007;23:357–62. https://doi.org/10.1016/j.pt.2007.06.005.

[18] Dreesen O, Cross GAM. Consequences of telomere shortening at an active VSG expression site in telomerase-deficient Trypanosoma brucei. Eukaryot Cell 2006;5:2114–9. https://doi.org/10.1128/EC.00059-06.

[19] Zhang A, Zheng C, Hou M, Lindvall C, Li KJ, Erlandsson F, et al. Deletion of the telomerase reverse transcriptase gene and haploinsufficiency of telomere maintenance in cri du chat syndrome. Am J Hum Genet 2003;72:940–8. https://doi.org/10.1086/374565.

[20] Assis LHC, Andrade-Silva D, Shiburah ME, de Oliveira BCD, Paiva SC, Abuchery BE, et al. Cell cycle, telomeres, and telomerase in *Leishmania* spp.: What do we know so far? Cells 2021;10. https://doi.org/10.3390/cells10113195.

[21] Conte FF, Cano MIN. Genomic organization of telomeric and subtelomeric sequences of *Leishmania* (Leishmania) amazonensis. Int J Parasitol 2005;35:1435–43. https://doi.org/10.1016/j.ijpara.2005.05.011.

[22] Cano MIN, Dungan JM, Agabian N, Blackburn EH. Telomerase in kinetoplastid parasitic protozoa. Proc Natl Acad Sci U S A 1999;96:3616–21. https://doi.org/10.1073/pnas.96.7.3616.

[23] Giardini MA, Segatto M, Da Silva MS, Nunes VS, Cano MIN. Telomere and telomerase biology. vol. 125. 2014. https://doi.org/10.1016/B978-0-12-397898-1.00001-3.

[24] Fu G, Barker DC. Characterisation of *Leishmania* telomeres reveals unusual telomeric repeats and conserved telomere-associated sequence. vol. 26. 1998.

[25] Galindo MM, Rodriguez E, Rojas MG, Figarella K, Campelo R, Ramírez JL. A heat-activated and thermoresistant telomerase activity in *Leishmania major* Friedlin. Acta Trop 2009;111:86–9. https://doi.org/10.1016/j.actatropica.2009.02.002.

[26] Giardini MA, Lira CBB, Conte FF, Camillo LR, De Siqueira Neto JL, Ramos CHI, et al. The putative telomerase reverse transcriptase component of *Leishmania* amazonensis: Gene cloning and characterization. Parasitol Res 2006;98:447–54. https://doi.org/10.1007/s00436-005-0036-4.

[27] Campelo R, Lozano ID, Figarella K, Osuna A, Ramírez JL. *Leishmania major* telomerase TERT protein has a nuclear/mitochondrial eclipsed distribution that is affected by oxidative stress. Infect Immun 2015;83:57–66. https://doi.org/10.1128/IAI.02269-14.

[28] Elton JRV, Vinícius SN, Marcelo SDS, Marcela S, Peter JM, Maria INC. The putative *Leishmania* telomerase rna (LeishTer) undergoes trans-splicing and contains a conserved template sequence. PLoS One 2014;9:17–20. https://doi.org/10.1371/journal.pone.0112061.

[29] Giardini MA, Fernández MF, Lira CBB, Cano MIN. *Leishmania* amazonensis: Partial purification and study of the biochemical properties of the telomerase reverse transcriptase activity from promastigote-stage. Exp Parasitol 2011;127:243–8. https://doi.org/10.1016/j.exppara.2010.08.001.

[30] Zvereva MI, Shcherbakova DM, Dontsova OA. Telomerase: Structure, functions, and activity regulation. Biochemistry (Moscow) 2010;75:1563–83. https://doi.org/10.1134/S0006297910130055.

[31] Dey A, Chakrabarti K. Current perspectives of telomerase structure and function in eukaryotes with emerging views on telomerase in human parasites. Int J Mol Sci 2018;19. https://doi.org/10.3390/ijms19020333.

[32] Xia J, Peng Y, Saira Mian I, Lue NF. Identification of Functionally Important Domains in the N-Terminal Region of Telomerase Reverse Transcriptase. vol. 20. 2000.

[33] Lai AG, Pouchkina-Stantcheva N, Di Donfrancesco A, Kildisiute G, Sahu S, Aziz Aboobaker A. The protein subunit of telomerase displays patterns of dynamic evolution and conservation across different metazoan taxa. BMC Evol Biol 2017;17. https://doi.org/10.1186/s12862-017-0949-4.

[34] Pestana A, Vinagre J, Sobrinho-Simões M, Soares P. TERT biology and function in cancer: Beyond immortalisation. J Mol Endocrinol 2017;58:R129–46. https://doi.org/10.1530/JME-16-0195.

[35] Cao Y, Li H, Deb S, Liu J-P. TERT regulates cell survival independent of telomerase enzymatic activity n.d. https://doi.org/10.1038/sj/onc/1205419.

[36] Lee J, Sung YH, Cheong C, Choi YS, Jeon HK, Sun W, et al. TERT promotes cellular and organismal survival independently of telomerase activity. Oncogene 2008;27:3754–60. https://doi.org/10.1038/sj.onc.1211037.

[37] Tan J, Liu R, Zhu G, Umbricht CB, Xing M. TERT promoter mutation determines apoptotic and therapeutic responses of BRAF-mutant cancers to BRAF and MEK inhibitors: Achilles Heel. Proc Natl Acad Sci U S A 2020;117:15846–51. https://doi.org/10.1073/pnas.2004707117.

[38] Xi L, Schmidt JC, Zaug AJ, Ascarrunz DR, Cech TR. A novel two-step genome editing strategy with CRISPR-Cas9 provides new insights into telomerase action and TERT gene expression. Genome Biol 2015;16:1–17. https://doi.org/10.1186/s13059-015-0791-1.

[39] Beneke T, Madden R, Makin L, Valli J, Sunter J, Gluenz E. A CRISPR Cas9 high-throughput genome editing toolkit for kinetoplastids. R Soc Open Sci 2017;4:1–16. https://doi.org/10.1098/rsos.170095.

[40] Hewitt G, Jurk D, Marques FDM, Correia-Melo C, Hardy T, Gackowska A, et al. Telomeres are favoured targets of a persistent DNA damage response in ageing and stress-induced senescence. Nat Commun 2012;3. https://doi.org/10.1038/ncomms1708.

[41] Ale-Agha N, Dyballa-Rukes N, Jakob S, Altschmied J, Haendeler J. Cellular functions of the dual-targeted catalytic subunit of telomerase, telomerase reverse transcriptase - Potential role in senescence and aging. Exp Gerontol 2014;56:189–93. https://doi.org/10.1016/j.exger.2014.02.011.

[42] Dobson DE, Scholtes LD, Myler PJ, Turco SJ, Beverley SM. Genomic organization and expression of the expanded SCG/L/R gene family of *Leishmania major*: Internal clusters and telomeric localization of SCGs mediating species-specific LPG modifications. Mol Biochem Parasitol 2006;146:231–41. https://doi.org/10.1016/j.molbiopara.2005.12.012.

[43] Dobson DE, Kamhawi S, Lawyer P, Turco SJ, Beverley SM, Sacks DL. *Leishmania major* survival in selective Phlebotomus papatasi sand fly vector requires a specific SCG-encoded lipophosphoglycan galactosylation pattern. PLoS Pathog 2010;6. https://doi.org/10.1371/journal.ppat.1001185.

[44] Wang T, Birsoy K, Hughes NW, Krupczak KM, Post Y, Wei JJ, et al. Identification and characterization of essential genes in the human genome. Science (1979) 2015;350:1096–101. https://doi.org/10.1126/science.aac7041.

[45] Beneke T, Gluenz E. LeishGEdit: A Method for Rapid Gene Knockout and Tagging Using CRISPR-Cas9. Methods in Molecular Biology 2019;1971:189–210. https://doi.org/10.1007/978-1-4939-9210-2_9.

[46] Martel D, Beneke T, Gluenz E, Späth GF, Rachidi N. Characterisation of Casein Kinase 1.1 in *Leishmania donovani* Using the CRISPR Cas9 Toolkit. Biomed Res Int 2017;2017. https://doi.org/10.1155/2017/4635605.

[47] Khamchun S, Thongboonkerd V. Cell cycle shift from G0/G1 to S and G2/M phases is responsible for increased adhesion of calcium oxalate crystals on repairing renal tubular cells at injured site. Cell Death Discov 2018;4. https://doi.org/10.1038/s41420-018-0123-9.

[48] Wheeler RJ, Gluenz E, Gull K. The cell cycle of Leishmania: Morphogenetic events and their implications for parasite biology. Mol Microbiol 2011;79:647–62. https://doi.org/10.1111/j.1365-2958.2010.07479.x.

[49] Xu X, Hamhouyia F, Thomas SD, Burke TJ, Girvan AC, McGregor WG, et al. Inhibition of DNA Replication and Induction of S Phase Cell Cycle Arrest by G-rich Oligonucleotides. Journal of Biological Chemistry 2001;276:43221–30. https://doi.org/10.1074/jbc.M104446200.

[50] Basmaciyan L, Casanova M. La mort cellulaire chez Leishmania. Parasite 2019;26:71. https://doi.org/10.1051/parasite/2019071.

[51] Kroemer G, El-Deiry WS, Golstein P, Peter ME, Vaux D, Vandenabeele P, et al. Classification of cell death: Recommendations of the nomenclature committee on cell death. Cell Death Differ 2005;12:1463–7. https://doi.org/10.1038/sj.cdd.4401724.

[52] Saraiva EM, Pinto-Da-Silva LH, Wanderley JLM, Bonomo AC, Barcinski MA, Moreira MEC. Flow cytometric assessment of *Leishmania* spp metacyclic differentiation: Validation by morphological features and specific markers. Exp Parasitol 2005;110:39–47. https://doi.org/10.1016/j.exppara.2005.01.004.

[53] Weingärtner A, Kemmer G, Müller FD, Zampieri RA, Gonzaga dos Santos M, Schiller J, et al. *Leishmania* promastigotes lack phosphatidylserine but bind annexin V upon permeabilization or miltefosine treatment. PLoS One 2012;7. https://doi.org/10.1371/journal.pone.0042070.

[54] Zandbergen van G, Bollinger A, Wenzel A, Kamhawi S, Voll R, Klinger M, et al. Leishmaniadisease development depends on thepresence of apoptotic promastigotes in the virulent inoculum. Proceedings of the National Academy of Sscience 2006;103:13837–42. https://doi.org/doi10.1073pnas.0607935103.

[55] El Maï M, Bird M, Allouche A, Targen S, Şerifoğlu N, Lopes-Bastos B, et al. Gut-specific telomerase expression counteracts systemic aging in telomerase-deficient zebrafish. Nat Aging 2023;3:567–84. https://doi.org/10.1038/s43587-023-00401-5.

[56] Xu Z, Fallet E, Paoletti C, Fehrmann S, Charvin G, Teixeira MT. Two routes to senescence revealed by real-time analysis of telomerase-negative single lineages. Nat Commun 2015;6:7680. https://doi.org/10.1038/ncomms8680.

[57] Bryan TM, Goodrich KJ, Cech TR. Telomerase RNA Bound by Protein Motifs Specific to Telomerase Reverse Transcriptase merase activity (Lingner et al TERTs also contain a telo-merase-specific motif T located just N-terminal to the. vol. 6. 2000.

[58] Dreesen O, Li B, Cross GAM. Telomere structure and shortening in telomerase-deficient Trypanosoma brucei. Nucleic Acids Res 2005;33:4536–43. https://doi.org/10.1093/nar/gki769.

[59] Lim CJ, Zaug AJ, Kim HJ, Cech TR. reveals unexpected stoichiometry and dual pathways to enhance telomerase processivity. Nat Commun 2017;8:1075. https://doi.org/10.1038/s41467-017-01313-w.

[60] Cunningham DD, Collins K. Biological and Biochemical Functions of RNA in the Tetrahymena Telomerase Holoenzyme. Mol Cell Biol 2005;25:4442–54. https://doi.org/10.1128/mcb.25.11.4442-4454.2005.

[61] Strong MA, Vidal-Cardenas SL, Karim B, Yu H, Guo N, Greider CW. Phenotypes in mTERT+/- and mTERT-/- Mice Are Due to Short Telomeres, Not Telomere-Independent Functions of Telomerase Reverse Transcriptase. Mol Cell Biol 2011;31:2369–79. https://doi.org/10.1128/mcb.05312-11.

[62] Zhu J, Liu W, Chen C, Zhang H, Yue D, Li C, et al. TPP1 OB - fold domain protein suppresses cell proliferation and induces cell apoptosis by inhibiting telomerase recruitment to telomeres in human lung cancer cells. J Cancer Res Clin Oncol 2019;145:1509–19. https://doi.org/10.1007/s00432-019-02921-3.

[63] Sacks DL, Brodin TN, Turco SJ. Developmental modification of the lipophosphoglycan from *Leishmania major* promastigotes during metacyclogenesis. 1990.

[64] Diniz MC, Pacheco ACL, Girão KT, Araujo FF, Walter CA, Oliveira DM. The tetratricopeptide repeats (TPR)-like superfamily of proteins in *Leishmania* spp., as revealed by multi-relational data mining. Pattern Recognit Lett 2010;31:2178–89. https://doi.org/10.1016/j.patrec.2010.04.008.

[65] Sealey DC, Kostic AD, LeBel C, Pryde F, Harrington L. The TPR-containing domain within Est1 homologs exhibits species-specific roles in telomerase interaction and telomere length homeostasis. BMC Mol Biol 2011;12:45. https://doi.org/10.1186/1471-2199-12-45.

[66] Kelly FD, Yates PA, Landfear SM. Nutrient sensing in *Leishmania* : Flagellum and cytosol. Mol Microbiol 2021;115. https://doi.org/10.1111/mmi.14635.

[67] Das-Bradoo S, Bielinsky A. DNA Replication and Checkpoint Control in S Phase. Nature Education 2010:616–27. https://doi.org/10.1038/nrm2450.

[68] Damasceno JD, Reis-Cunha J, Crouch K, Beraldi D, Lapsley C, Tosi LRO, et al. Conditional knockout of RAD51-related genes in *Leishmania major* reveals a critical role for homologous recombination during genome replication. PLoS Genet 2020;16. https://doi.org/10.1371/journal.pgen.1008828.

[69] Huffman KE, Levene SD, Tesmer VM, Shay JW, Wright WE. Telomere shortening is proportional to the size of the G-rich telomeric 3'-overhang. Journal of Biological Chemistry 2000;275:19719–22. https://doi.org/10.1074/jbc.M002843200.

[70] Zhang JM, Zou L. Alternative lengthening of telomeres: From molecular mechanisms to therapeutic outlooks. Cell Biosci 2020;10. https://doi.org/10.1186/s13578-020-00391-6.

[71] Londoñ O-Vallejo JA, Der-Sarkissian H, Cazes L, Bacchetti S, Reddel RR. Alternative Lengthening of Telomeres Is Characterized by High Rates of Telomeric Exchange. vol. 64. 2004.

[72] Bryan TM, Englezou A, Oalla-Pozza2 L, Ounham MA, Reddel RR. Evidence for an alternative mechanism for maintaining telomere length in human tumors and tumor-derived cell lines. 1997.

[73] Dreesen O, Cross GAM. Telomerase-Independent Stabilization of Short Telomeres in Trypanosoma brucei . Mol Cell Biol 2006;26:4911–9. https://doi.org/10.1128/mcb.00212-06.

[74] Grandin N, Charbonneau M. Protection against chromosome degradation at the telomeres. Biochimie 2008;90:41–59. https://doi.org/10.1016/j.biochi.2007.07.008.

[75] Owiti NA, Nagel ZD, Engelward BP. Fluorescence Sheds Light on DNA Damage, DNA Repair, and Mutations. Trends Cancer 2021;7:240–8. https://doi.org/10.1016/j.trecan.2020.10.006.

[76] Glover L, Horn D. Trypanosomal histone γh2A and the DNA damage response. Mol Biochem Parasitol 2012;183:78–83. https://doi.org/10.1016/j.molbiopara.2012.01.008.

[77] Karanam K, Loewer A, Lahav G. Dynamics of the DNA damage response: Insights fromlive-cell imaging. Brief Funct Genomics 2013;12:109–17. https://doi.org/10.1093/bfgp/els059.

[78] Mersaoui SY, Gravel S, Karpov V, Wellinger RJ. DNA damage checkpoint adaptation genes are required for division of cells harbouring eroded telomeres. Microbial Cell 2015;2:394–405. https://doi.org/10.15698/mic2015.10.229.

[79] Doksani Y. The response to dna damage at telomeric repeats and its consequences for telomere function. Genes (Basel) 2019;10:1–17. https://doi.org/10.3390/genes10040318.

[80] Black JA, Crouch K, Lemgruber L, Lapsley C, Dickens N, Tosi LRO, et al. Trypanosoma brucei ATR Links DNA Damage Signaling during Antigenic Variation with Regulation of RNA Polymerase I-Transcribed Surface Antigens. Cell Rep 2020;30:836-851.e5. https://doi.org/10.1016/j.celrep.2019.12.049.

[81] Crauwels P, Bohn R, Thomas M, Gottwalt S, Jäckel F, Krämer S, et al. Apoptotic-like *Leishmania* exploit the host´s autophagy machinery to reduce T-cell-mediated parasite elimination. Autophagy 2015;11:285–97. https://doi.org/10.1080/15548627.2014.998904.

[82] Grandin N. Cdc13 prevents telomere uncapping and Rad50-dependent homologous recombination. EMBO J 2001;20:6127–39. https://doi.org/10.1093/emboj/20.21.6127.

[83] Basmaciyan L, Azas N, Casanova M. Calcein+/PI- as an early apoptotic feature in Leishmania. PLoS One 2017;12. https://doi.org/10.1371/journal.pone.0187756.

[84] Basmaciyan L, Casanova M. Cell death in Leishmania. Parasite 2019;26. https://doi.org/10.1051/parasite/2019071.

[85] Zangger H, Mottram JC, Fasel N. Cell death in *Leishmania* induced by stress and differentiation: Programmed cell death or necrosis? Cell Death Differ 2002;9:1126–39. https://doi.org/10.1038/sj.cdd.4401071.

[86] Ardestani SK, Poorrajab F, Razmi S, Foroumadi A, Ajdary S, Gharegozlou B, et al. Cell death features induced in *Leishmania major* by 1,3,4-thiadiazole derivatives. Exp Parasitol 2012;132:116–22. https://doi.org/10.1016/j.exppara.2012.06.002.

[87] Basmaciyan L, Azas N, Casanova M. A potential acetyltransferase involved in *Leishmania major* metacaspase-dependent cell death. Parasit Vectors 2019;12:1–8. https://doi.org/10.1186/s13071-019-3526-4.

[88] Aureliano DP, Lindoso JAL, de Castro Soares SR, Takakura CFH, Pereira TM, Ribeiro MS. Cell death mechanisms in *Leishmania amazonensis*triggered by methylene blue-mediated antiparasitic photodynamic therapy. Photodiagnosis Photodyn Ther 2018;23:1–8. https://doi.org/10.1016/j.pdpdt.2018.05.005.

[89] Britta EA, Scariot DB, Falzirolli H, Ueda-Nakamura T, Silva CC, Filho BPD, et al. Cell death and ultrastructural alterations in *Leishmania amazonensis*caused by new compound 4-Nitrobenzaldehyde thiosemicarbazone derived from S-limonene. BMC Microbiol 2014;14. https://doi.org/10.1186/s12866-014-0236-0.

[90] Proto WR, Coombs GH, Mottram JC. Cell death in parasitic protozoa: Regulated or incidental? Nat Rev Microbiol 2013;11:58–66. https://doi.org/10.1038/nrmicro2929.

[91] Wanderley JLM, da Silva LHP, Deolindo P, Soong L, Borges VM, Prates DB, et al. Cooperation between apoptotic and viable metacyclics enhances the pathogenesis of leishmaniasis. PLoS One 2009;4. https://doi.org/10.1371/journal.pone.0005733.

[92] Sarkari B, Ashrafmansouri M, Hatam G, Habibi P, Abdolahi Khabisi S. Performance of an ELISA and Indirect Immunofluorescence Assay in Serological Diagnosis of Zoonotic Cutaneous Leishmaniasis in Iran. Interdiscip Perspect Infect Dis 2014;2014. https://doi.org/10.1155/2014/505134.

[93] Ministério da Saúde Secretaria de Vigilância em Saúde Departamento de Vigilância das Doençaas Transmissíveis B. Manual de vigilância da leishmaniose tegumentar [recurso eletrônico]. n.d.

[94] Basmaciyan L, Berry L, Gros J, Azas N, Casanova M. Temporal analysis of the autophagic and apoptotic phenotypes in *Leishmania* parasites. Microbial Cell 2018;5:404–17. https://doi.org/10.15698/mic2018.09.646.

[95] Parzych KR, Klionsky DJ. An overview of autophagy: Morphology, mechanism, and regulation. Antioxid Redox Signal 2014;20:460–73. https://doi.org/10.1089/ars.2013.5371.

[96] Da Silva R, Sacks DL. Metacyclogenesis is a *major* determinant of *Leishmania* promastigote virulence and attenuation. Infect Immun 1987;55:2802–6. https://doi.org/10.1128/iai.55.11.2802-2806.1987.

[97] Pandey SC, Pande V, Samant M. DDX3 DEAD-box RNA helicase (Hel67) gene disruption impairs infectivity of *Leishmania* donovani and induces protective immunity against visceral leishmaniasis. Sci Rep 2020;10. https://doi.org/10.1038/s41598-020-75420-y.

[98] Yagoubat A, Crobu L, Berry L, Kuk N, Lefebvre M, Sarrazin A, et al. Universal highly efficient conditional knockout system in Leishmania, with a focus on untranscribed region preservation. Cell Microbiol 2020;22:1–11. https://doi.org/10.1111/cmi.13159.

[99] Kent M, Chandler R, Wachtel S. DNA analysis by flow cytometry. Cytogenet Cell Genet 1988;47:88–9. https://doi.org/10.1159/000132514.

[100] Darzynkiewicz Z, Huang X, Zhao H. Analysis of cellular DNA content by flow cytometry. Curr Protoc Immunol 2017;2017:5.7.1-5.7.20. https://doi.org/10.1002/cpim.36.

[101] de Oliveira BCD, Shiburah ME, Paiva SC, Vieira MR, Morea EGO, da Silva MS, et al. Possible Involvement of Hsp90 in the Regulation of Telomere Length and Telomerase Activity During the *Leishmania amazonensis*Developmental Cycle and Population Proliferation. Front Cell Dev Biol 2021;9. https://doi.org/10.3389/fcell.2021.713415.

[102] Santos Da Silva M, Andrea P, Muñoz M, Aguirre Armelin H, Elias MC. Differences in the Detection of BrdU/EdU Incorporation Assays Alter the Calculation for G1, S, and G2 Phases of the Cell Cycle in Trypanosomatids 2017. https://doi.org/10.1111/jeu.12408-4940.

[103] Damasceno JD, Marques CA, Beraldi D, Crouch K, Lapsley C, Obonaga R, et al. Genome duplication in *Leishmania major* relies on persistent subtelomeric DNA replication. Elife 2020;9. https://doi.org/10.7554/eLife.58030.

[104] Fantoni NZ, El-Sagheer AH, Brown T. A Hitchhiker's Guide to Click-Chemistry with Nucleic Acids. Chem Rev 2021;121:7122–54. https://doi.org/10.1021/acs.chemrev.0c00928.

[105] Nikic I, Kang JH, Girona GE, Aramburu IV, Lemke EA. Labeling proteins on live mammalian cells using click chemistry. Nat Protoc 2015;10:780–91. https://doi.org/10.1038/nprot.2015.045.

[106] Buck SB, Bradford J, Gee KR, Agnew BJ, Clarke ST, Salic A. Detection of S-phase cell cycle progression using 5-ethynyl-2′- deoxyuridine incorporation with click chemistry, an alternative to using 5-bromo-2′-deoxyuridine antibodies. Biotechniques 2008;44:927–9. https://doi.org/10.2144/000112812.

[107] Sangenito LS, Rodrigues HD, Santiago SO, Bombaça ACS, Menna-Barreto RFS, Reddy A, et al. In vitro effects of bis(N- [4-(hydroxyphenyl)methyl]-2-pyridinemethamine)zinc perchlorate monohydrate 4 on the

physiology and interaction process of *Leishmania* amazonensis. Parasitol Int 2021;84. https://doi.org/10.1016/j.parint.2021.102376.

[108] Rebello KM, Menna-Barreto RFS, Chagas-Moutinho VA, Mota EM, Perales J, Neves-Ferreira AGC, et al. Morphological aspects of Angiostrongylus costaricensis by light and scanning electron microscopy. Acta Trop 2013;127. https://doi.org/10.1016/j.actatropica.2013.05.002.

[109] Fragaki K, Ferrua B, Mograbi B, Waldispühl J, Kubar J. A novel *Leishmania* infantum nuclear phosphoprotein Lepp12 which stimulates IL1-beta synthesis in THP-1 transfectants. BMC Microbiol 2003;3:7. https://doi.org/10.1186/1471-2180-3-7.

[110] Rappsilber J, Mann M, Ishihama Y. Protocol for micro-purification, enrichment, pre-fractionation and storage of peptides for proteomics using StageTips. Nat Protoc 2007;2:1896–906. https://doi.org/10.1038/nprot.2007.261.

[111] Zecha J, Satpathy S, Kanashova T, Avanessian SC, Kane MH, Clauser KR, et al. TMT Labeling for the Masses: A Robust and Cost-efficient, In-solution Labeling Approach. Molecular & Cellular Proteomics 2019;18:1468–78. https://doi.org/10.1074/mcp.TIR119.001385.

[112] Cox J, Mann M. MaxQuant enables high peptide identification rates, individualized p.p.b.-range mass accuracies and proteome-wide protein quantification. Nat Biotechnol 2008;26:1367–72. https://doi.org/10.1038/nbt.1511.

[113] Amos B, Aurrecoechea C, Barba M, Barreto A, Basenko EY, Bażant W, et al. VEuPathDB: the eukaryotic pathogen, vector and host bioinformatics resource center. Nucleic Acids Res 2022;50:D898–911. https://doi.org/10.1093/NAR/GKAB929.

[114] Alshaweesh J, Nakamura R, Tanaka Y, Hayashishita M, Musa A, Kikuchi M, et al. *Leishmania major* Strain-Dependent Macrophage Activation Contributes to Pathogenicity in the Absence of Lymphocytes. Microbiol Spectr 2022;10. https://doi.org/10.1128/spectrum.01126-22.

[115] Brazil. Departamento de Vigilância Epidemiológica. Manual de vigilância e controle da leishmaniose visceral. Editora MS; 2003.

[116] Oliveira GC, Paiz LM, Menozzi BD, Lima M de S, Moraes CCG de, Langoni H. Antibodies to *Leishmania* spp. in domestic felines. Revista Brasileira de Parasitologia Veterinária 2015;24. https://doi.org/10.1590/S1984-29612015071.

Supplementary information

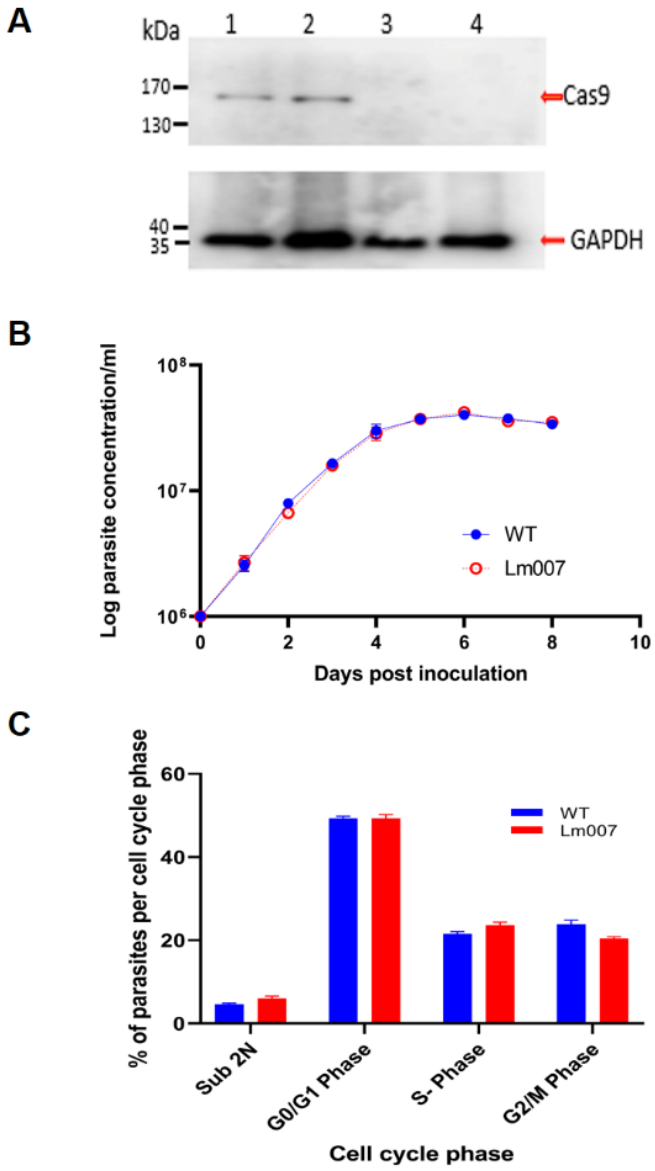

S1 Fig. Expression of pTB007 in *L. major* (*Lm*007) does not affect the growth and cell cycle of the parasite. (A) Western blot image for Cas9 expression validation. Lanes 1 and 2: selected *Lm*007 clone; Lanes 3 and 4 WT *L. major* electroporated and nonelectroporated, respectively. (B) Growth profile of WT and *Lm*007 (C) DNA content assessment of WT and *Lm*007.

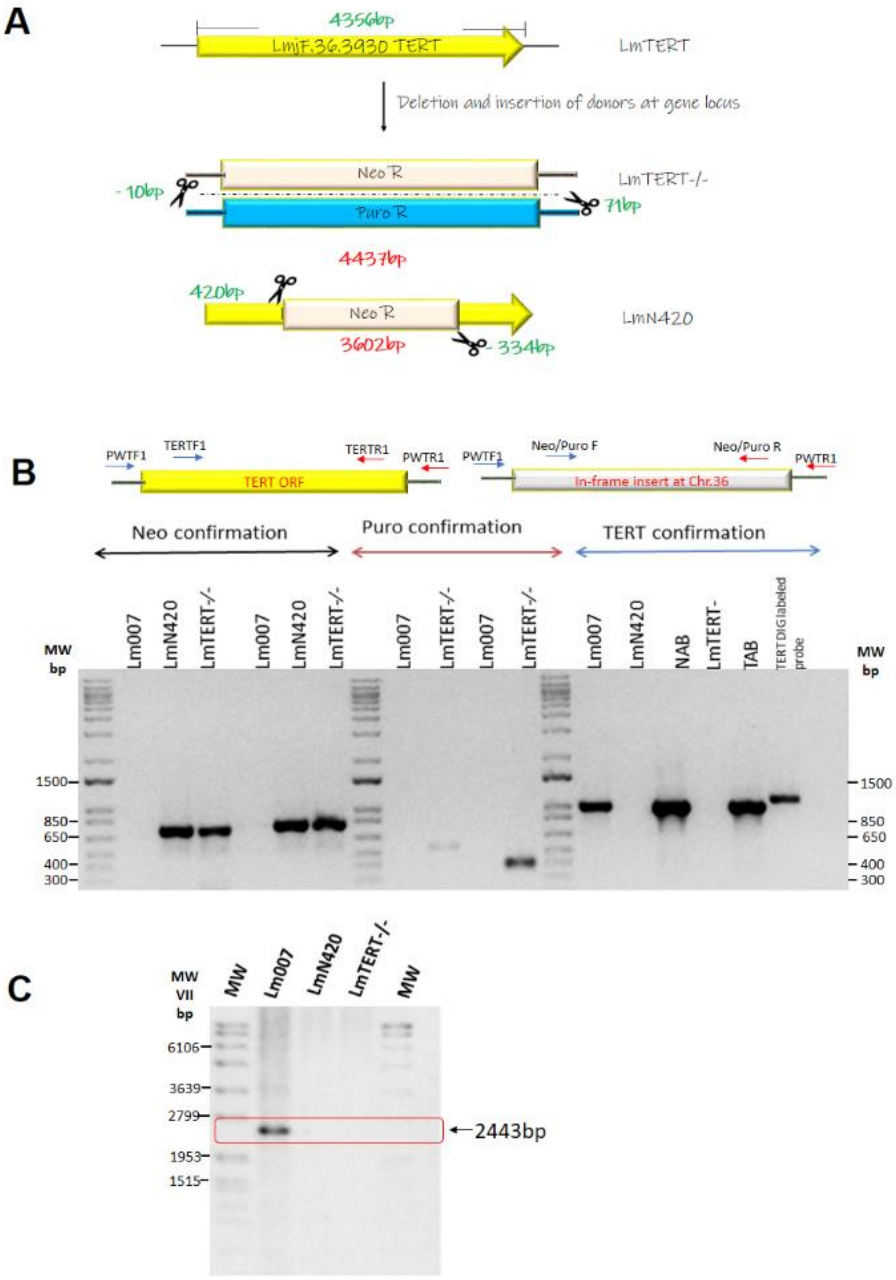

S2 Fig. Strategies for the deletion of *Lm*TERT and the methods of confirmation. (A) Schematic showing the two strategies used in ablating *Lm*TERT. The top schematic shows the full TERT gene and its corresponding size in green. The middle schematic shows the deletion of the full TERT gene (*Lm*TERT-/-) being replaced by Puromycin (PuroR) and Neomycin (NeoR) resistance genes. The bottom schematic shows the deletion of an internal region of the TERT gene leaving 420bp upstream and 334bp downstream. The *Lm*N420 cut site is replaced by a NeoR. The size of deleted regions in both lineages is given in red, and the cut site of the Cas 9 endonuclease relative to the start and stop codons is written in green (Middle and bottom schematic). (B) PCR amplifications confirm the successful ablation of the *Lm*TERT and the proper integration of donor templates. Schematic maps show the positioning of primers used in the confirmation (C) Southern blot confirmation of *Lm*TERT absence in both knockout lineages using dig labelled probe and digesting genomic DNA with *Xho*1.

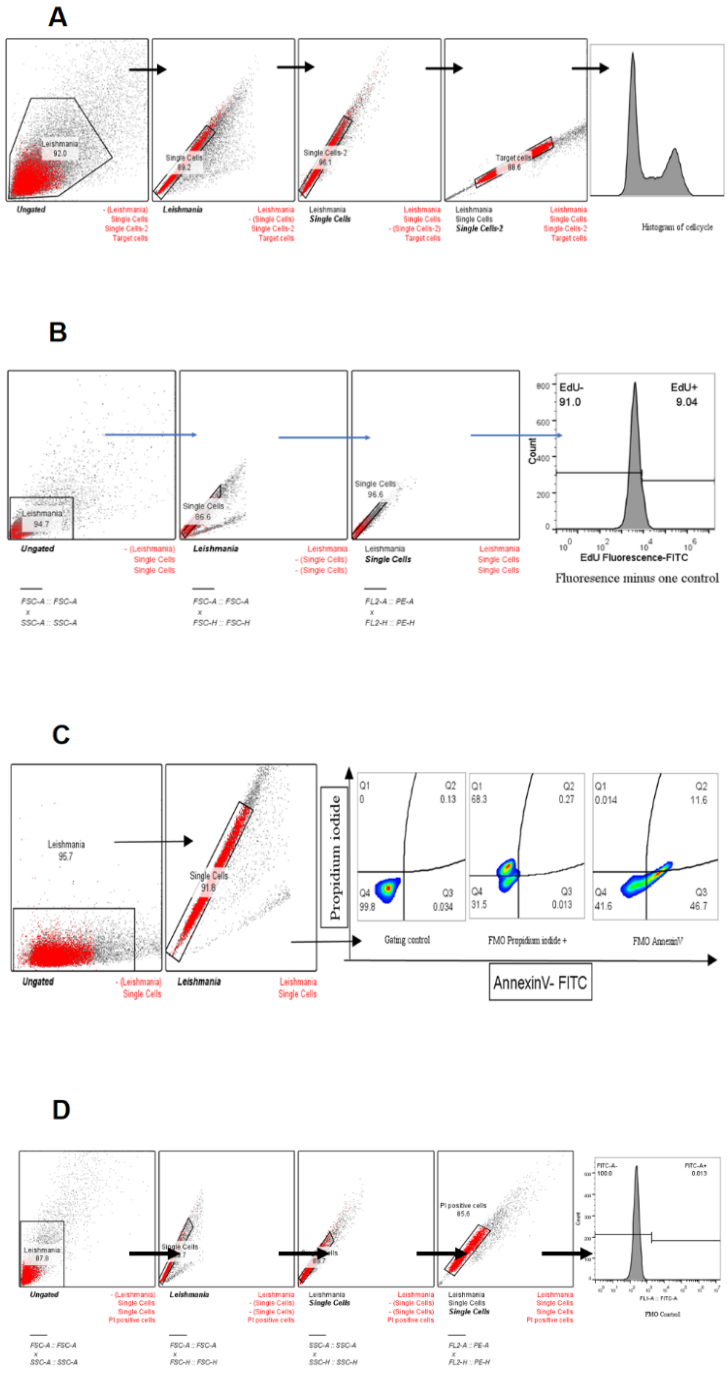

S3 Fig. Representative gating paths used in analysing flow cytometry data. (A) Gating strategies used to select cells for DNA content analysis (B) EdU gating steps to select parasites undergoing synthesis and parasites that are not (C) Annexin assay gating strategies to select for cells that are positive, negative, both or neither for the stains used (Annexin V and Propidium iodide). (D) Gating paths are used to determine the percentage of DNA fragmentation. All data were analysed using Flowjo V.10.0.7r2. The final number of cells considered for statistical treatment was within the same range for all groups considered. Fluorescence Minus One (FMO) controls were used to gate out flow-through fluorescence signals.

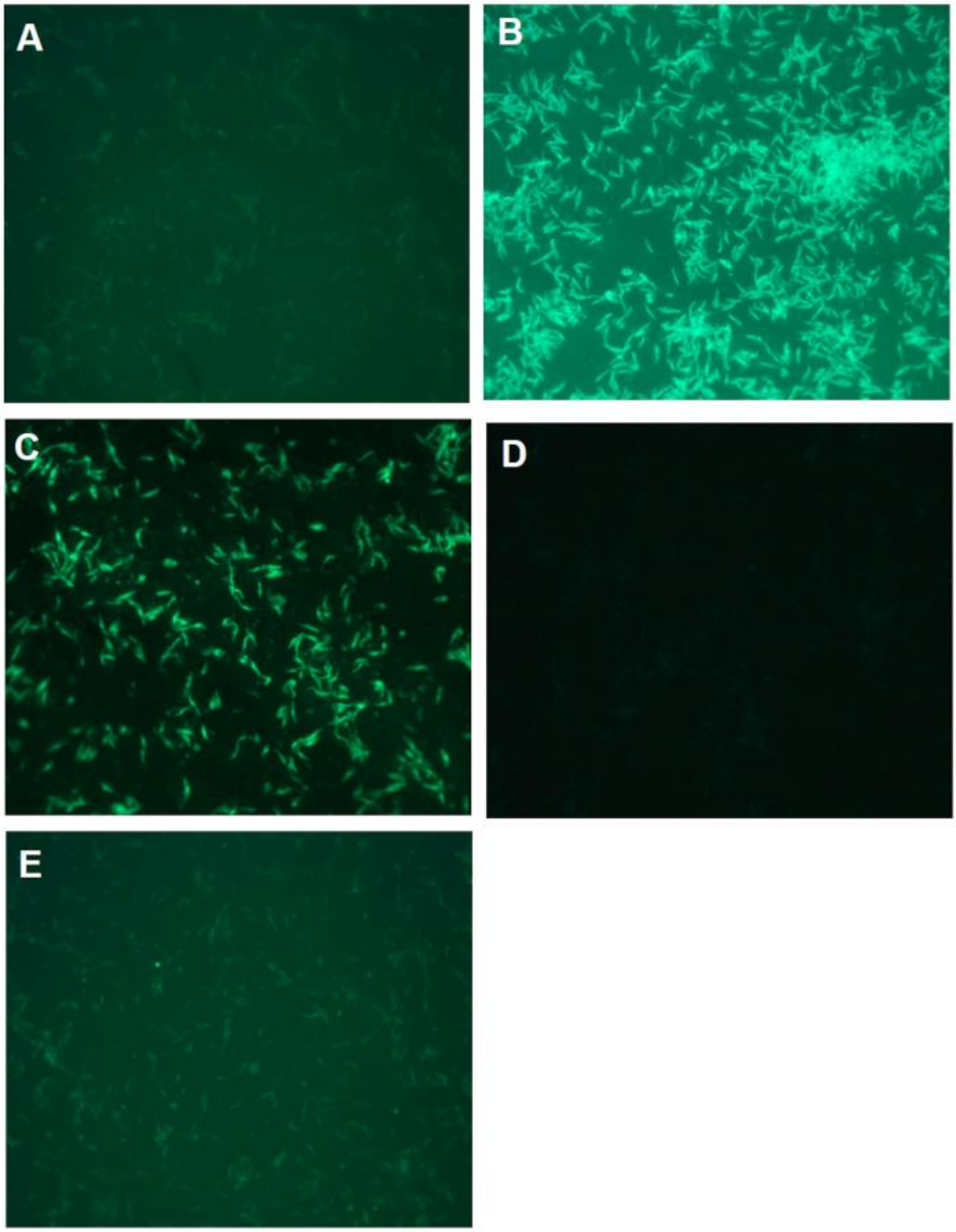

S4 Fig. Fluorescent antibody test of *Leishmania major* infection in experimentally infected mice. Images from the indirect immunofluorescence of sera were obtained from infected mice in this study. **(A)** Negative control and **(B)** positive control of the technical procedure **(C)** Results from *Lm*007. **(D)** and **(E)** *Lm*N420 and *Lm*TERT-/-, respectively.

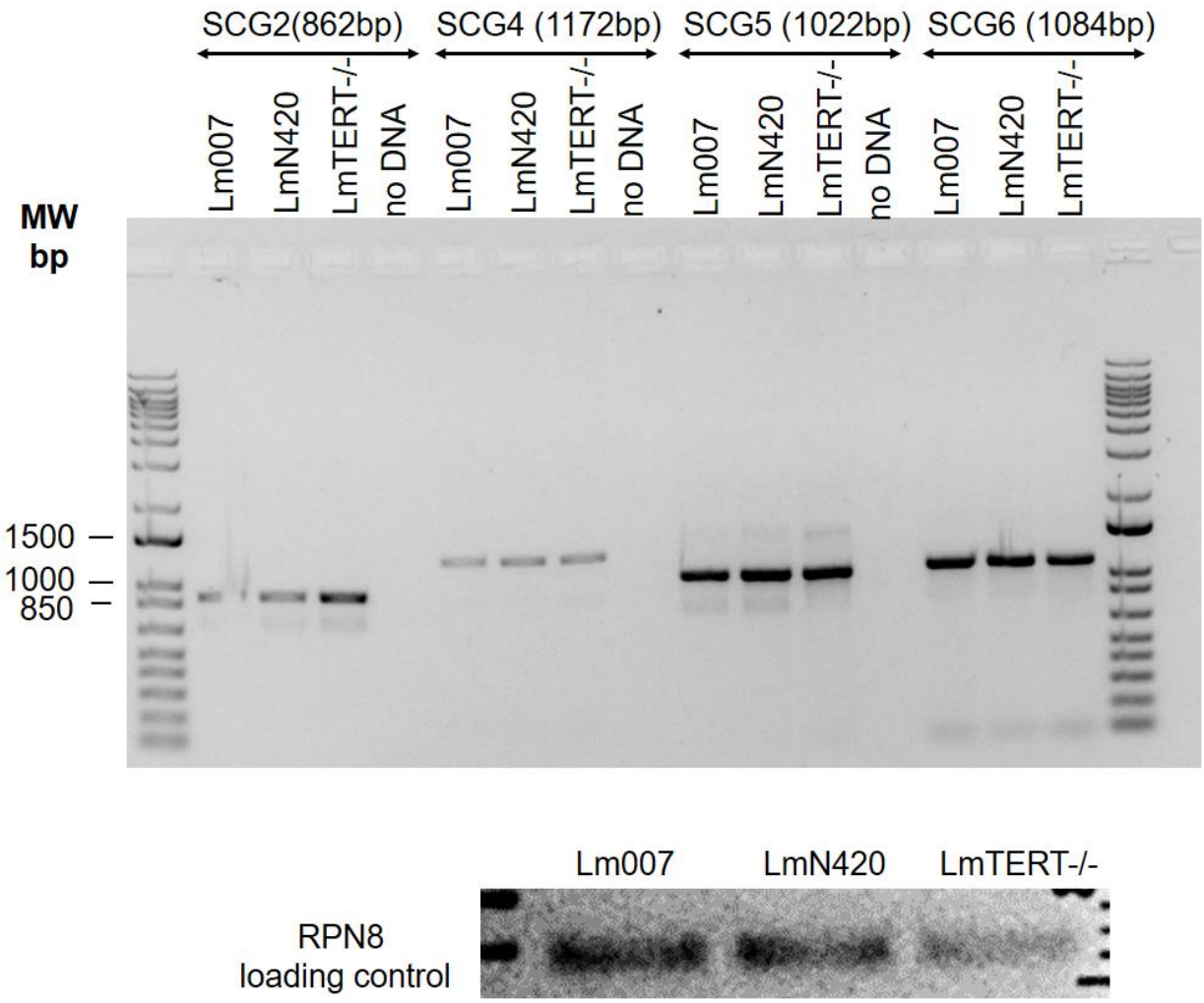

S5 Fig. SCG gene amplifications. Agarose gel images of the amplicons for *SCG2*, SCG4, *SCG5* and *SCG6*

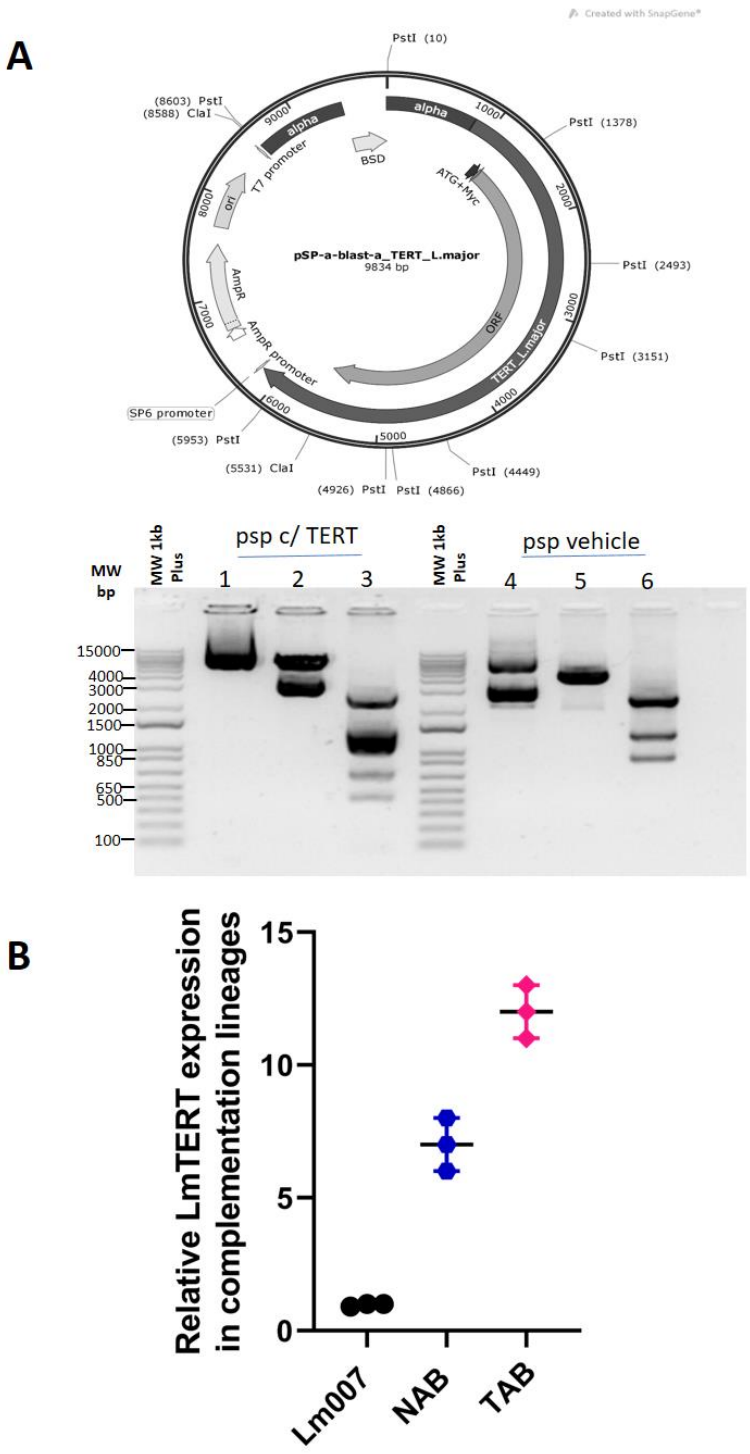

S6 Fig. Plasmid engineering for *Lm*TERT reintroduction in knockout lineages (complementation). (A) Map of Psp plasmid inserted with WT *Lm*TERT gene sequence. The map also shows the restriction sites used in restriction fragment length polymorphism confirmation. Restriction digestion of plasmid DNA to confirm the presence (left panel) and absence (right panel) of *Lm*TERT. 1 and 4 are undigested plasmids, 2 and 5 are plasmids digested with *Cla*I, and 3 and 6 are plasmids digested with *Pst*1. (B) Expression of *Lm*TERT after complementation in knockout lines compared to *Lm*007.

A

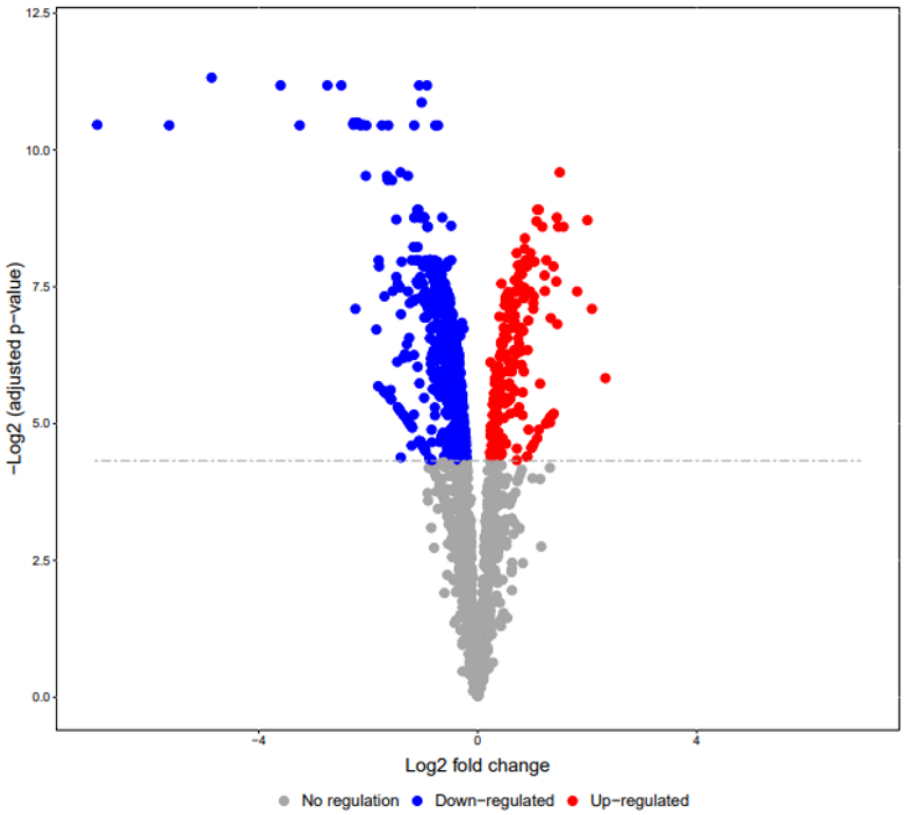

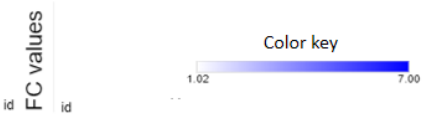

B

	2.16	voltage-dependent anion-selective channel - putative
	3.52	Thioredoxin - putative
	2.17	short chain 3-hydroxyacyl-CoA dehydrogenase - putative
	2.05	Ras-related protein Rab5A - putative
	2.27	outer dynein arm docking complex - putative
→	2.78	**META domain containing protein - putative**
	2.02	hypothetical protein - conserved
	2.03	hypothetical protein - conserved
	4.01	histone H4
	2.82	histone H4
	2.52	histone H3 variant - putative
	2.96	histone H2B
	2.11	histone H2A
	2.20	heat shock protein 83
	2.70	Dynein light chain LC6 - flagellar outer arm - putative
	5.04	dynein light chain - flagellar outer arm - putative
	2.12	dynein heavy chain - putative
	2.56	cytochrome c - putative
	2.72	Cytochrome b5-like Heme/Steroid binding domain containing protein - putative

S7 Fig. Differential protein expression. (A) The volcano plot shows differential protein expression between *Lm*007 and *Lm*TERT. **(B)** A Morpheus derived heatmap depicting significantly downregulated proteins and of interest is the META domain containing protein boldly highlighted. **(C)** Heatmap of significantly upregulated proteins after TERT ablation, in bold is the TPR overexpression.

S1 Table. List of oligonucleotides used in this study

Primer Tag	Source	Identifier
Oligonucleotides used in knockout procedure		
G00 (is a primer sequence, common sgRNA primer for amplification)	[39]	N/A
sgRNA_TERT_420 (for generating *Lm*N420): GGAGGAGTTCTGTCGGTCGG	This paper	N/A
sgRNA_TERT_4022 (for generating *Lm*N420): GGACCTCTTTAAAAGGGCGG	This paper	N/A
sgRNA_TERT_5'-UTR (for generating *Lm*TERT-/-): GTACCATGAACGAGGCAAGG	This paper	N/A
sgRNA_TERT_3'-UTR (for generating *Lm*TERT-/-): TAACCCCAACACTCACAGAG	This paper	N/A
Donor Primer (Forward): TCCCCCCTACCAGTACCCCTCGCGTCTCCGgtataatgcagacctgctgc	This paper	N/A
Donor Primer (Reverse): ACGCGGTAGATACCGAGGCACCGTCAGAGGccaatttgagagacctgtgc	This paper	N/A
Oligonucleotides used in knockout confirmation		
PWTF1-(TERT 5' UTR): GGTACGTCATAGGCACTTGAAAG	This paper	N/A
PWNeoF2 (NeoR ORF): CAGACAATCGGCTGCTCTGA	This paper	N/A
PWNeoR1 (NeoR ORF): AGGTCGGTCTTGACAAAAAGAACC	This paper	N/A
PWNeoF3 (NeoR ORF): TGACGAGTTCTTCAGCTCCG	This paper	N/A
PWNeoR2 (NeoR ORF): GAAACATCGCACACGGATGG	This paper	N/A
PWTR7 (TERT 3' UTR): TGTGTGTCTGCAATCAGCC	This paper	N/A
Puro1 UTR 5' Rv (Puro ORF): TTCGTGAGAGAAACCTGTAG	This paper	N/A
Puro2 UTR 3' Fw (Puro ORF): AATACAGGCACGGTCCT	This paper	N/A
Primers used in complementation (addbaack) confirmations (RT-qPCR)		
*Lmj*TERT2R for Target gene: CACCCGCTCTTGTGGTAAGT	This paper	N/A
TERTF2 for Target gene: CAGTTTTTGCGAGGAGGTGC	This paper	N/A
RPN8 F for Reference gene: ATGAACCGCCGCAAGCT	[117]	N/A
RPN8 R for Reference gene: GGCGCGCGACGACGATCTTTGATT	[117]	N/A
Primers used for *SCG* genes		

SCGU3F (Forward primer used in combination with all other reverse primers-universal): CTCGACCCTCTTCAGCTGC	This paper	N/A
SCG7R1 (Primer for SCG 7 confirmation): CGCTGTGTAGTCAGAATCC	This paper	N/A
SCG6R1 (Primer for SCG 6 confirmation): TTGCTGCGGCGTACTCGA	This paper	N/A
SCG54R1 (Primer for SCG5 and Forward primer for 4): GAGTCCTCAGAATCATGCTCC	This paper	N/A
SCG4F (Primer for SCG4): ATGCAGCCAAGCGTGTGC	This paper	N/A
SCG2R1 (Primer for SCG2): CCAACACGATCAAGTGTCT	This paper	N/A
SCG3R1 (Primer for SCG 2): TCGCCAAGGATGACCGCAA	This paper	N/A

3.2 Chapter 2

A brief report on the consequences of BIBR1532 inhibition of telomerase in *Leishmania major*

Mark Ewusi Shiburah[1,2]; Veronica S. Fontes[1]; Stephanie C. Paiva[1]; Maria I.N Cano[1*]

Abstract

There is a need for new therapeutics against leishmaniasis. The telomerase reverse transcriptase component (TERT) of *Leishmania* telomerase has been previously shown to be a useful target. Our goal in this study was to demonstrate the possibility of using small molecules to target *Leishmania major* telomerase and evaluate the effect. BIBR1532 is a non-nucleoside inhibitor known to bind a hydrophobic pocket of the TERT. Its effects on telomerase activity elected it as telomerase-specific inhibitor in some species. We treated *Leishmania major* promastigotes with different doses of BIBR1532 and observed that it causes proliferative decline and telomere attrition. Our results summarily suggest that it is possible to pharmacologically inhibit the telomerase in *Leishmania major* and that the molecule acts in a dose-dependent manner. These findings open the frontiers to the use of small molecules as specific inhibitors against *Leishmania*.

Keywords: Telomerase, BIBR1532, telomere shortening, growth decline

[1] Department of Chemical and Biological Sciences, Institute of Biological Sciences, UNESP, Botucatu, Sao Paulo, Brazil
[2] Animal Research Institute, Council for Scientific and Industrial Research (CSIR-ARI), Accra, Ghana
*Correspondence: maria.in.cano@unesp.br

Introduction

The telomerase reverse transcriptase (TERT) is a core component of the telomerase holoenzyme, along with the telomerase RNA (TER), they both interact to help with genomic stability and integrity by ensuring telomere homeostasis ([1–4]). For long-lived organisms like *Leishmania* and in cancerous cells, the telomerase enzyme has a relatively stable expression compared to normal human cells [2,5–7]. The question of whether the parasite depends on the enzyme for longevity as has been reported in other cells is still unanswered. The current data we have in our lab shows some deficiency in the parasite when the TERT was deleted suggesting that it has an immense potential to be used as a drug target [8].

TERT has been implicated in cell proliferation, apoptosis, and other cellular survival functions [7,9–13]. In metazoans, TERT presents four domains consisting of 11 motifs showing some moderate variations and high synteny in its TERT sequence with humans [14]. Among these motifs, the GQ is reported to be essential for the telomere maintenance mechanism of the TERT and its manipulation can potentially influence cell growth [15]. The CTE domain is responsible for the telomeric DNA positioning, while the TEN facilitates the telomeric DNA and pseudoknot binding. The polymerization activity is reserved for the RT domain as the TRBD facilitates the binding and stability of the RNA template from TER [16,17].

The telomerase RNA provides the template sequence for the *de novo* synthesis of telomeric repeats to chromosome termini. The non-template region of TER, however, comprises of the template boundary element (TBE) that associates with the TERT RBD domain, the pseudoknot, and the stem terminus element (STE) [18]. An important and well-conserved domain of the TER is the CR4/5 domain, which in flagellates is termed Helix IV domain [18,19]. The association

between TERT and TER via the TRBD, and thumb domain is considered necessary for telomerase activity to take place [17,20].

Strategies to inhibit telomerase are underway in the fight against cancer. Chemical molecules such as 2'-O-MeRNA, 3,11-difluoro-6,8,13-trimethyl-8H-quino[4,3,2-kl]acridinium methosulfate (RHPS4), and 2-[[(E)-3-naphthalen-2-ylbut-2-enoyl]amino]benzoic acid (BIBR1532) are some of the proposed therapeutics directed at telomerase [21,22]. Advanced *in vitro* and *in vivo* studies with BIBR1532 have shown promising anti-tumor effect [21,23,24].

2-[[(E)-3-naphthalen-2-ylbut-2-enoyl] amino] benzoic acid (BIBR1532), is a small molecule that is described as a non-nucleoside, and non-competitive inhibitor of telomerase [25]. The activity of BIBR1532 leads to proliferative defects in leukemia cells but not in normal hematopoietic cells [26,27]. Annealing omit maps were used to show the structural basis for the inhibitory activity of TERT in *Tribolium castenum* is related to the binding of the molecule to a hydrophobic pocket on the outer surface of the thumb domain adjacent to the TRBD, at a motif denoted FVYL [20].

Our goal in this study was to evaluate the effect of this molecule on the parasite's proliferation and telomere length maintenance. Based on the binding site of the molecule, we predicted that the telomerase activity would be hampered by the presence of the inhibitor. Preliminary results from the study proved growth impairment in the parasite upon treatment with the inhibitor. The growth impairment and telomere shortening observed corroborate data presented by Shiburah *et al* [8].

Results

BIBR1532 affects the proliferative capacity of *L. major* in a dose-dependent manner

A standard growth curve by cell count was mounted to estimate the impact of the inhibitory activity of BIBR1532 on the growth of *L. major* promastigotes. In a previous study by our group, we estimated the IC50 of BIBR1532 as 65 μM (data not shown) for promastigote forms of *Leishmania major*. Here we show that the parasite growth reduced with concentrations of the inhibitor below and above the previously estimated IC50 (Fig 1A). At 24 h of incubation, the growth of the parasite was showed difference between the control and the BIBR1532-treated parasites (Fig 1B). We evaluated the percentage of growth at each of these days for the concentrations tested and found that, at 24 h, 35 μM of BIBR1532 reduced the parasite proliferation by approximately 40% while 65 μM and 100 μM respectively, reduced about 50% and 60% of the parasite proliferative capacities (Fig 1B). At 48 h, parasites treated with 100 μM BIBR1532 showed about 19% proliferative capacity, which declined further to about 11% at 72 h (Fig 1C and 1D). A similar result was observed for the lower-concentration treated parasites. At 72 h, the growth capacity of parasites treated with 35 μM was at 50% and of parasites treated with 65 μM was about 30% (Fig 1D). These results indicate that, the proliferative defect induced by BIBR1532 is dose dependent, and acts stronger over the duration of treatment. Moreover, the DMSO used as the drug diluent had no effect on parasite growth (Fig 1A).

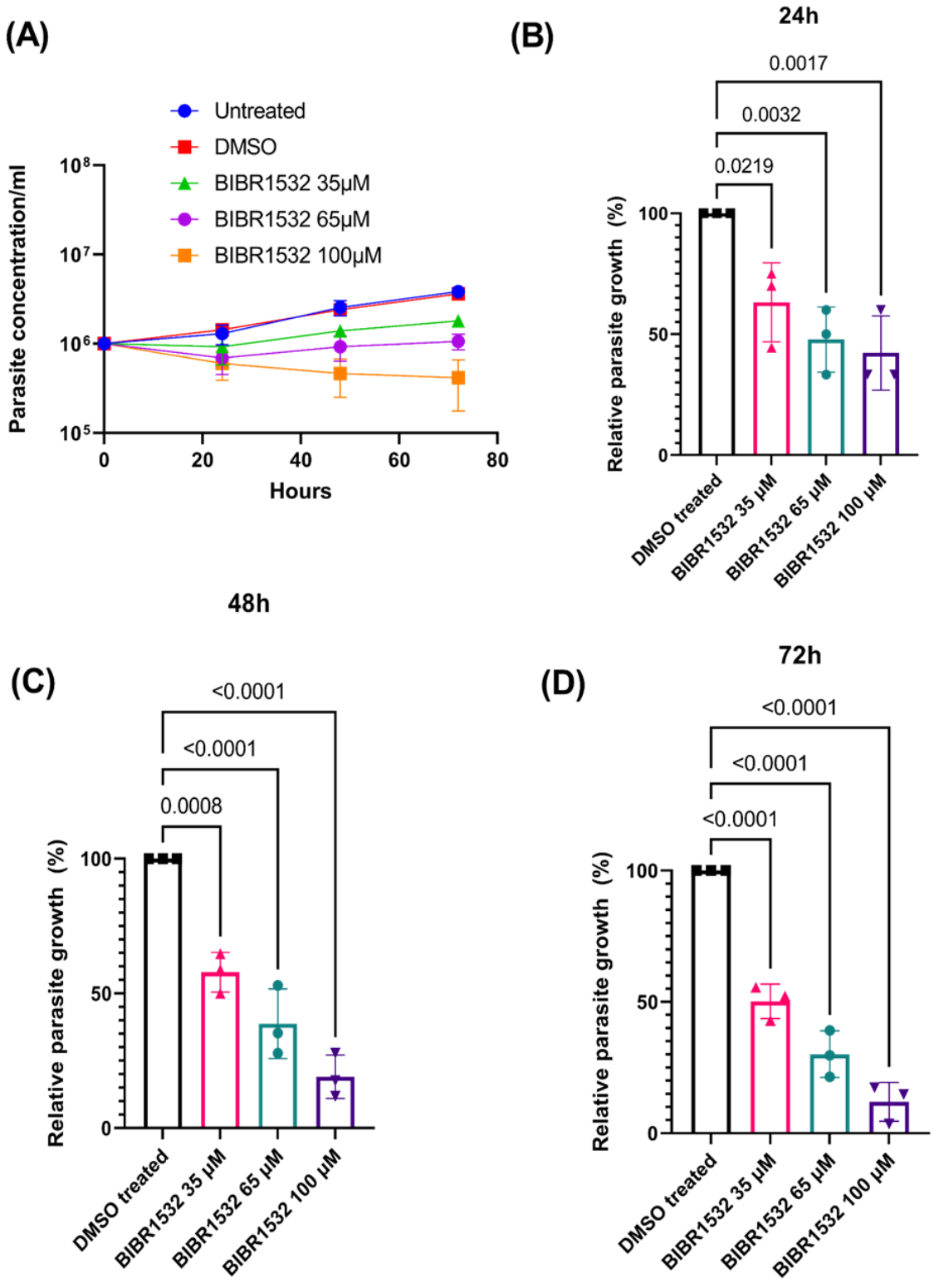

FIG 1. Growth comparisons of BIBR1532 treated and non-treated parasites. (A) Growth comparisons between untreated parasites and parasites treated with three different concentrations of BIBR1532. **(B)**, **(C)**, **(D)** comparative proliferation in percentages of parasites at 24, 48, and 72 h respectively.

Dose dependent telomere shortening after BIBR1532 treatment

We checked the impact of the BIBR1532 treatment on the telomere size of promastigotes 72 h after treatment. We found that the telomere sizes reduced with increased concentrations of BIBR1532 (Fig. 2). The results also revealed that the diluent used (DMSO) had no effect on the telomere size (Fig. 2). The WALTER assessment of TRF intensities revealed the mean of the untreated and DMSO-treated, to be approximately, 4638.7 bp and 4652.1 bp. The means obtained for the treated groups were 4177.9 bp for the 35 μM and 3314.3 bp for the 100 μM, a difference of about 200 bp and 1300 bp when respectively compared to the untreated.

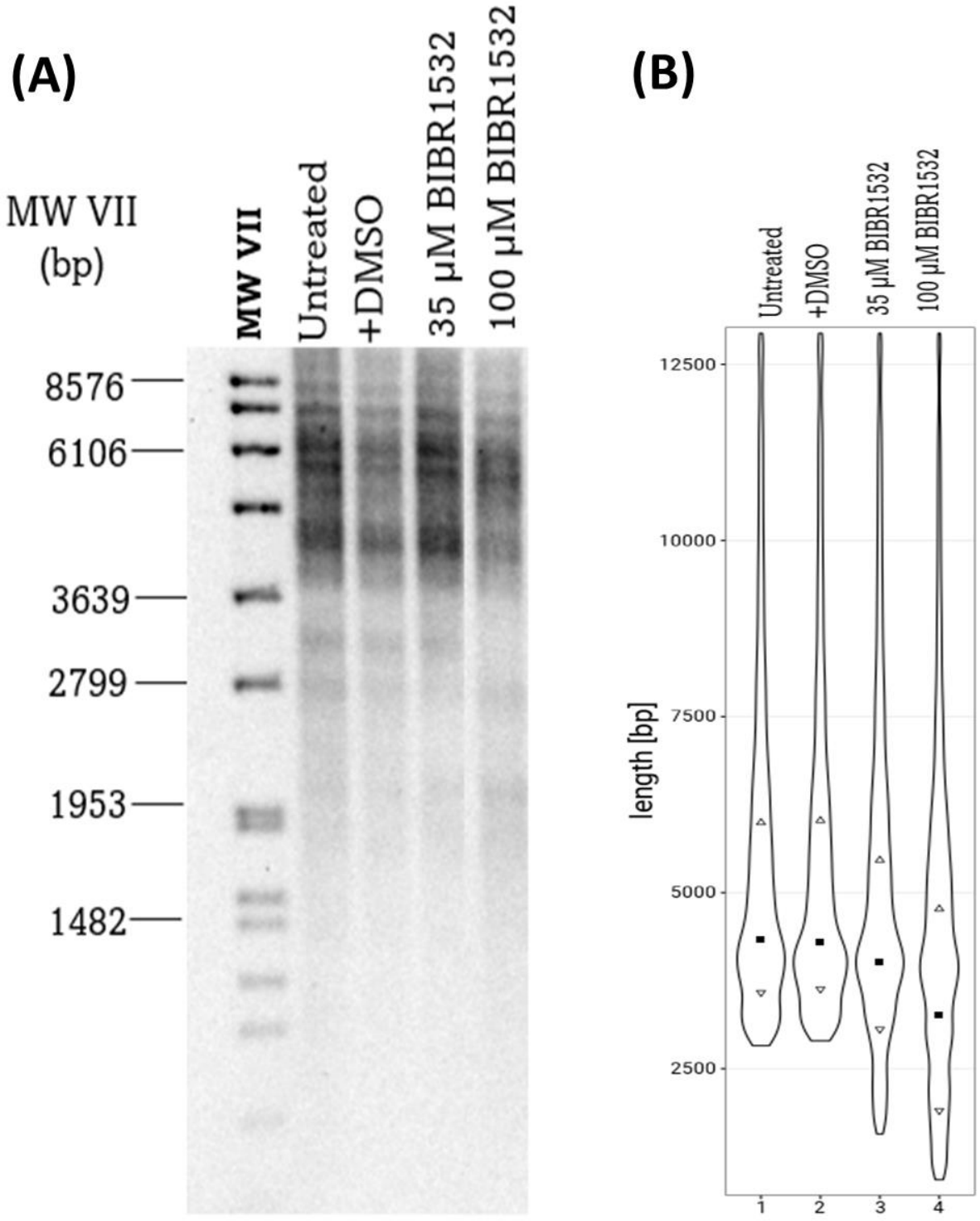

FIG 2. Telomere length attrition due to BIBR1532 treatment. (A) Southern blot TRF assessment of the sizes of telomeres in the parasites 72 h after treatment of BIBR1532. **(B)** WALTER intensity profiles of the TRF sizes obtained from the southern blot.

Discussion

Given the results obtained from the knockout of LmTERT [8], we hypothesised the possibility of targeting the TERT using small molecules as a means to effectively study the potential of TERT as a drug target against *Leishmania*. Our knowledge from the knockout study indicated that the parasite loses its ability to proliferate and undergoes telomere attrition due to the inactivity of TERT. Using BIBR1532, a well-established telomerase specific inhibitor, we have shown that indeed telomerase is essential in the growth of the parasite and the maintenance of telomere length. We also observed the parasites to be sensitive to the drug at a concentration lower than the estimated IC50 following prolonged exposure time. Altamura et al. [28] reported differences in cell responsiveness to varied concentrations. Zhang et al. [26] showed 25 μM to be sufficient to cause a response in multiple myeloma cell lines. Both studies and other earlier reports have shown that BIBR1532 acts in a dose dependent manner, with telomerase activity, and drug effect on cells being profoundly impacted with increasing concentrations [26,28]. Our results corroborates results presented by studies on the inhibition of telomerase in human cell lines, *Tribolium castenum* and others [25–27]. Based on these results it is probable that telomerase could be a good target for drugs against leishmaniasis. However, efficacy of a drug must consider safety. Telomerase is absent in normal somatic cells but present in embryonic, hematopoietic, rapidly renewing cells, and germline cells [29]. Ding et al. [29] showed that longer exposure of such cells to lower concentrations (5-10 μM) of BIBR1532 resulted in telomerase inactivation without affecting proliferation and telomere length due to residual telomerase. The low concentrations however delimited the cells' ability to overcome DNA damage without any other cytotoxic defect detection in male germline cells. Pandya and colleagues [30] on the other hand reported BIBR1532 concentrations above 1 μM to

be toxic to feeder-free induced pluripotent stem cells (iPSCs). They go further to show that non-cytotoxic concentrations were ineffective.

Our experimental design tested the effects of BIBR1532 in vitro and in the insect form of *Leishmania major.* But, to cause leishmaniasis in mammals, the parasite transforms into the intracellular amastigotes, which would probably be a more challenging scenario for drug testing. Therefore, the above studies leads us to make proposals for further studies to look at the structural binding, least concentration necessary, and specificity of the BIBR1532 to the parasite´s telomerase. The possibility of designing LmTERT specific small-molecule inhibitors should also be considered alongside the treatment duration to achieve results.

Materials and Methods

Cell culture and pharmacological treatment

Leishmania major (Friedelin strain, MHOM/IL/1980/FRIEDLIN) used in this study was cultured with M199 medium (Cultilab) supplemented with 10% (v/v) foetal bovine serum (FBS), 41.75mM HEPES, 0.35g/l NaHCO3, 104.38 µM Adenine, 0.0001% Biotin, 1X antibiotic solution. Cells were incubated inside a biological oxygen demand (BOD) chamber at 26 °C. Treatment of parasites with BIBR1532 was done by diluting the BIBR1532 in DMSO (10%). Cells were counted using Neubauer chamber.

Telomeric Southern blot

Genomic DNA extracted from the parasites at Day 3 were digested with 5 U *Afa*1 (Roche) at 37 °C overnight. Terminal restriction fragments (TRF) were fractionated in a 0.8% EtBr-stained agarose gel and transferred to the Hybond N+ nylon membrane (Cytivia) overnight. The membrane was crosslinked after the transfer and taken through stringent washes before being hybridized with a 5'-DIG-labelled telomeric probe (TELC) (5'-DIG-CCCTAACCCTAACCCTAACCCTAACCCTAA). The hybridization signals were developed with an anti-DIG-HRP conjugate antibody and CSPD-Star (Roche).

Statistical Analysis

Data collected, unless otherwise stated, were from at least three replicates conducted in parallel. Each assay is subjected to statistical treatment using GraphPad Prism V.9. Statistical analysis was done using one-way ANOVA with further Dunnett post-hoc analysis for multi-comparisons. All graph is represented as mean ±SD, and significance was tested at $P \leq 0.05$ at all times (specific P values are stated).

References

[1] Greider CW, Blackburn EH. A telomeric sequence in the RNA of Tetrahymena telomerase required for telomere repeat synthesis. Nature 1989;337:331–7. https://doi.org/10.1038/337331a0.

[2] Cano MIN, Dungan JM, Agabian N, Blackburn EH. Telomerase in kinetoplastid parasitic protozoa. Proc Natl Acad Sci U S A 1999;96:3616–21. https://doi.org/10.1073/pnas.96.7.3616.

[3] Ségal-Bendirdjian E, Geli V. Non-canonical Roles of Telomerase: Unraveling the Imbroglio. Front Cell Dev Biol 2019;7:1–12. https://doi.org/10.3389/fcell.2019.00332.

[4] Ale-Agha N, Dyballa-Rukes N, Jakob S, Altschmied J, Haendeler J. Cellular functions of the dual-targeted catalytic subunit of telomerase, telomerase reverse transcriptase - Potential role in senescence and aging. Exp Gerontol 2014;56:189–93. https://doi.org/10.1016/j.exger.2014.02.011.

[5] Mozdy AD, Cech TR. Low abundance of telomerase in yeast: Implications for telomerase haploinsufficiency. Rna 2006;12:1721–37. https://doi.org/10.1261/rna.134706.

[6] Giardini MA, Segatto M, Da Silva MS, Nunes VS, Cano MIN. Telomere and telomerase biology. vol. 125. 2014. https://doi.org/10.1016/B978-0-12-397898-1.00001-3.

[7] Zhang A, Zheng C, Hou M, Lindvall C, Li KJ, Erlandsson F, et al. Deletion of the telomerase reverse transcriptase gene and haploinsufficiency of telomere maintenance in cri du chat syndrome. Am J Hum Genet 2003;72:940–8. https://doi.org/10.1086/374565.

[8] Shiburah ME, Cristina Dias de Oliveira B, Bisetegn H, Silva A, Henrique de Castro Assis L, Menna Barreto R, et al. Ablation of telomerase reverse transcriptase in *Leishmania major* results in a senescent-like 2 phenotype and loss of infectivity 3 n.d. https://doi.org/10.1101/2023.11.10.566596.

[9] Haendeler J, Hoffmann J örg, Rahman S, Zeiher AM, Dimmeler S. Regulation of telomerase activity and anti-apoptotic function by protein-protein interaction and phosphorylation. FEBS Lett 2003;536:180–6. https://doi.org/10.1016/S0014-5793(03)00058-9.

[10] Xi L, Schmidt JC, Zaug AJ, Ascarrunz DR, Cech TR. A novel two-step genome editing strategy with CRISPR-Cas9 provides new insights into telomerase action and TERT gene expression. Genome Biol 2015;16:1–17. https://doi.org/10.1186/s13059-015-0791-1.

[11] Zhu J, Liu W, Chen C, Zhang H, Yue D, Li C, et al. TPP1 OB - fold domain protein suppresses cell proliferation and induces cell apoptosis by inhibiting telomerase recruitment to telomeres in human lung cancer cells. J Cancer Res Clin Oncol 2019;145:1509–19. https://doi.org/10.1007/s00432-019-02921-3.

[12] Lee J, Sung YH, Cheong C, Choi YS, Jeon HK, Sun W, et al. TERT promotes cellular and organismal survival independently of telomerase activity. Oncogene 2008;27:3754–60. https://doi.org/10.1038/sj.onc.1211037.

[13] Zhou J, Ding D, Wang M, Cong YS. Telomerase reverse transcriptase in the regulation of gene expression. BMB Rep 2014;47:8–14. https://doi.org/10.5483/BMBRep.2014.47.1.284.

[14] Lai AG, Pouchkina-Stantcheva N, Di Donfrancesco A, Kildisiute G, Sahu S, Aziz Aboobaker A. The protein subunit of telomerase displays patterns of dynamic evolution and conservation across different metazoan taxa. BMC Evol Biol 2017;17. https://doi.org/10.1186/s12862-017-0949-4.

[15] Zvereva MI, Shcherbakova DM, Dontsova OA. Telomerase: Structure, functions, and activity regulation. Biochemistry (Moscow) 2010;75:1563–83. https://doi.org/10.1134/S0006297910130055.

[16] Nguyen THD, Tam J, Wu RA, Greber BJ, Toso D, Nogales E, et al. Cryo-EM structure of substrate-bound human telomerase holoenzyme. Nature 2018;557:190–5. https://doi.org/10.1038/s41586-018-0062-x.

[17] Wang Y, Feigon J. Structural biology of telomerase and its interaction at telomeres. Curr Opin Struct Biol 2017;47:77–87. https://doi.org/10.1016/j.sbi.2017.06.010.

[18] Davis JA, Chakrabarti K. Telomerase ribonucleoprotein and genome integrity—An emerging connection in protozoan parasites. WIREs RNA 2021. https://doi.org/10.1002/wrna.1710.

[19] Elton JRV, Vinícius SN, Marcelo SDS, Marcela S, Peter JM, Maria INC. The putative *Leishmania* telomerase rna (LeishTer) undergoes trans-splicing and contains a conserved template sequence. PLoS One 2014;9:17–20. https://doi.org/10.1371/journal.pone.0112061.

[20] Bryan C, Rice C, Hoffman H, Harkisheimer M, Sweeney M, Skordalakes E. Structural Basis of Telomerase Inhibition by the Highly Specific BIBR1532. Structure 2015;23:1934–42. https://doi.org/10.1016/j.str.2015.08.006.

[21] Berardinelli F, Coluzzi E, Sgura A, Antoccia A. Targeting telomerase and telomeres to enhance ionizing radiation effects in in vitro and in vivo cancer models. Mutat Res Rev Mutat Res 2017;773:204–19. https://doi.org/10.1016/j.mrrev.2017.02.004.

[22] Herbert B, Pitts AE, Baker SI, Hamilton SE, Wright WE, Shay JW, et al. Inhibition of human telomerase in immortal human cells leads to progressive telomere shortening and cell death. 1999.

[23] Ding X, Cheng J, Pang Q, Wei X, Zhang X, Wang P, et al. BIBR1532, a Selective Telomerase Inhibitor, Enhances Radiosensitivity of Non-Small Cell Lung Cancer Through Increasing Telomere Dysfunction and ATM/CHK1 Inhibition. Int J Radiat Oncol Biol Phys, vol. 105, Elsevier Inc.; 2019, p. 861–74. https://doi.org/10.1016/j.ijrobp.2019.08.009.

[24] Amin A, Morello M, Petrara MR, Rizzo B, Argenton F, De Rossi A, et al. Short-Term TERT Inhibition Impairs Cellular Proliferation via a Telomere Length-Independent Mechanism and Can Be Exploited as a Potential Anticancer Approach. Cancers (Basel) 2023;15. https://doi.org/10.3390/cancers15102673.

[25] Pascolo E, Wenz C, Lingner J, Hauel N, Priepke H, Kauffmann I, et al. Mechanism of human telomerase inhibition by BIBR1532, a synthetic, non-nucleosidic drug candidate. Journal of Biological Chemistry 2002;277:15566–72. https://doi.org/10.1074/jbc.M201266200.

[26] Zhang Y, Yang X, Zhou H, Yao G, Zhou L, Qian C. BIBR1532 inhibits proliferation and enhances apoptosis in multiple myeloma cells by reducing telomerase activity. PeerJ 2023;11:e16404. https://doi.org/10.7717/peerj.16404.

[27] Turkmen E, Sogutlu F, Erdogan M, Biray Avci C. Evaluation of the anticancer effect of telomerase inhibitor BIBR1532 in anaplastic thyroid cancer in terms of apoptosis, migration and cell cycle. Medical Oncology 2023;40. https://doi.org/10.1007/s12032-023-02063-0.

[28] Altamura G, degli Uberti B, Galiero G, De Luca G, Power K, Licenziato L, et al. The Small Molecule BIBR1532 Exerts Potential Anti-cancer Activities in Preclinical Models of Feline Oral Squamous Cell

Carcinoma Through Inhibition of Telomerase Activity and Down-Regulation of TERT. Front Vet Sci 2021;7. https://doi.org/10.3389/fvets.2020.620776.

[29] Ding X, Cheng J, Pang Q, Wei X, Zhang X, Wang P, et al. BIBR1532, a Selective Telomerase Inhibitor, Enhances Radiosensitivity of Non-Small Cell Lung Cancer Through Increasing Telomere Dysfunction and ATM/CHK1 Inhibition. Int J Radiat Oncol Biol Phys, vol. 105, Elsevier Inc.; 2019, p. 861–74. https://doi.org/10.1016/j.ijrobp.2019.08.009.

[30] Pandya VA, Crerar H, Mitchell JS, Patani R. A non-toxic concentration of telomerase inhibitor BIBR1532 fails to reduce tert expression in a feeder-free induced pluripotent stem cell model of human motor neurogenesis. Int J Mol Sci 2021;22. https://doi.org/10.3390/ijms22063256.

4. General conclusion and perspectives

Our data on the study of the TERT as a potential drug target against leishmaniasis has provided useful insights on the possible effects on the biology of the parasite. Particularly, the druggability of the target was successfully confirmed by the use of BIBR1532. However, there are still lingering questions on the mechanism of action and whether the BIBR1532 acts in similar ways as in other tested models. Additionally, the proposed model of action after TERT ablation will need to be experimentally proven to aid in therapeutic modulation of the target. Future studies may look at the processivity of the telomerase during the inhibition at different concentrations. Toxicity levels of the various concentrations can also be tested to avert potential threats to normal cells with telomerase activity.

Lastly, studying further the infectivity *in vitro* and *in vivo* will be an additional benefit to developing potential therapeutics.

5. References

References in this section refer to the citations made before the beginning of the objectives section.

---

[1] Wheeler RJ, Gluenz E, Gull K. The cell cycle of Leishmania: Morphogenetic events and their implications for parasite biology. Mol Microbiol 2011;79:647–62. https://doi.org/10.1111/j.1365-2958.2010.07479.x.

[2] Da Silva R, Sacks DL. Metacyclogenesis is a major determinant of *Leishmania* promastigote virulence and attenuation. Infect Immun 1987;55:2802–6. https://doi.org/10.1128/iai.55.11.2802-2806.1987.

[3] Calderano SG, Moretti NS, Araujo C, Silva MS, Cristina T, Jesus L de, et al. CHAPTER 1 The Cellular Organization of Trypanosomatids During Life Cycle. Frontiers in Parasitology 2016;1:3–60.

[4] Sunter J, Gull K. Shape, form, function and *Leishmania* pathogenicity: from textbook descriptions to biological understanding. Open Biol 2017;7. https://doi.org/10.1098/rsob.170165.

[5] Ramos CS, Franco FAL, Smith DF, Uliana SRB. Characterisation of a new *Leishmania* META gene and genomic analysis of the META cluster. FEMS Microbiol Lett 2004;238:213–9. https://doi.org/10.1016/j.femsle.2004.07.037.

[6] Kweku MA, Odoom S, Puplampu N, Desewu K, Nuako GK, Gyan B, et al. An outbreak of suspected cutaneous leishmaniasis in Ghana: lessons learnt and preparation for future outbreaks. Glob Health Action 2011;4. https://doi.org/10.3402/gha.v4i0.5527.

[7] Faulde M, Schrader J, Heyl G, Amirih M, Hoerauf A. Zoonotic cutaneous leishmaniasis outbreak in Mazar-e Sharif, northern Afghanistan: An epidemiological evaluation. International Journal of Medical Microbiology 2008;298:543–50. https://doi.org/10.1016/j.ijmm.2007.07.015.

[8] Kwakye-Nuako G, Mosore MT, Duplessis C, Bates MD, Puplampu N, Mensah-Attipoe I, et al. First isolation of a new species of *Leishmania* responsible for human cutaneous leishmaniasis in Ghana and classification in the *Leishmania* enriettii complex. Int J Parasitol 2015;45:679–84. https://doi.org/10.1016/j.ijpara.2015.05.001.

[9] Kanyina EW. Characterization of visceral leishmaniasis outbreak, Marsabit County, Kenya, 2014. BMC Public Health 2020;20. https://doi.org/10.1186/s12889-020-08532-9.

[10] Handman E, Kedzierski L, Uboldi AD, Goding JW. Fishing for anti-*Leishmania* drugs: Principles and problems. Adv Exp Med Biol 2008;625:48–60. https://doi.org/10.1007/978-0-387-77570-8_5.

[11] Weekly epidemiological record Relevé épidémiologique hebdomadaire. n.d.

[12] Lindoso JAL, Lindoso AABP. Neglected tropical diseases in Brazil. Rev Inst Med Trop Sao Paulo 2009;51:247–53. https://doi.org/10.1590/S0036-46652009000500003.

[13] Cano MIN. Telomere biology of Trypanosomatids: More questions than answers. Trends Parasitol 2001;17:425–9. https://doi.org/10.1016/S1471-4922(01)02014-1.

[14] Geneva: World Health Organization. Ending the neglect to attain the Sustainable Development Goals: a road map for neglected tropical diseases 2021–2030. 2020.

[15] Kamhawi S. Phlebotomine sand flies and *Leishmania* parasites: friends or foes? Trends Parasitol 2006;22:439–45. https://doi.org/10.1016/j.pt.2006.06.012.

[16] Reis-cunha JL, Valdivia HO, Castanheira D. CHAPTER 2 Trypanosomatid Genome Organization and Ploidy. Frontiers in Parasitology 2016;1:61–103.

[17] Wheeler RJ. The trypanolytic factor-mechanism, impacts and applications. Trends Parasitol 2010;26:457–64. https://doi.org/10.1016/j.pt.2010.05.005.

[18] Calado R, Young N. Telomeres in disease. F1000 Med Rep 2012;4. https://doi.org/10.3410/M4-8.

[19] Srinivas N, Rachakonda S, Kumar R. Telomeres and telomere length: A general overview. Cancers (Basel) 2020;12. https://doi.org/10.3390/cancers12030558.

[20] blackburn_and_gall_1978 n.d.

[21] Moyzis RK, Buckingham JM, Crams LS, Dani M, Deavent LL, Jones MD, et al. A highly conserved repetitive DNA sequence, (TTAGGG)., present at the telomeres of human chromosomes (human repetitive DNA/in situ hybridization/trypanosome telomeres/BAL-31 nuclease/flow cytometry). vol. 85. 1988.

[22] Blackburn EH, Challoner PB. Identification of a Telomeric DNA Sequence in Trypanosoma brucei. vol. 36. 1984.

[23] Cano MIN, Dungan JM, Agabian N, Blackburn EH. Telomerase in kinetoplastid parasitic protozoa. Proc Natl Acad Sci U S A 1999;96:3616–21. https://doi.org/10.1073/pnas.96.7.3616.

[24] Ohki R, Tsurimoto T, Ishikawa F. In Vitro Reconstitution of the End Replication Problem. Mol Cell Biol 2001;21:5753–66. https://doi.org/10.1128/mcb.21.17.5753-5766.2001.

[25] Barbé-Tuana F, Kich Grun L, Pierdoná V, Dias De Oliveira BC, Paiva SC, Shiburah ME, et al. Human genome structure, function and clinical considerations. 2021. https://doi.org/https://doi.org/10.1007/978-3-030-73151-9_7#DOI.

[26] Dreesen O, Li B, Cross GAM. Telomere structure and shortening in telomerase-deficient Trypanosoma brucei. Nucleic Acids Res 2005;33:4536–43. https://doi.org/10.1093/nar/gki769.

[27] Bryan TM. G-quadruplexes at telomeres: Friend or foe? Molecules 2020;25. https://doi.org/10.3390/molecules25163686.

[28] Martínez P, Blasco MA. Cardiovascular Aging Compendium. Circ Res 2018;123:787–802. https://doi.org/10.1161/CIRCRESAHA.118.312202.

[29] Lange T De. How Shelterin Solves the Telomere End-Protection Problem. Cold Spring Harb Symp Quant Biol 2011;75:167–77. https://doi.org/10.1101/sqb.2010.75.017.

[30] Diotti R, Loayza D. Shelterin complex and associated factors at human telomeres. Nucleus 2011;2:2:119–35. https://doi.org/10.4161/nucl.2.2.15135.

[31] Lange T De. Shelterin : the protein complex that shapes and safeguards human telomeres. Genes Dev 2005;19:2100–10. https://doi.org/10.1101/gad.1346005.quence.

[32] Schmutz I, Lange T De. Quick guide Shelterin. Current Biology 2016;26:R387–407. https://doi.org/10.1016/j.cub.2016.01.056.

[33] Jones M, Bisht K, Savage SA, Nandakumar J, Keegan CE, Maillard I. The shelterin complex and hematopoiesis. J Clin Invest 2016;126:1621–9. https://doi.org/10.1172/JCI84547.unit.

[34] Janovič T, Stojaspal M, Veverka P, Horáková D, Hofr C. Human Telomere Repeat Binding Factor TRF1 Replaces TRF2 Bound to Shelterin Core Hub TIN2 when TPP1 Is Absent. Journal of Environmental Issues and Agriculture in Developing Countries 2019;431:3289–301. https://doi.org/10.1016/j.jmb.2019.05.038.

[35] Lan J, Zhu Y, Xu L, Yu H, Yu J, Liu X, et al. The 68-kDa Telomeric Repeat Binding Factor 1 (TRF1) - associated Protein (TAP68) Interacts with and Recruits TRF1 to the Spindle Pole during Mitosis. Journal of Biological Chemistry 2014;289:14145–56. https://doi.org/10.1074/jbc.M113.526244.

[36] Chen Y. The structural biology of the shelterin complex. Biol Chem 2019;400:457–66. https://doi.org/10.1515/hsz-2018-0368.

[37] Conte FF, Cano MIN. Genomic organization of telomeric and subtelomeric sequences of *Leishmania* (Leishmania) amazonensis. Int J Parasitol 2005;35:1435–43. https://doi.org/10.1016/j.ijpara.2005.05.011.

[38] T Van der Ploeg LH, C Liu AY, Borst P. Structure of the Growing Telomeres of Trypanosomes. vol. 36. 1964.

[39] Dossin F de M, Dufour A, Dusch E, Siqueira-Neto JL, Moraes CB, Yang GS, et al. Automated nuclear analysis of *Leishmania major* telomeric clusters reveals changes in their organization during the parasite's life cycle. PLoS One 2008;3. https://doi.org/10.1371/journal.pone.0002313.

[40] Fu G, Barker DC. Characterisation of *Leishmania* telomeres reveals unusual telomeric repeats and conserved telomere-associated sequence. vol. 26. 1998.

[41] Zvereva MI, Shcherbakova DM, Dontsova OA. Telomerase: Structure, functions, and activity regulation. Biochemistry (Moscow) 2010;75:1563–83. https://doi.org/10.1134/S0006297910130055.

[42] Collins K, Mitchell JR. Telomerase in the human organism. Oncogene 2002;21:564–79. https://doi.org/10.1038/sj/onc/1205083.

[43] Greider CW, Blackburn EH. A telomeric sequence in the RNA of Tetrahymena telomerase required for telomere repeat synthesis. Nature 1989;337:331–7. https://doi.org/10.1038/337331a0.

[44] Gilley D, Lee MS, Blackburn EH. Altering specific telomerase RNA template residues affects active site function. Genes Dev 1995;9:2214–26. https://doi.org/10.1101/gad.9.18.2214.

[45] Davis JA, Chakrabarti K. Telomerase ribonucleoprotein and genome integrity—An emerging connection in protozoan parasites. WIREs RNA 2021. https://doi.org/10.1002/wrna.1710.

[46] Zhang A, Zheng C, Hou M, Lindvall C, Li KJ, Erlandsson F, et al. Deletion of the telomerase reverse transcriptase gene and haploinsufficiency of telomere maintenance in cri du chat syndrome. Am J Hum Genet 2003;72:940–8. https://doi.org/10.1086/374565.

[47] Pestana A, Vinagre J, Sobrinho-Simões M, Soares P. TERT biology and function in cancer: Beyond immortalisation. J Mol Endocrinol 2017;58:R129–46. https://doi.org/10.1530/JME-16-0195.

[48] Giardini MA, Lira CBB, Conte FF, Camillo LR, De Siqueira Neto JL, Ramos CHI, et al. The putative telomerase reverse transcriptase component of *Leishmania* amazonensis: Gene cloning and characterization. Parasitol Res 2006;98:447–54. https://doi.org/10.1007/s00436-005-0036-4.

[49] Giardini MA, Segatto M, Da Silva MS, Nunes VS, Cano MIN. Telomere and telomerase biology. vol. 125. 2014. https://doi.org/10.1016/B978-0-12-397898-1.00001-3.

[50] Giardini MA, Fernández MF, Lira CBB, Cano MIN. *Leishmania* amazonensis: Partial purification and study of the biochemical properties of the telomerase reverse transcriptase activity from promastigote-stage. Exp Parasitol 2011;127:243–8. https://doi.org/10.1016/j.exppara.2010.08.001.

[51] Dey A, Chakrabarti K. Current perspectives of telomerase structure and function in eukaryotes with emerging views on telomerase in human parasites. Int J Mol Sci 2018;19. https://doi.org/10.3390/ijms19020333.

[52] Lai AG, Pouchkina-Stantcheva N, Di Donfrancesco A, Kildisiute G, Sahu S, Aziz Aboobaker A. The protein subunit of telomerase displays patterns of dynamic evolution and conservation across different metazoan taxa. BMC Evol Biol 2017;17. https://doi.org/10.1186/s12862-017-0949-4.

[53] Xia J, Peng Y, Saira Mian I, Lue NF. Identification of Functionally Important Domains in the N-Terminal Region of Telomerase Reverse Transcriptase. vol. 20. 2000.

[54] Bhattacharyya A, Blackburn EH. A functional telomerase RNA swap in vivo reveals the importance of nontemplate RNA domains. vol. 94. 1997.

[55] Theimer CA, Feigon J. Structure and function of telomerase RNA. Curr Opin Struct Biol 2006;16:307–18. https://doi.org/10.1016/j.sbi.2006.05.005.

[56] Elton JRV, Vinícius SN, Marcelo SDS, Marcela S, Peter JM, Maria INC. The putative *Leishmania* telomerase rna (LeishTer) undergoes trans-splicing and contains a conserved template sequence. PLoS One 2014;9:17–20. https://doi.org/10.1371/journal.pone.0112061.

[57] Chen Q, Ijpma A, Greider CW. Two Survivor Pathways That Allow Growth in the Absence of Telomerase Are Generated by Distinct Telomere Recombination Events. Mol Cell Biol 2001;21:1819–27. https://doi.org/10.1128/MCB.21.5.1819-1827.2001.

[58] Dreesen O, Cross GAM. Telomerase-Independent Stabilization of Short Telomeres in Trypanosoma brucei . Mol Cell Biol 2006;26:4911–9. https://doi.org/10.1128/mcb.00212-06.

[59] Bryan TM, Englezou A, Oalla-Pozza2 L, Ounham MA, Reddel RR. Evidence for an alternative mechanism for maintaining telomere length in human tumors and tumor-derived cell lines. 1997.

[60] Bryan TM, Englezou A, Gupta J, Bacchetti S, Reddel RR. Telomere elongation in immortal human cells without detectable telomerase activity. EMBO Journal 1995;14:4240–8. https://doi.org/10.1002/j.1460-2075.1995.tb00098.x.

[61] Guterres AN, Villanueva J. Targeting telomerase for cancer therapy. Oncogene 2020;39:5811–24. https://doi.org/10.1038/s41388-020-01405-w.

[62] Londoñ O-Vallejo JA, Der-Sarkissian H, Cazes L, Bacchetti S, Reddel RR. Alternative Lengthening of Telomeres Is Characterized by High Rates of Telomeric Exchange. vol. 64. 2004.

[63] Seimiya H. Crossroads of telomere biology and anticancer drug discovery. Cancer Sci 2020;111:3089–99. https://doi.org/10.1111/cas.14540.

[64] Zhang JM, Zou L. Alternative lengthening of telomeres: From molecular mechanisms to therapeutic outlooks. Cell Biosci 2020;10. https://doi.org/10.1186/s13578-020-00391-6.

[65] Ale-Agha N, Dyballa-Rukes N, Jakob S, Altschmied J, Haendeler J. Cellular functions of the dual-targeted catalytic subunit of telomerase, telomerase reverse transcriptase - Potential role in senescence and aging. Exp Gerontol 2014;56:189–93. https://doi.org/10.1016/j.exger.2014.02.011.

[66] Haendeler J, Hoffmann J örg, Rahman S, Zeiher AM, Dimmeler S. Regulation of telomerase activity and anti-apoptotic function by protein-protein interaction and phosphorylation. FEBS Lett 2003;536:180–6. https://doi.org/10.1016/S0014-5793(03)00058-9.

[67] de Oliveira BCD, Shiburah ME, Paiva SC, Vieira MR, Morea EGO, da Silva MS, et al. Possible Involvement of Hsp90 in the Regulation of Telomere Length and Telomerase Activity During the *Leishmania amazonensis*Developmental Cycle and Population Proliferation. Front Cell Dev Biol 2021;9. https://doi.org/10.3389/fcell.2021.713415.

[68] Campelo R, Lozano ID, Figarella K, Osuna A, Ramírez JL. *Leishmania major* telomerase TERT protein has a nuclear/mitochondrial eclipsed distribution that is affected by oxidative stress. Infect Immun 2015;83:57–66. https://doi.org/10.1128/IAI.02269-14.

[69] Mozdy AD, Cech TR. Low abundance of telomerase in yeast: Implications for telomerase haploinsufficiency. Rna 2006;12:1721–37. https://doi.org/10.1261/rna.134706.

[70] Lee J, Sung YH, Cheong C, Choi YS, Jeon HK, Sun W, et al. TERT promotes cellular and organismal survival independently of telomerase activity. Oncogene 2008;27:3754–60. https://doi.org/10.1038/sj.onc.1211037.

[71] Lee MK, Hande MP, Sabapathy K. Ectopic mTERT expression in mouse embryonic stem cells does not affect differentiation but confers resistance to differentiation- and stress-induced p53-dependent apoptosis. J Cell Sci 2005;118:819–29. https://doi.org/10.1242/jcs.01673.

[72] Strong MA, Vidal-Cardenas SL, Karim B, Yu H, Guo N, Greider CW. Phenotypes in mTERT+/- and mTERT-/- Mice Are Due to Short Telomeres, Not Telomere-Independent Functions of Telomerase Reverse Transcriptase. Mol Cell Biol 2011;31:2369–79. https://doi.org/10.1128/mcb.05312-11.

6. Appendix

This section captures the scientific engagement of the candidate during his PhD until the time of defence. It mainly focuses on his contribution to scientific publications and presentations at conferences and symposiums.

---

1. **Mark Ewusi Shiburah,** Beatriz Cristina Dias de Oliveira, Habtye Bisetegn, Débora Andrade Silva, Luiz Henrique de Castro Assis, Rubem Menna Barreto, Marcos Meuser Batista, Maria de Nazaré Correia Soeiro, Benedito D. Menozzi, Helio Langoni, Juliana Ide Aoki, Adriano Capellazzo Coelho, Maria Isabel N. Cano. Ablation of telomerase reverse transcriptase in *Leishmania major* results in a senescent-like phenotype and loss of infectivity. bioRxiv 2023.11.10.566596; doi: https://doi.org/10.1101/2023.11.10.566596

2. Beatriz Cristina Dias de Oliveira, **Mark Ewusi Shiburah**, Luiz Henrique de Castro Assis, Veronica Silva Fontes, Pedro Henrique Gallo-Francisco, Selma Giorgio, Marcos Meuser Batista, Maria Nazaré Correia Soeiro, Rubem Figueiredo Sadok Menna-Barreto, Juliana Ide Aoki, Adriano Cappellazzo Coelho, Maria Isabel Nogueira Cano. The impact of knocking out the *Leishmania major* telomerase RNA (LeishTER): from altered cell proliferation to decreased parasite infectivity. bioRxiv 2023.11.10.566567; doi: https://doi.org/10.1101/2023.11.10.566567

3. **Mark Ewusi Shiburah,** Beatriz Cristina Dias de Oliveira, Habtye Bisetegn, Débora Andrade Silva, Luiz Henrique de Castro Assis, Rubem Menna Barreto, Marcos Meuser Batista, Maria de Nazaré Correia Soeiro, Benedito D. Menozzi, Helio Langoni, Juliana Ide Aoki, Adriano Capellazzo Coelho, Maria Isabel N. Cano. Growing without TERT: Insights on the absence of telomerase reverse transcriptase in *Leishmania major.* 2nd International symposium on Trypanosomatids, October 27-28, 2023

4. **Mark Ewusi Shiburah**; Beatriz Cristina Dias de Oliveira; Veronica S. Fontes; Noemi Nosomi Taniwaki; Maria Isabel Nogueira Cano. Is the tert in *L. major* a pleiotropic gene: genome editing with CRISPR-Cas9 reveals the possible involvement of TERT in multiple cellular events in the parasite- 51st annual meeting of Brazilian society of biochemistry and molecular biology, and 46th congress of the Brazilian biophysical society. Sep 7, 2022

5. Beatriz C. D. de Oliveira, Luiz H. C. Assis, **Mark E. Shiburah,** Stephany C. Paiva, Veronica S. Fontes, Leilane S. de Oliveira Vitor L. da Silva & Marcelo S. da Silva& Maria Isabel N. Cano. Synchronization of *Leishmania amazonensis* cell cycle using

hydroxyurea. Springer Nature (2022) doi https://doi.org/10.1007/978-1-0716-2736-5_10

6. **Mark Ewusi Shiburah;** Bryan Abuchery; Marcelo S. da Silva; Maria I.N. Cano Beyond telomere maintenance: Uncovering new roles of the Telomerase Reverse Transcriptase (TERT) in *Leishmania major* Cold Spring Harbor Laboratory-Telomeres and Telomerase Meeting. Dec 14, 2021

7. Assis, L.H.C.; Andrade-Silva, D.; **Shiburah, M.E**.; de Oliveira, B.C.D.; Paiva, S.C.; Abuchery, B.E.; Ferri, Y.G.; Fontes, V.S.; de Oliveira, L.S.; da Silva, M.S.; et al. Cell Cycle, Telomeres, and Telomerase in Leishmania spp.: What Do We Know So Far? Cells 2021, 10, 3195. https://doi.org/10.3390/cells10113195

8. de Oliveira BCD, **Shiburah ME**, Paiva SC, Vieira MR, Morea EGO, da Silva MS, Alves CS, Segatto M, Gutierrez-Rodrigues F, Borges JC, Calado RT, and Cano MIN (2021) Possible Involvement of Hsp90 in the Regulation of Telomere Length and Telomerase Activity During the Leishmania amazonensis Developmental Cycle and Population Proliferation. Front. Cell Dev. Biol. doi:10.3389/fcell.2021.713415

9. **Mark Ewusi Shiburah**; Beatriz Cristina Dias De Oliveira; Stephany Cacete de Paiva; Maria Isabel Nogueira Cano; Marcelo Santos da-Silva; Bryan Abuchery. Knockout of the Telomerase reverse transcriptase (TERT) in Leishmania major induces stunted growth and negatively impacts the cellular profile of the parasite. Knockout of the Telomerase reverse transcriptase (TERT) in Leishmania major induces stunted growth and negatively impacts the cellular profile of the parasite. 66th Brazilian Congress of Genetics. Sep 15, 2021

10. Florencia Barbé-Tuana, Lucas Kich Grun, Vinícius Pierdoná, Beatriz Cristina Dias de Oliveira, Stephany Cacete Paiva, **Mark Ewusi Shiburah**, Vítor Luiz da Silva, Edna Gicela Ortiz Morea, Verônica Silva Fontes & Maria Isabel Nogueira Cano. Human Chromosome Telomeres. Springer Nature (2021). doi https://doi.org/10.1007/978-3-030-73151-9_7

11. **Mark E. Shiburah;** Beatriz C. D. de Oliveira; Stepany C. Paiva; Marina R. Vieira; Edna Gicela O. Morea; Marcelo Santos da Silva; Cristiane de Santis Alves; Marcela Segatto; Fernanda Gutierrez; Julio C. Borges; Rodrigo T. Calado; Maria Isabel N. Cano. Regulation of Telomere Length and Telomerase Activity During the Leishmania amazonensis Developmental Cycle and Population ReplicationConference Paper: Regulation of Telomere Length and Telomerase Activity During the Leishmania amazonensis Developmental Cycle and Population Replication 30th Annual Molecular Parasitology and Vector Biology Symposium. (https://ctegd.uga.edu/files/2021/05/Book2021.pdf) May 4, 2021

12. Godson Aryee, Gabriel Adu-Aboagye, **Mark Ewusi Shiburah,** Theresah Nkrumah, David Amedorme. Correlation Between Egg Weight and Egg Characteristics in Japanese Quail, Animal and Veterinary Sciences. Volume 8, Issue 3, May 2020, pp. 51-54. doi: 10.11648/j.avs.20200803.11